

F/8 13/9

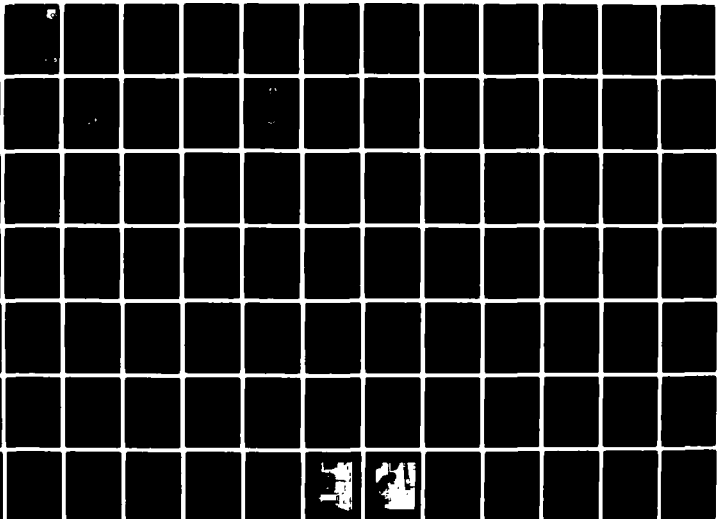
F33615-79-C-2037

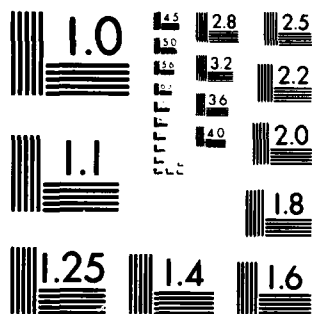
NL

142

As a result, the

Figure 1





MICROCOPY RESOLUTION TEST CHART
NATIONAL BUREAU OF STANDARDS 1963 A

AFWAL-TR-81-2095

GAS FOIL BEARING DEVELOPMENT PROGRAM



**FRANCIS J. SURIANO
GARRETT TURBINE ENGINE COMPANY
A DIVISION OF THE GARRETT CORPORATION
111 S. 34th STREET
PHOENIX, ARIZONA 85010**

DA114002

September 1981

Final Report for Period 1 July 1979 — 28 February 1981

Approved for public release; distribution unlimited.

**AERO PROPULSION LABORATORY
AIR FORCE WRIGHT AERONAUTICAL LABORATORIES
AIR FORCE SYSTEMS COMMAND
WRIGHT-PATTERSON AIR FORCE BASE, OHIO 45433**



DTIC FILE COPY

82 05 20 052


NOTICE

When Government drawings, specifications, or other data are used for any purpose other than in connection with a definitely related Government procurement operation, the United States Government thereby incurs no responsibility nor any obligation whatsoever; and the fact that the government may have formulated, furnished, or in any way supplied the said drawings, specifications, or other data, is not to be regarded by implication or otherwise as in any manner licensing the holder or any other person or corporation, or conveying any rights or permission to manufacture, use, or sell any patented invention that may in any way be related thereto.

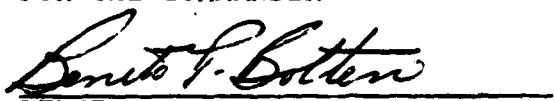
This report has been reviewed by the Office of Public Affairs (ASD/PA) and is releasable to the National Technical Information Service (NTIS). At NTIS, it will be available to the general public, including foreign nations.

This technical report has been reviewed and is approved for publication.


LEON J. DEBROHUN
Project Engineer


HOWARD F. JONES
Chief, Lubrication Branch

FOR THE COMMANDER


BENITO P. BOTTERI, Actg Chief
Fuels and Lubrication Division
Aero Propulsion Laboratory

"If your address has changed, if you wish to be removed from our mailing list, or if the addressee is no longer employed by your organization please notify AFWAL/POSL, W-PAFB, OH 45433 to help us maintain a current mailing list".

Copies of this report should not be returned unless return is required by security considerations, contractual obligations, or notice on a specific account.

SECURITY CLASSIFICATION OF THIS PAGE (When Data Entered)

DD FORM 1473 EDITION OF 1 NOV 68 IS OBSOLETE

SECURITY CLASSIFICATION OF THIS PAGE (When Data Entered)

Unclassified

SECURITY CLASSIFICATION OF THIS PAGE(When Data Entered)

20.

The bearing test rig used was the rig designed for the GTCP165 APU foil bearing program under Contract F33615-78-C-2044. Similarity of journal diameters made this possible. A total of six bearing configurations were tested, two ambient temperature configurations using Teflon-S coated foils with a chrome-plated journal, and four with high-temperature foil and journal coatings. The high-temperature bearings used foil coatings Kaman DES, Kaman DES + Au, Co-20 Ni, and TiC, all of which were run with a Kaman SCA-coated journal. Program goals were met with both ambient-temperature bearing configurations and Kaman SCA versus Kaman DES and TiC high-temperature configurations. ←

Unclassified

SECURITY CLASSIFICATION OF THIS PAGE(When Data Entered)

PREFACE

This report was prepared by the Garrett Turbine Engine Company, a Division of The Garrett Corporation, under Contract F33615-79-C-2037 per the Air Force Wright Aeronautical Laboratories, Wright-Patterson Air Force Base, Ohio 45433. Mr. Leon DeBrohun and Mr. Ron Dayton administered the program for the Air Force. The principal investigator at Garrett was Dr. Francis J. Suriano; program testing was accomplished by Mr. John Ruggles.

Accession For	
NTIS GRA&I	<input checked="" type="checkbox"/>
DTIC TAB	<input type="checkbox"/>
Unannounced	<input type="checkbox"/>
Justification	
By _____	
Distribution/	
Availability Codes	
Dist	Avail and/or Special
A	



TABLE OF CONTENTS

SECTION	PAGE
I INTRODUCTION	1
1. Background	1
a. Advantages	1
b. Related Programs	4
2. Program Objectives	6
3. Program Approach	8
II SUMMARY	9
1. Analysis/Design	9
2. Bearing Development and Testing	11
III DISCUSSION	13
1. Engine Characteristics	13
2. Analysis/Design	14
a. Mechanical	14
b. Thermal Design/Analysis	32
c. Integrated Mechanical-Thermal Design/Analysis	32
d. Similitude of Data for TJE331-1029 and GTCPl65 Basic Simulator Test Rig Bearings	44
e. Alternate Bearing Cooling Designs	44
f. Hydrodynamic Analysis	55
3. Test Rig	75
a. Test Rig Configuration	75
b. Test Rig Instrumentation	75
c. Displacement Probe Monitoring During Load Application	75
4. Basic Bearing Testing	83
a. Bearing Configuration 1	83
b. Bearing Configuration 2	88
c. Bearing Configurations 3, 3a, 3b	91
d. Bearing Configurations 4, 4a, 4b, 4c	95
5. Alternate Foil Coatings	99
a. Bearing Configuration 5	102
b. Bearing Configuration 6	103

TABLE OF CONTENTS (Contd)

SECTION	PAGE
6. Instrumented Journal Testing	105
a. Test Rig Setup	105
b. Pressure Measurement Test Results	110
c. Film Thickness Measurement	122
d. Additional Comments	124
IV CONCLUSIONS AND RECOMMENDATIONS	128
1. Analysis/Design	128
a. Mechanical Design - Conclusions	128
b. Mechanical Design - Recommendations	128
c. Thermal Design - Conclusions	128
d. Thermal Design - Recommendations	130
e. Integrated Mechanical-Thermal Design - Conclusions	130
f. Integrated Mechanical-Thermal Design - Recommendations	130
g. Hydrodynamic Analysis - Conclusions	130
h. Hydrodynamic Analysis - Recommendations	131
2. Basic Bearing Test Rig - Conclusions	131
a. Basic Bearing Test Rig - Conclusions	131
b. Basic Bearing Test Rig - Recommendations	131
3. Basic Bearing Testing/Ambient Facility	132
a. Basic Bearing Testing/Ambient Facility - Conclusions	132
b. Basic Bearing Testing/Ambient Facility - Recommendations	132
4. Basic Bearing Testing/High-Temperature Facility	132
a. Basic Bearing Testing/High-Temperature Facility - Conclusions	132
b. Basic Bearing Testing/High-Temperature Facility - Recommendations	132
5. Alternate Foil Coating Testing	133
a. Alternate Foil Coating Testing - Conclusions	133
b. Alternate Foil Coating Testing - Recommendations	133

TABLE OF CONTENTS (Contd)

SECTION	PAGE
6. Instrumented Journal Testing	133
a. Instrumented Journal Testing - Conclusions	133
b. Instrumented Journal Testing - Recommendations	134
7. Overall Conclusions and Recommendations	134

LIST OF ILLUSTRATIONS

FIGURE		PAGE
1	The Hydrodynamic Gas Bearing Concept	2
2	Self-Acting Gas-Lubricated Compliant Foil Bearing Concept	5
3	TJE331-1029 Thrust Engine 4.5-Inch Diameter Journal	17
4	TJE331-1029 Turbine End Foil Bearing, 4.5-Inch Journal	19
5	TJE331-1029 Turbine End Foil Bearing, 3.5-Inch Diameter Journal	20
6	TJE331-1029 Thrust Engine, 3.5-Inch Diameter Journal	22
7	Flight Maneuver Load Diagrams (MIL-E-5007D)	23
8	Critical Speed vs Bearing Spring Rate for TJE331-1029 with 3.5-Inch Journal Foil Bearings	26
9	Journal Finite-Element Stress Grid	27
10	Journal Stress/Displacement Under Centrifugal Load Including 0.1 Inch Copper Shunt	29
11	Journal Displacement Under Centrifugal Load Plus 16,000 Lb Tie-Shaft Load	30
12	Journal Stress and Displacement Under Combined Centrifugal and Tieshaft Loads	31
13	TJE331-1029 Hot End Foil Bearing Thermal Model; 3.5-Inch Diameter, 4.2-Inch Length Bearing	34
14	Effect of Cooling Flow Rate and Heat Generation on Bearing Component Temperatures	35
15	Effect of Copper Thermal Shunt Thickness on Foil Bearing Journal Axial Temperature Distribution	36
16	Axial Bearing Thermal Distortion for Various Configurations. Variation (δ) in Running Radial Clearance Between Bearing Center and Ends	37

LIST OF ILLUSTRATIONS (CONTD)

FIGURE		PAGE
17	TJE331-1029 Hot End Foil Bearing Thermal Response at 500 Watts Power Dissipation and 0.01 Lb/Sec Cooling Flow at 500°F Inlet Temperature	38
18	TJE331-1029 Hot End Foil Bearing Thermal Response at 500 Watts Power Dissipation and 0.04 Lb/Sec Cooling Flow at 500°F Inlet Temperature	39
19	TJE331-1029 Hot End Foil Bearing Diametral Change in Sway Space Due to Combined Thermal and Centrifugal Effects	41
20	TJE331-1029 Hot End Foil Bearing Diametral Change in Sway Space Due to Combined Thermal and Centrifugal Effects	42
21	TJE331-1029 Hot End Foil Bearing Diametral Change In Sway Space Due to Combined Thermal and Centrifugal Effects	43
22	Solid-Web Journal Centrifugal Stress (ksi) 38,800 rpm	45
23	Foil Bearing Thermal Responses With 500 Watt Bearing Power Dissipation and 0.04 Lb/Sec Cooling Flow at 500°F Inlet Temperature	47
24	Schematic of Multiple Entry Cooling Flow	49
25	TJE331-1029 Hot End Foil Bearing Thermal Response With Configuration 2 Cooling Flow at 500°F Inlet Temperature	51
26	TJE331-1029 Hot End Foil Bearing Diametral Change in Sway Space for 2 Cooling Configurations	52
27	Self-Acting Compliant Foil Bearing Geometry	56
28	Load Deflection Curve for the 12-Foil Bearing	58
29	Comparison of Measured to Calculated Load Deflection Curve, Twelve-Segment Foil Bearing	59

LIST OF ILLUSTRATIONS (CONTD)

FIGURE		PAGE
30	Deflected Foil State Under 1.0-Pound Load for 12-Foil Bearing	61
31	Deflected Foil State at Assembly (3-Pound Load)	62
32	Deflected Foil State Under 5.5-Pound Load	63
33	TJE331-1029/Foil Load-Deflection Curve for the 10-Foil Bearing	64
34	TJE331-1029 10-Foil Bearing Assembly State	65
35	TJE331-1029/Foil Load-Deflection Curve for the 8-Foil Bearing	66
36	TJE331-1029 8-Foil Bearing Assembly State	68
37	TJE331-1029 Normalized Pressure on Foil Segment for the Concentric 12-Foil Bearing	69
38	TJE331-1029 Normalized Pressure on Foil Segment for the Concentric 10-Foil Bearing	70
39	TJE331-1029 Normalized Pressure on Foil Segment for the Concentric 8-Foil Bearing	71
40	TJE331-1029 Foil Shape Under Pressure Load for the Concentric 12-Foil Bearing	72
41	TJE331-1029 Foil Shape Under Pressure for the Concentric 10-Foil Bearing	73
42	TJE331-1029 Foil Shape Under Pressure for the Concentric 8-Foil Bearing	74
43	Basic Simulator Test Rig	76
44	Basic Test Rig with Ambient Box Installed Over Test Bearing	77
45	Instrumentation Locations	79
46	Instrumentation Locations	80
47	Instrumentation Locations	81
48	Typical Signals from Wayne-Kerr Capacitance Type Displacement Probes	82

LIST OF ILLUSTRATIONS (CONTD)

FIGURE		PAGE
49	Foil Backing Spring Modification for 10-Foil Bearing	85
50	10-Foil Bearing Wear Pattern View of "LOAD CARRYING" Region	89
51	10-Foil Bearing Post-Test Foil Condition	90
52	Configuration 3a Post-Test Foil Wear Pattern	94
53	Configuration 4 Variations	95
54	Configuration 4C Bearing. Post-Test Condition After High-Temperature, High-Load Testing	100
55	Configuration 4C Journal. Post-Test Condition After High-Temperature, High-Load Testing	100
56	Configuration 6 TiC Coated Foils After Testing at 1200°F	104
57	Test Rig Assembly Without Instrument Holder or Slip-Ring Assembly	106
58	Probe Slip-Ring Installation on Basic Bearing Rig	107
59	Pressure and Displacement Probe Locations	108
60	Detail of Pressure Probe Installation in Journal	109
61	Instrumented Journal Data, 3.5-Inch Foil Bearing (Photo No. 1)	111
62	Instrumented Journal Data, 3.5-Inch Foil Bearing (Photo No. 2)	112
63	Instrumented Journal Data, 3.5-Inch Foil Bearing (Photo No. 3)	113
64	Instrumented Journal Data, 3.5-Inch Foil Bearing (Photo No. 4)	114
65	Instrumented Journal Data, 3.5-Inch Foil Bearing (Photo No. 5)	115

LIST OF ILLUSTRATIONS (CONTD)

FIGURE		PAGE
66	Instrumented Journal Data, 3.5-Inch Foil Bearing (Photo No. 6)	116
67	Instrumented Journal Data, 3.5-Inch Foil Bearing (Photo No. 7)	117
68	Instrumented Journal Data, 3.5-Inch Foil Bearing (Photo No. 8)	118
69	Instrumented Journal Data, 3.5-Inch Foil Bearing (Photo No. 9)	119
70	Instrumented Journal Data, 3.5-Inch Foil Bearing (Photo No. 10)	120
71	Instrumented Journal Data, 3.5-Inch Foil Bearing (Photo No. 11)	121
72	Pressure Field Relationship With Foils and Backing Springs	122
73	Measured Pressure Field Relationship With Foils and Backing Springs	123
74	Bearing Showing Damage Resulting From Pressure Probe Disintegration	125
75	Instrumented Journal; Inboard Pressure Probe in Place. Outboard Pressure Probe Missing. Scarring is a Result of Probe Centrifuging Out and Breaking Up	126
76	Instrumented Journal; Wayne-Kerr Probe Installation	127

LIST OF TABLES

TABLE		PAGE
1	Foil Bearing Applications	7
2	Summary of Requirements and Accomplishments	10
3	Rotor System Parameters and Limiting Case Bearing Loads	25
4	Foil Bearing Journal Stress Results Centrifugal (33,200 RPM) and Tieshaft (16,000 Lb) Loads	33
5	Solid Web GTCPl65 Journal Stress and Displacements	46
6	TJE331-1029 Multiple Entry Cooling Flow Distribution	50
7	TJE331-1029 Hot End Foil Bearing Relative Load Carrying Capacity (Compared to Axially Uniform 0.001-Inch Film)	54
8	TJE331-1029 Foil Bearing Hydrodynamic Analysis Results	67
9	Foil Bearing Basic Simulator Instrumentation	78
10	Configuration Description	84
11	Bearing Configuration 3, 3a, 3b Characteristics	92
12	Configuration and Performance Description	130

SECTION I

INTRODUCTION

1. BACKGROUND

For many years, gas bearings have been a natural candidate for high-speed turbomachinery design because of the convenience and simplicity of using the process fluid, plant air, or ambient atmosphere as the lubricant. Consequently, a system concept that can capitalize on the advantages of gas bearings has been the object of intensive research throughout the world.

Air bearings constitute one type of the more general class of process fluid, film-lubricated bearings. (Process fluid is the fluid most readily available as the lubricant.) The fluid-film bearing developed during this program is the self-acting (hydrodynamic) type. The load carrying capacity of this self-acting bearing is derived from the pressure generated in the fluid film by the relative motion of two converging surfaces. A foil bearing based on this concept is shown in Figure 1.

Gas-lubricated foil bearings show potential for providing the advantages of simplicity, reduced maintenance, added reliability, reduced vulnerability, high-temperature operation, reduced weight, and cost savings to an advanced engine system.

a. Advantages

Gas-lubricated foil bearings inherently provide the following advantages:

(1) Simplicity

A complicated oil delivery and scavenge network is not required. This consideration is especially critical at the

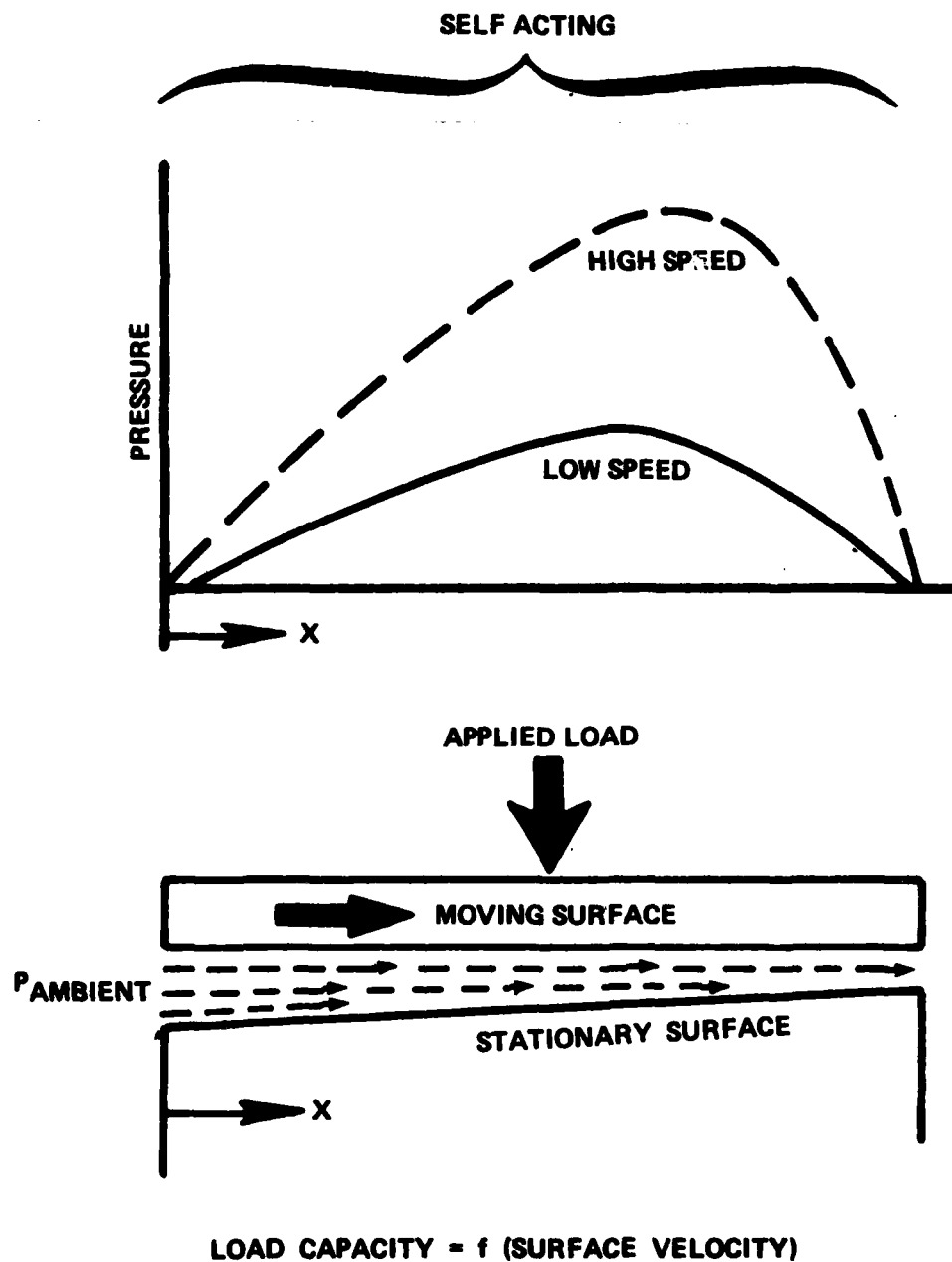


Figure 1. The Hydrodynamic Gas Bearing Concept.

hot end bearings, where oil crosses the engine exhaust path upon entering and leaving the bearing cavity. In this area, extensive development is sometimes necessary to prevent high oil temperature during soakback. Such soak-back often reduces engine reliability and time-between-overhaul.

(2) Reduced Maintenance and Added Reliability

Endurance capability has been proven by foil bearing-equipped cooling turbines used in the DC-10 aircraft environmental control system (ECS). Reliability also is being demonstrated in several military aircraft ECS.

Foil bearings can achieve a longer life because there is no contact between the bearing and shaft during normal operation. Wear-resistant coatings provide adequate wear protection for contact during starts and stops.

Eliminating the need for a viscous bearing lubricant reduces the load on the lubrication pump and enhances cold weather starting capability.

(3) Reduced Vulnerability

Since foil bearings do not require external engine hardware, such as oil lines and an oil heat exchanger, engine vulnerability is reduced.

(4) High-Temperature Operation

Advancements in foil coating temperature tolerance were achieved during this program. Because air viscosity increases with temperature, a hotter-running bearing provides higher load capacity, thus making high-temperature operation desirable.

(5) Reduced Weight

Foil bearings effect system weight savings by reducing the required oil capacity even when an engine gearbox is required. The reduced oil capacity, in turn, reduces capacity requirements for the oil heat exchanger and the oil pump. Eliminating oil delivery and scavenge networks results in a less complex, more uniform, and lighter weight assembly.

(6) Cost Saving

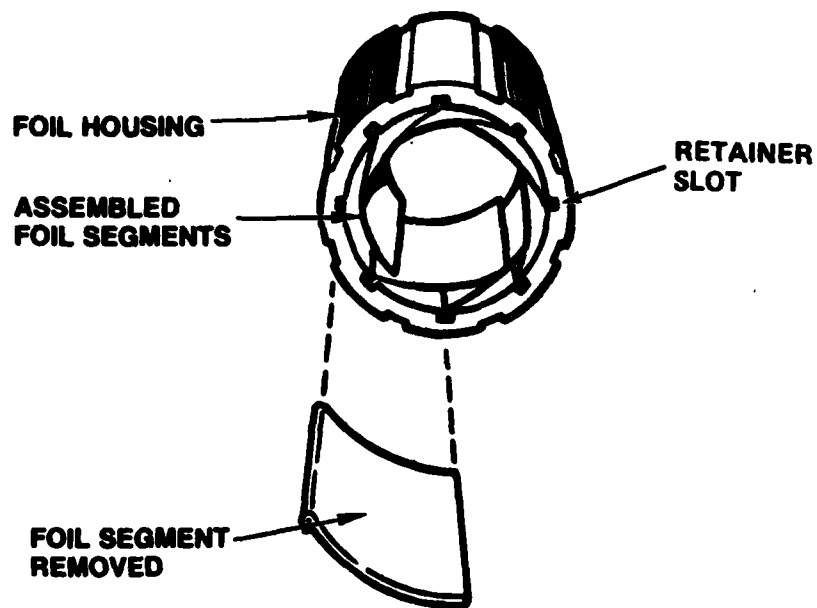
The simplicity of foil bearings augments rapid and easy fabrication. After an initial investment in tooling, foils can be stamped or rolled out at low cost. The greatest cost saving is realized by elimination of the oil network.

b. Related Programs

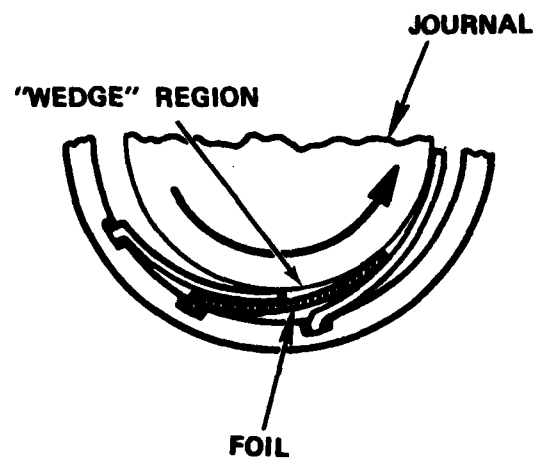
The gas-lubricated foil bearing utilized for this program is of a design patented by The Garrett Corporation. The bearing initially was developed for experimental use in cooling turbines of the Boeing 727 air conditioning system. The general bearing design is depicted in Figure 2.

Observing the successful application of the Garrett foil bearing to the cooling turbines, and recognizing the advantages that foil bearings offer to advanced military engines, the U.S. Air Force sponsored a feasibility study of the application of gas-lubricated, compliant foil bearings to gas turbine engines. This initial program was completed and is described in Technical Report AFAPL-TR-72-41, dated June 1972.

During a follow-on program, a foil bearing demonstrator was designed and fabricated from a Garrett Model JFS100-13A Jet Fuel Starter gas generator, used on the U.S. Air Force A7D



(a) GENERAL ARRANGEMENT (LESS JOURNAL)



(b) CONVERGING SURFACES (JOURNAL INSTALLED)

Figure 2. Self-Acting Gas-Lubricated Compliant Foil Bearing Concept.

light-attack aircraft. Modifications to the original production equipment included replacing the rolling element bearings with compliant foil gas bearings and replacing the power turbine module with an exhaust thrust nozzle. The resultant engine is a 95-pound static thrust turbojet engine, mounted on compliant foil gas bearings totally free of oil and external air supply, and operating at 72,000 rpm. The demonstrator was operated continuously for five hours and underwent 135 start/stop cycles. This activity was reported in Technical Report AFAPL-TR-73-56 dated June 1973.

In another follow-on effort, the program objective was to extend and demonstrate the state-of-the-art of gas-lubricated, compliant surface foil bearings to 1000 to 3000-pound thrust class full scale turbomachine requirements and constraints. The analytical, material development and test results in both thrust and journal foil bearings on this program are described in Technical Report AFAPL-TR-76-114.

Other foil bearing application and demonstration vehicles are tabulated in Table 1.

2. PROGRAM OBJECTIVES

The primary program objective was to develop a compliant gas-lubricated foil bearing of an advanced design to meet the applied load requirement of the TJE331-1029 when subjected to MIL-E-5007D maneuver loads. Secondary goals were to demonstrate bearing operational capability at component maximum temperatures to 1200°F, low starting torque, and repeated start/stop capability. The total program effort comprised design, fabrication, and rig development-testing of a 3.5-inch advanced, gas-lubricated journal foil bearing for application to a gas turbine engine rated at approximately 750 pounds thrust.

TABLE 1. FOIL BEARING APPLICATIONS

	Shaft Speed (Nom) rpm x 100	Rotor Weight (lb)	Rotor Polar Moment of Inertia (in-lb/sec ²)	Journal Foil Bearings (quantity)	Thrust Foil Bearings (quantity)	Gas Temperature to Foils (°F)	Process Fluid Temperature (°F)
Miniature Turbo- alternator	350	0.222	--	2 (Conical)		-370	-380
Nitrogen Compressor	135	1.85	--	2	2	220	300
C5A Tire Pump Turbocompressor	96	2.6	--	2	2 Hydrost	450	600
F-4 Cooling Turbine	74	2.85	--	2	2 Hydrost	350	800
Helium Gas Bearing Compressor	85	3.0	--	2	2	150	300
727 Cooling Turbine	76	2.9	--	2	2	375	850
Waste Heat Vapor- Cycle Refrigeration Turbo Compressor	52	3.8	--	2	2 Hydrost	150	325
JFSL100 Foil Bearing Demonstration	72	4.9	0.013	2	2	350	1500
Brayton Cycle Space	48	7.5	0.0098	2	2	N/A	1550
DC-10 3-Wheel, Air Cycle Machine	46	8.0	0.062	2	2	400	800
GTP30 Gas Turbine	38	13.5	--	2	2	N/A	1350
Nuclear Brayton TAC	24	152	1.746	2	2	350	1550

3. PROGRAM APPROACH

The program approach was to:

- o Establish the loads imposed on the journal and thrust bearings by the selected turbomachine rotor
- o Apply existing analytical design tools for bearing development and for the proper application of these bearings to a 750-pound thrust turbomachine
- o Design, fabricate and develop a journal bearing test rig for baseline bearing testing and development to meet the selected turbomachine requirements, while subjected to MIL-E-5007D maneuver loads
- o Select a base material and coatings with a thermal capability of 1200°F, based on previous data and experience. Kaman coatings DES and SCA were two coatings tested
- o Conduct a bearing development program with the support of analytical tools. Development activities goal was to achieve the load capacity, high-temperature operation, and other turbomachine application requirements

SECTION II

SUMMARY

The program consisted of the following two major, inter-dependent divisions of effort:

- o Analysis/Design
- o Bearing Development and Testing

Accomplishments within these areas are summarized in the following paragraphs. A summary of program and TJE331-1029 engine requirements and program accomplishments is provided in Table 2.

1. ANALYSIS/DESIGN

During the early stages of the analysis/design portion of the program, thermal and structural isolation requirements necessitated a request for reduced bearing size. This change to the program statement of work was negotiated, resulting in a reduction in bearing size from 4.5 inches to 3.5 inches. Analysis and design continued, based on a 3.5-inch journal diameter. Bearing loads were calculated in accordance with the requirements of MIL-E-5007D.

A rotor dynamics analysis of the TJE331-1029 rotor incorporating a 3.5-inch diameter journal was performed and indicated that the rotating group bending critical occurred at 147 percent of operating speed, a sufficient margin.

The mechanical design objective was to minimize journal radial growth, and achieve acceptable stress levels. A thermal analysis was performed. Modeling was correlated with test data from Contract F33615-78-C-2044. Power dissipation was in the range of 500-1000 watts for steady-state 1-g loads and

TABLE 2. SUMMARY OF REQUIREMENTS AND ACCOMPLISHMENTS

Requirement	Requirement for TJE331-1029 Engine	Basic Bearing Rig	
		Level Achieved	Satisfy TJE331 Requirement
<u>Steady State</u>			
Load (lb)	31	200	Yes
Temperature (°F)*	750	870	Yes
<u>Flight Maneuver</u>			
Load (lb)	410	435	Yes
Temperature (°F)*	750	855	Yes
Duration (sec)	15	30	Yes
<u>Gyroscopic</u>			
Load (lb)	454	490	Yes
Temperature (°F)*	750	900	Yes
Duration (sec)	15	15	Yes
<u>Total Operating Time (hr)</u>	--	30.4	--
<u>Total Starts</u>	--	119	--
<u>Secondary Goal</u> (Operation at 1200°F)			
<u>Steady State</u>			
Load (lb)		150	
Temperature (°F)		1210	
<u>Transient Load</u>			
Load (lb)		410	
Temperature (°F)		1256	

*Estimated turbine end requirement

1500-3000 watts at maximum loads. Thermal analysis was integrated with mechanical design to determine a bearing cooling design compatible with bearing installation in the TJE331-1029.

The 3.5-inch foil bearing design was analyzed using an elasto-hydrodynamic analysis program. Bearing configurations with 10 and 8 foils were identified as having the potential to exceed the performance of the 12-foil GTCPl65 APU bearing.

2. BEARING DEVELOPMENT AND TESTING

The bearing test rig used was the rig designed for the GTCPl65 APU foil bearing program under contract F33615-78-C-2044. Similarity of journal diameters made this possible. All rig mechanical parts were the same except for the number of foils used. The test bearing was enclosed in a thermally insulated ambient box allowing testing at temperatures ranging from -65 to 1200°F. Instrumentation was provided to monitor journal and bearing motion and temperatures, friction, load, vibration, and cooling air flows and temperatures. Data was recorded electronically as well as manually.

A total of six bearing configurations were tested, two ambient temperature configurations, using Teflon-S coated foils with a chrome-plated journal, and four with high-temperature foil and journal coatings. The high-temperature bearings used foil coatings Kaman DES, (chemically adherent Cr_2O_3), Kaman DES + Gold Overcoat, Co-20Ni, and TiC, all of which were run with a Kaman SCA (chemically adherent oxide composite ceramic containing Al_2O_3 , SiO_2 and Cr_2O_3) coated journal. Program goals were met with both ambient-temperature bearing configurations and Kaman SCA versus Kaman DES and TiC high-temperature configurations.

A low-temperature bearing journal was instrumented with two pressure probes and two proximity probes for air film pressure

field and thickness measurement. Pressure measurements were successful but film thickness measurements were inconclusive. Sufficient pressure data was generated for correlation with hydrodynamic analysis. Test data and analysis of air film pressures were in reasonable agreement. This portion of testing was limited by the extremely short life span of the pressure and proximity probes.

SECTION III

DISCUSSION

A 4.5-inch diameter journal foil bearing was initially proposed for this program. This size foil bearing and the proposed bearing installation configuration were consistent with those identified under the preceding program (Contract F33615-73-C-2058). Subsequently, design and analysis conducted on the ongoing "APU Gas-Lubricated Foil Turbine End Bearing Development Program" (Contract F33615-78-C-2044) emphasized the necessity for adhering to certain foil bearing installation considerations. Structural and thermal isolation of the foil bearing in the engine installation are key considerations for maintaining dimensional control of bearing components, which is required for successful bearing operation in the engine. The TJE331-1029 foil bearing installation proposed under Contract F33615-73-C-2058 did not incorporate the features subsequently developed for the GTCPl65 APU foil bearing installation. Reevaluation of the proposed TJE331-1029 engine foil bearing installation relative to mounting and thermal considerations initiated a review of the bearing design for the TJE331-1029 engine.

As a result of this reevaluation, a revised foil journal bearing and installation configuration were identified. The revised TJE331-1029 engine foil bearing application incorporates the latest installation considerations from the GTCPl65 APU application, and has a journal diameter of 3.5 inches, instead of the proposed 4.5-inch diameter journal.

1. ENGINE CHARACTERISTICS

The TJE331-1029 engine (the foil bearing version of the ETJ341-P1) was selected as the vehicle for the application of foil bearings. Specific advantages achieved by selecting this turbomachine are as follows:

- o The selected configuration is a high technology turbomachine, representative of that required for future advanced cruise missile or remotely piloted vehicle applications. Also, final demonstration of the bearing system in this turbomachine would provide a firm basis for a near-term flight test of the same machine in several potential flight test vehicles
- o The selected turbomachine has excellent operational and production potential:
 - The selected turbomachine is an advanced technology design. Low-cost engine design studies performed by Garrett¹ under contract to the U.S. Air Force showed that turbomachinery design configurations similar to that proposed for use in this program will be required for future applications; i.e., all-axial aerodynamic components
 - Turbine inlet temperatures are representative of the state of the art (1700 to 1900°F) for this type of application

2. ANALYSIS/DESIGN

a. Mechanical

(1) Design Considerations

Dimensional control of bearing components is an essential consideration in the application of foil bearings. The

¹Six, L.D., F.W. Lewis, and C.S. Stone, Low Cost, Limited Life Turbine Engine Analysis, AFAPL-TR-71-102, January 19, 1972.

annular dimension between the foil bearing journal and bearing housing inside surface is a crucial design parameter. This dimension, when combined with each foil and backing spring thickness, is commonly referred to as "sway space". The first order importance of sway space on bearing performance necessitates that it be controlled within acceptable limits throughout the spectrum of operating conditions. The sway-space value at any operating condition is governed by bearing assembly dimensions, the respective operating temperatures of the bearing housing and journal, and the journal centrifugal growth. If the sway space is diminished due to a combination of these influences, the gas-film load that must be withstood by each foil increases, as does bearing power consumption. Net bearing load capacity is reduced, and bearing failure due to thermal overloading can result. The other extreme of excessive sway space can result in unacceptably large rotor radial excursions when accelerating through critical speeds, as well as increased susceptibility to self-excited whirl instability. The latter also can result in bearing failure. To preserve bearing operation within acceptable sway-space limits, it is necessary that:

- o Differential dimensional changes be minimized
- o Dimensional changes be defined and controlled through analytical design

Both requirements are best served if bearing housing thermal and structural isolation is maximized with respect to the external environment, so that bearing housing operating temperatures are governed largely by those of the bearing journal. In addition, structural isolation permits bearing housing operating temperatures to be distinctly different from those of the parent supporting structure, in the absence of significant thermally induced stresses and attendant housing distortions.

Consistent with the need to properly control sway space is the requirement for axial dimensional control of the bearing journal and housing. Minimum gas-film thicknesses of the order of 10^{-4} inch are realistic for foil bearings; thus, the effective axial length of the bearing is exploited only if axial dimensional variations are properly controlled. This requirement also is favored by thermal and structural isolation of the bearing housing.

First order concern also must be given to journal dimensional changes due to centrifugal and thermal effects. The severity of the bearing differential radial and axial dimensional control problems and external cooling design vary directly with the bearing power generation. To a first approximation, bearing power varies directly with (diameter)³ and linearly with bearing axial length for constant annular speed. Similarly, journal centrifugal stress and deflection vary directly with (diameter)² for constant annular speed.

(2) Envelope Constraint

The existing space envelopes to accommodate the foil journal bearing in the TJE331-1029 engine (Figure 3) are:

- o Bounded diametrically by the compressor inlet flow path at the engine front end
- o Bounded by the combustion system inlet transition member and combustion system at the turbine end

These constraints result in a diameter slightly greater than 4.5 inches into which the overall bearing system must be integrated. There is an axial dimension limitation at the turbine end, but it is less severe than the turbine end diametral limitation.

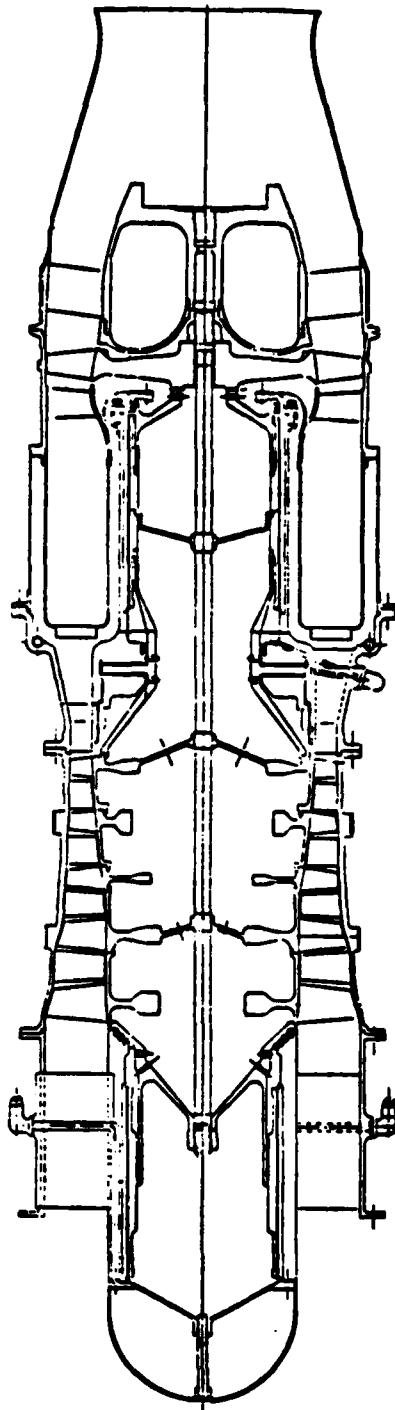


Figure 3. TJE331-1029 Thrust Engine 4.5-Inch Diameter Journal.

(3) 4.5-Inch Diameter Journal Installation

Figure 4 shows additional details of the originally proposed conceptual arrangement of a 4.5-inch diameter by 6.0-inch long journal foil bearing in the TJE331-1029 turbine end cavity. This installation was characterized by:

- o A bearing housing structurally integral to the engine support structure

This basic mounting arrangement provides virtually no thermal or structural isolation of the bearing housing.

- o A maximum available bearing housing thickness of approximately 0.28 inch. (The foil locating slots also must be cut into this housing thickness. Simply stated, this bearing housing is unacceptably thin.)

- o Limited bearing cooling design alternatives

(4) 3.5-Inch Diameter Journal Installation

Figure 5 shows the details of a conceptual arrangement of a 3.5-inch diameter by 4.2-inch long journal foil bearing in the TJE331-1029 turbine end cavity. This installation is characterized by:

- o A bearing housing installation incorporating the present design approach to structural and thermal isolation

The bearing housing is structurally tied to the neighboring static member by a number of beams. Each beam is designed to be highly flexible about one transverse axis and relatively stiff about the orthogonal transverse axis. These axes are oriented so that

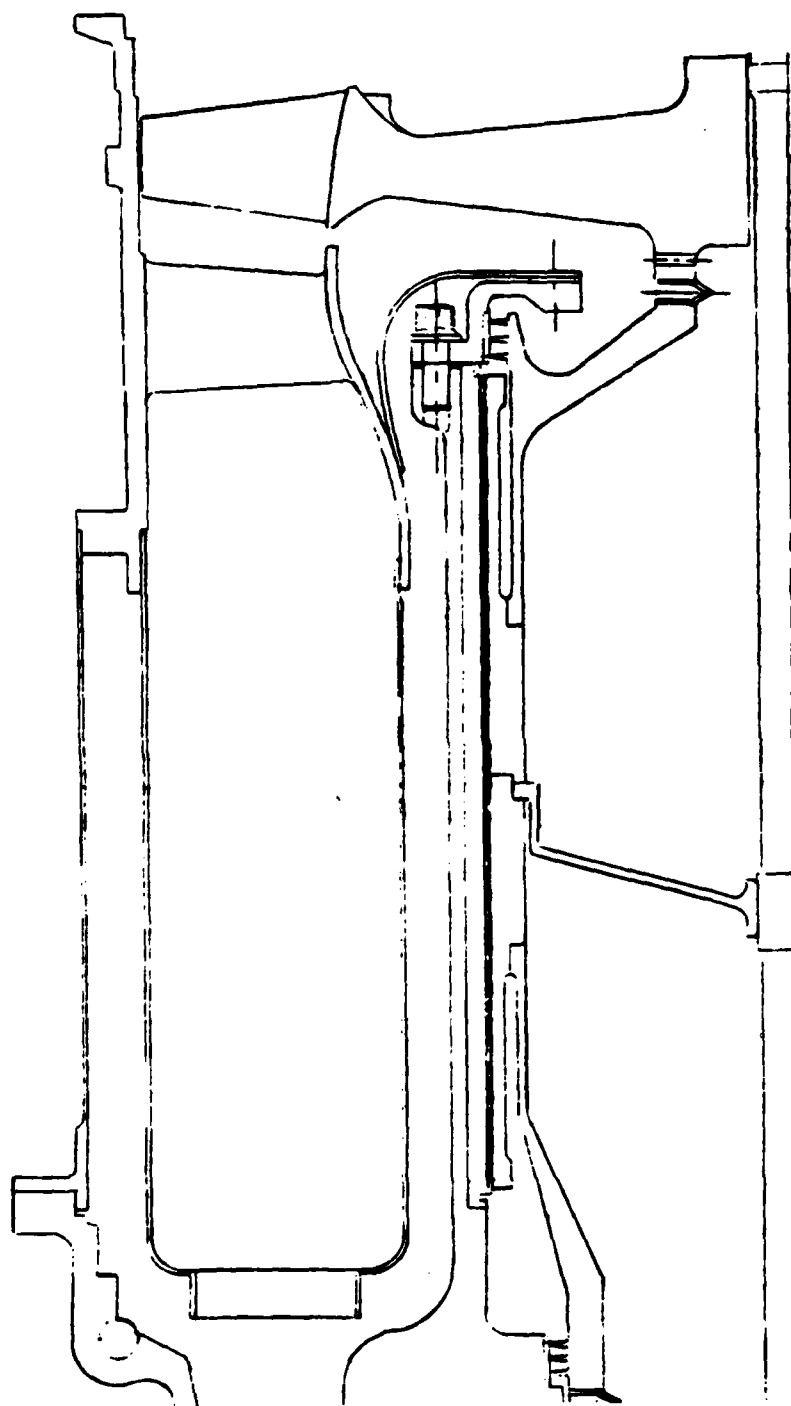


Figure 4. TJE331-1029 Turbine End Foil Bearing, 4.5-Inch Journal.

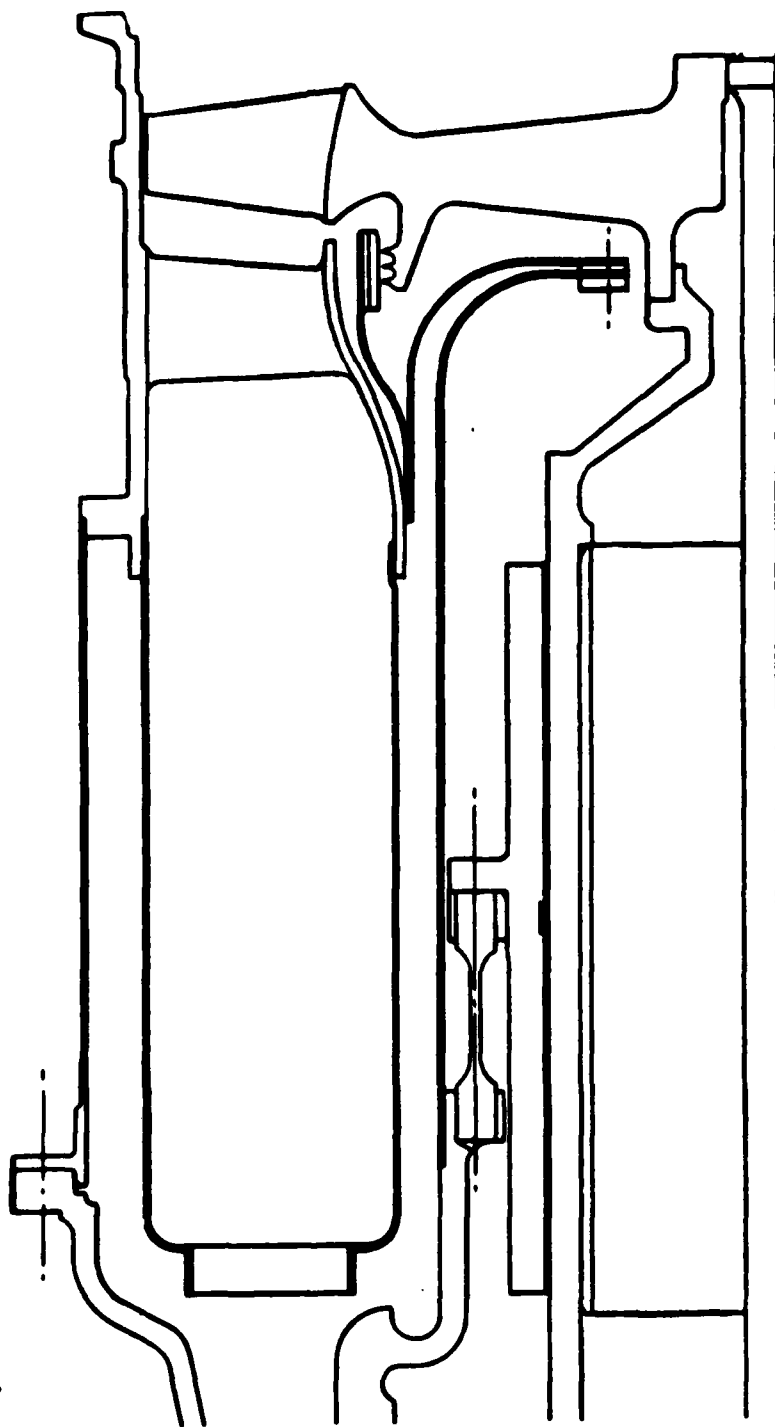


Figure 5. TJE331-1029 Turbine End Foil Bearing, 3.5-Inch Diameter Journal.

radial dimensional changes of the housing with respect to the adjacent structure are accommodated by the high flexibility of each beam. On the other hand, net bearing loads are reacted by bending and shear loads directed about the stiff transverse axis of a number of the beams. The local beams also provide a weak thermal conductance avenue. Because the housing external surfaces are wetted by virtually stagnant air, the housing is thermally well isolated from the external environment

- o A bearing housing of sufficient thickness to accept the foil mounting slots and maintain dimensional stability under thermal transients
- o A bearing cooling flow path incorporating mid-bearing span cooling air introduction

The 3.5-inch journal diameter bearing design accommodates the design considerations described in Section 2.1.1. The 3.5-inch diameter journal is nominally the maximum diameter that can be incorporated, within the diametral constraints imposed by the TJE331-1029 installation, and maintain the desired design approach of structural and thermal isolation from the hot structure. An overall view of the TJE331-1029 engine incorporating the 3.5-inch journal diameter foil bearings is presented in Figure 6.

(5) Foil Bearing Loads

The requirements to be met by the bearings in the TJE331-1029 thrust engine program are defined in accordance with MIL-E-5007D (Figure 7). The existing TJE331-1029 engine incorporates a cast steel compressor, principally for cost purposes.

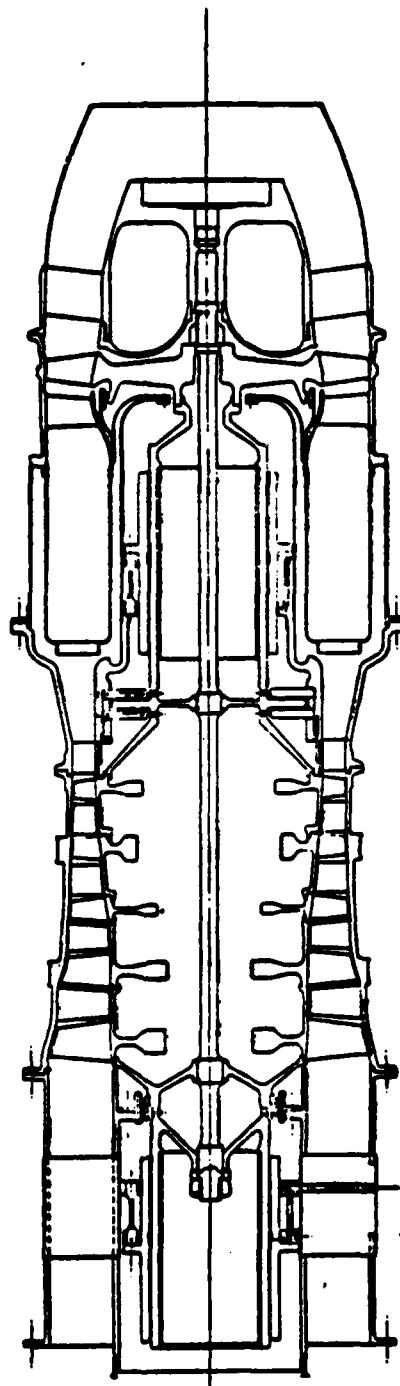


Figure 6. TJE331-1029 Thrust Engine, 3.5-Inch Diameter Journal.

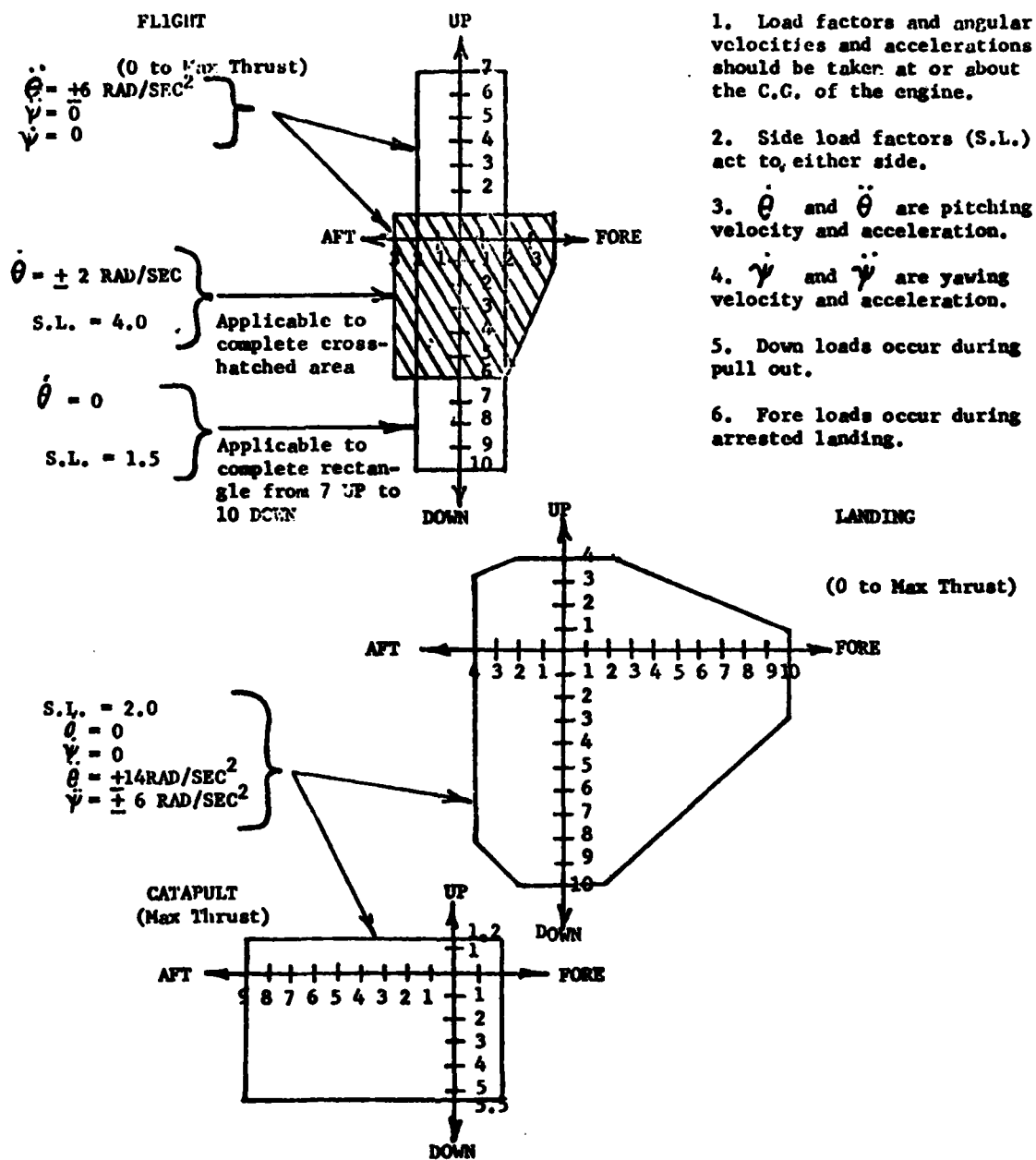


Figure 7. Flight Maneuver Load Diagrams (MIL-E-5007D).

Table 3 lists the rotor system parameters and limiting case load requirements for foil bearings applied to this reference engine.

(6) Rotor Dynamics

A rotor dynamics analysis of the TJE331-1029 rotor incorporating the 3.5-inch journal was performed. The analysis showed that this rotating group bending critical has more than a 40-percent margin, which is sufficient to assure satisfactory operation at maximum operating speed.

The first three critical speeds are shown in Figure 8 as a function of foil bearing spring rate for a 3.5-inch journal. The first two criticals are rigid body modes. The bending critical for a 3.5-journal (20,000 lb/in spring rate) occurs at about 147-percent speed. Margin above maximum operating speed for a 3.5-inch journal rotating group is satisfactory.

(7) Journal Mechanical Design

The primary objective of the journal design was to minimize axial variation in radial growth in the 4.2-inch long bearing region. Stress levels had to be acceptable as well.

The journal is axisymmetric and was therefore modeled using a two-dimensional finite-element stress analysis program. A typical finite-element grid is shown in Figure 9. The particular configuration shown includes a 0.10-inch thick copper shunt brazed to the journal inside diameter. To be conservative, the copper was assumed to have no hoop strength of its own, which will give growths and stresses in the journal that will be slightly higher than actual. The journal material is IN718.

TABLE 3. ROTOR SYSTEM PARAMETERS AND LIMITING
CASE BEARING LOADS

<u>TJE331-1029</u>	
Rotor Parameter (Steel Compressor)	
Rotor Weight (lb)	50.5
Design speed (rpm)	33,200
Bearing Diameter (in)	3.5
Polar Moment of Inertia (in-lb/sec ²)	0.71
<u>Bearing Loads (Turbine End)</u>	
1-g (lbs)	31.0
Flight Maneuver (lb)*	410
Gyroscopic-3.5 rad/sec plus 1-g (lb)	454 (15 sec)

*Limiting Flight Maneuver Conditions:

- o TJE331-1029 (per MIL-E-5007D)
2 rad/sec pitch at design speed, combined with 6-g down and 4-g sideload
- o GTCPl65 (per MIL-P-8686)
2 rad/sec pitch at design speed, combined with 6-g down and 1.5-g sideload
- o Flight maneuver and gyroscopic conditions not required to have 1.5 factor on loads

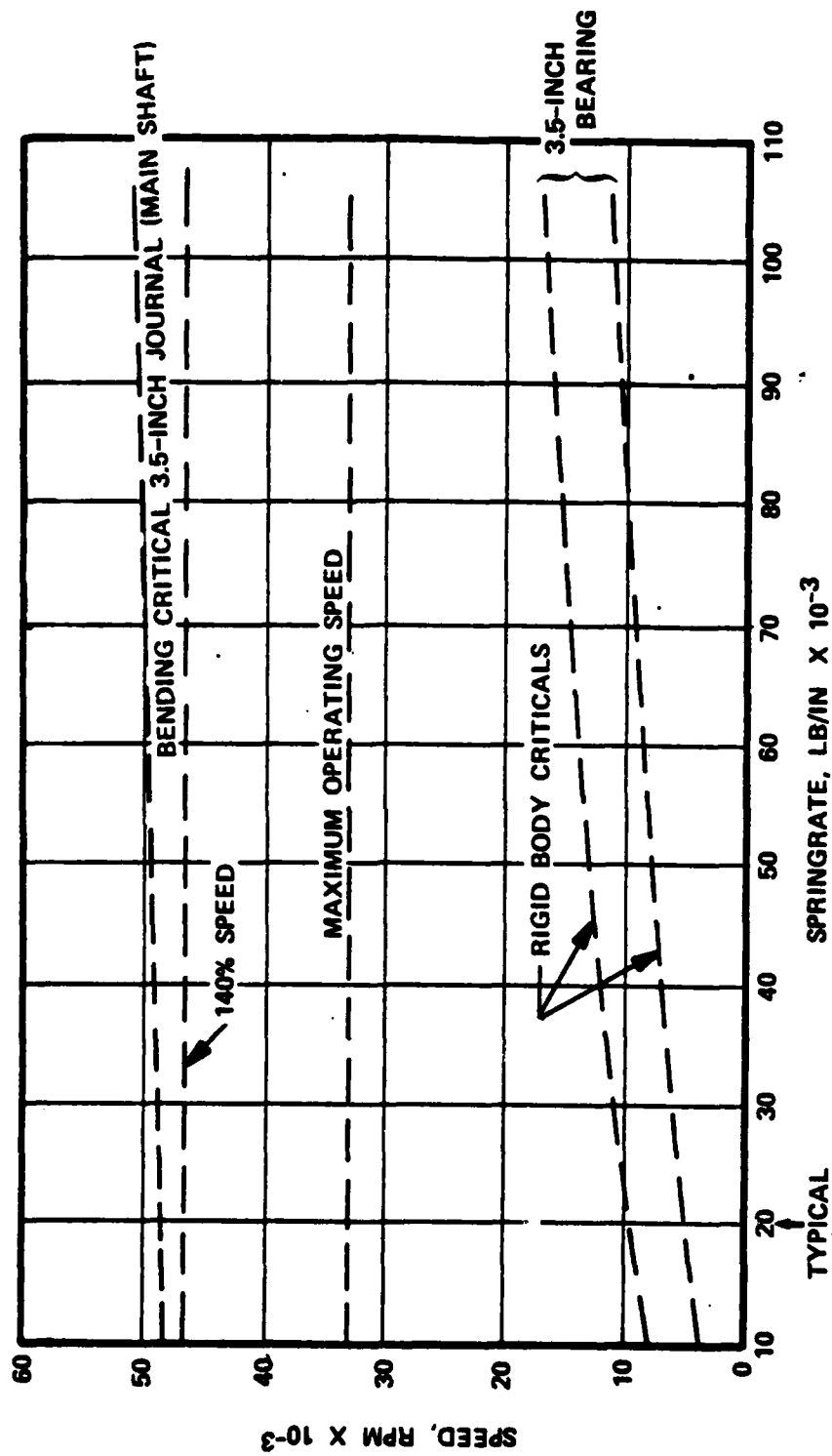


Figure 8. Critical Speed vs Bearing Spring Rate For TJE331-1029 with 3.5-Inch Journal Foil Bearings

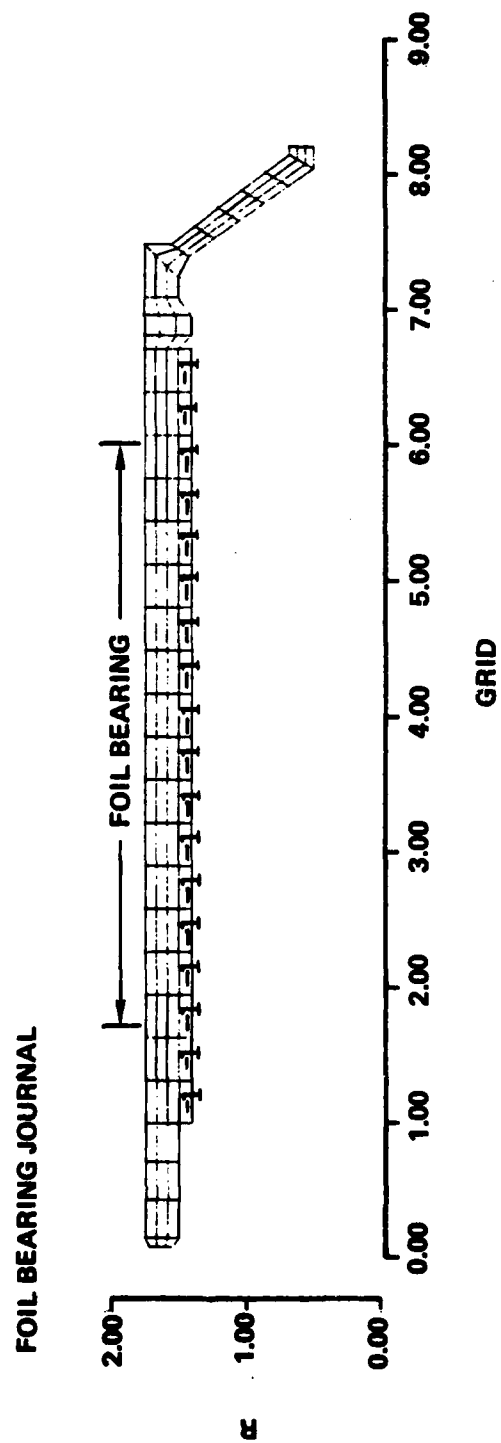


Figure 9. Journal Finite-Element Stress Grid.

Stress and displacement plots for this configuration are shown in Figure 10 for centrifugal load only. Values for the journal without a copper shunt are included in parenthesis for reference. Maximum effective stress in the journal is 36 ksi with, and 28 ksi without the copper shunt. The average journal radial centrifugal growth at the foil bearing is 0.00165 inch with an axial variation of 0.00005 inch, with the copper shunt as dead weight. Without the shunt, the average radial growth is 0.00129 inch with an axial variation of 0.00003 inch.

The copper shunt may or may not be required for controlling thermal distortions, but its influence on the centrifugal growths has been negligible.

The influence of an axial tieshaft load of 16,000 pounds also was considered and the displacements are shown in Figure 11. The average centrifugal growth increases to 0.00172 inch but the axial variation of the growth at the bearing is still very low at 0.00007 inch.

Some additional work was done to lower stresses at the journal turbine end inner diameter. A small modification was made to the journal design at the turbine attachment end to obtain acceptable stress levels under the centrifugal load plus 16,000 pound tieshaft load. The inner cylinder adjacent to the curvic was lengthened and fillet radii were increased.

The resulting stresses and displacements under the combined centrifugal-tieshaft loadings are pictured in Figure 12. Displacements of the journal outer cylinder essentially were as shown in Figure 11. Displacements in the turbine end curvic area were more favorable than previously experienced. The axial variation in radial growth of the journal cylinder was low at 0.00007 inch. The maximum effective stress was 53 ksi at the

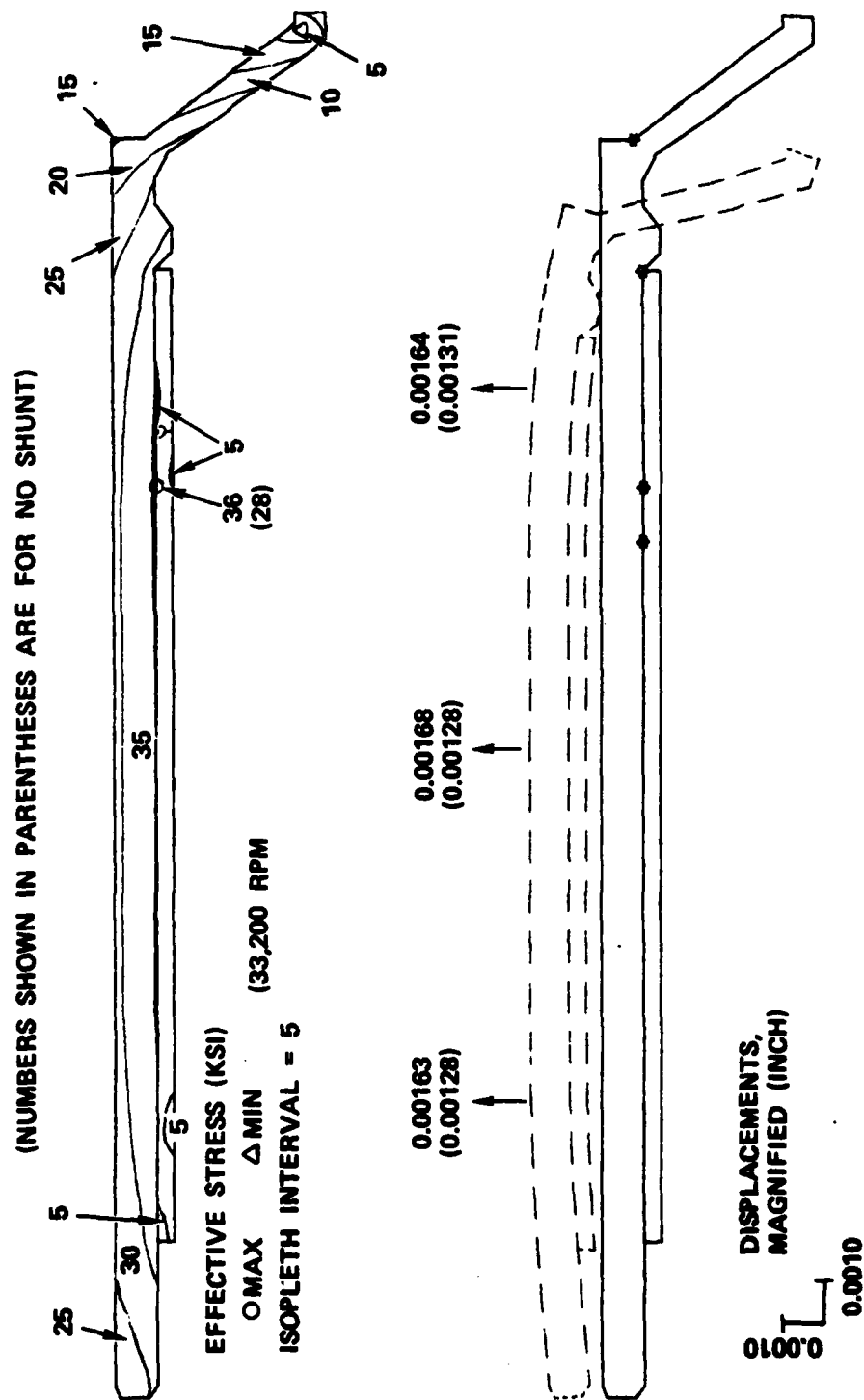


Figure 10. Journal Stress/Displacement Under Centrifugal Load Including 0.1 Inch Copper Shunt.

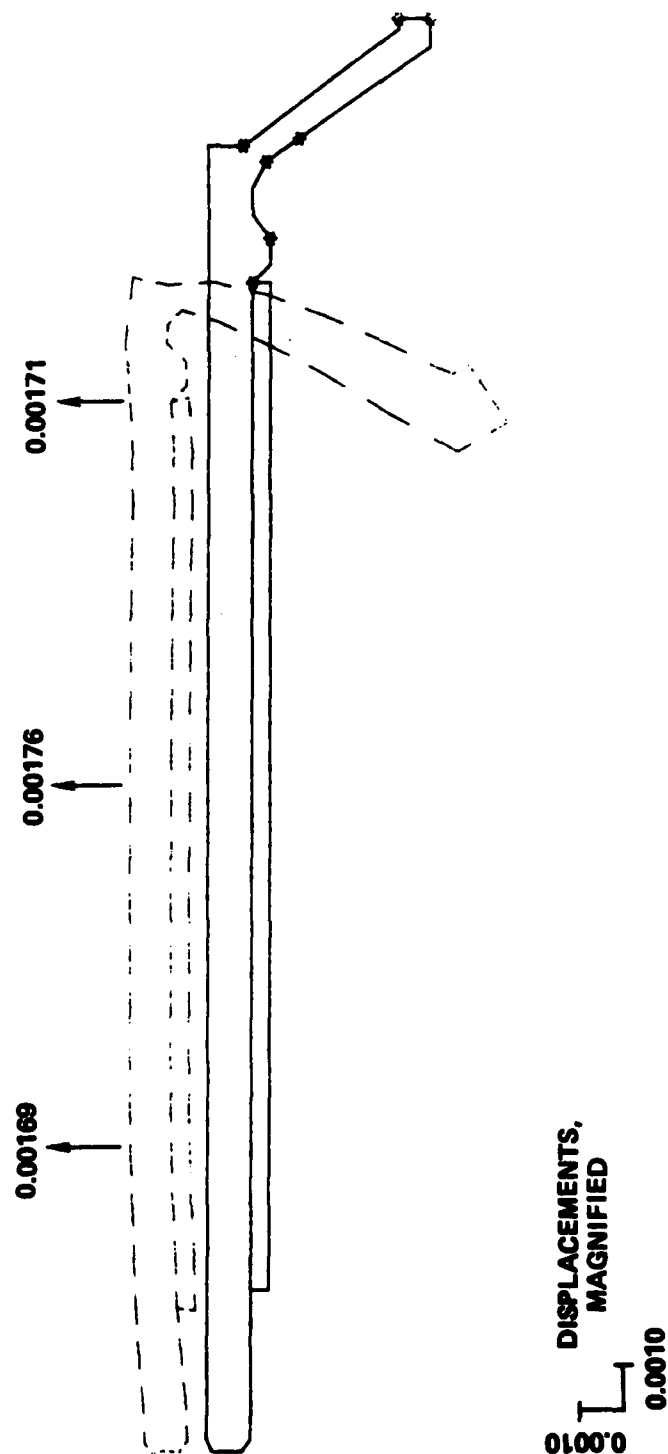


Figure 11. Journal Displacement Under Centrifugal Load Plus
16,000 Lb Tie-Shaft Load.

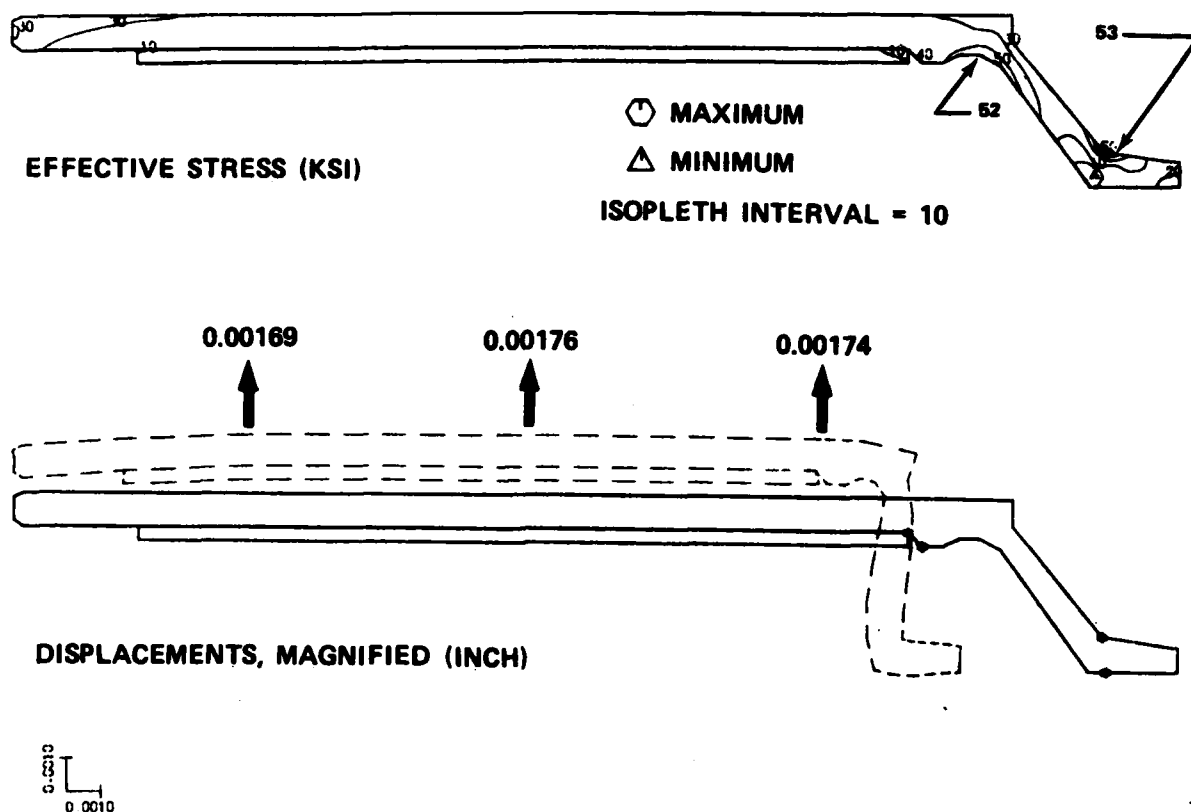


Figure 12. Journal Stress and Displacement Under Combined Centrifugal and Tieshaft Loads.

turbine end of the journal. This stress level is 40 percent of IN718 yield strength at 100°F, and provides for a creep life of about 10^6 hours at that temperature. Stress results are summarized in Table 4.

b. Thermal Design/Analysis

The engine thermal model reflects a bearing length of 4.2 inches and is shown in Figure 13. (Thermal analyses also were conducted on longer journal axial length bearings.) The thermal analysis was run using this model, with a 0.05-inch copper shunt and a friction heat generation rate of 500 watts. Journal, housing, and foil mid-point temperatures are plotted as a function of cooling flow rate in Figure 14. The influence of the copper shunt is pictured in Figure 15 for 500 watts, 0.01 lb/sec at 500°F. A 0.05-inch thick copper shunt is compared with no shunt.

Bearing performance will be influenced most by axial variation in sway space (or the net diametral growth) between journal and housing. The design goal is to minimize this axial distortion since it reduces the effective bearing length and consequent load capacity. For centrifugal loading, only the journal changes shape, and the axial distortion, as reported above, will be less than 0.0001 inch. However, Figure 16 shows that thermal distortions will dominate. The data of Figure 16 depicts the influence of various parameters. Note that axial distortions due to thermal effects range from 0.001 to 0.0002 inch, which exceed the centrifugal distortion above.

c. Integrated Mechanical-Thermal Design/Analysis

The following discussion integrates thermal effects with centrifugal effects for a total effect on bearing sway space. Figures 17 and 18 present foil bearing thermal response

**TABLE 4. FOIL BEARING JOURNAL STRESS RESULTS
CENTRIFUGAL (33,200 RPM) AND TIESHAFT
(16,000 LB) LOADS**

Average Tangential Stress	26.7 ksi
Burst Speed	74,700 rpm
Maximum Effective Stress	53.0 ksi
Yield Strength	129 ksi
MS	1.43
0.2 Percent Creep Life	10 ⁶ hours

NOTES:

- (1) Calculations are made for forged IN718 at 1000°F
- (2) MS = Margin-of-Safety = $\frac{\text{allowable}}{\text{actual}} - 1$

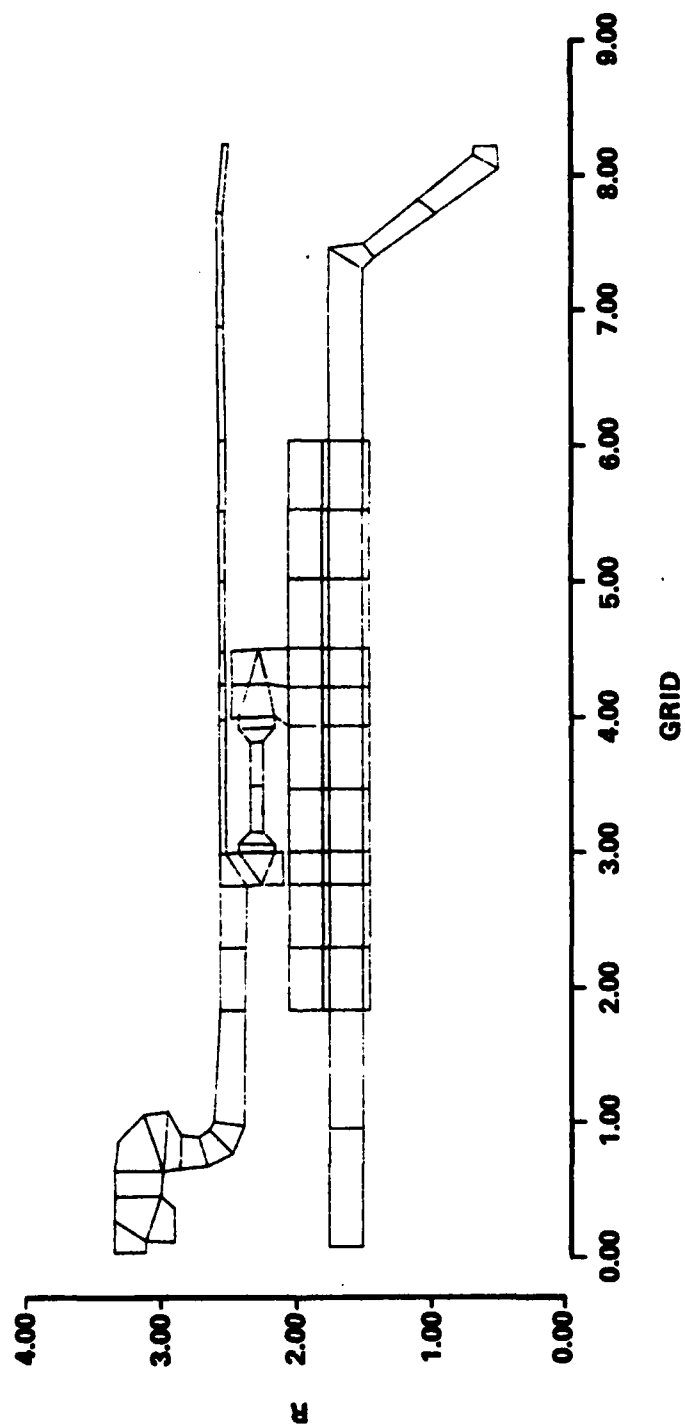


Figure 13. TJE331-1029 Hot End Foil Bearing Thermal Model;
3.5-Inch Diameter, 4.2-Inch Length Bearing.

NOTE: TEMPERATURES SHOWN ARE AT BEARING MID-POINT LOCATION

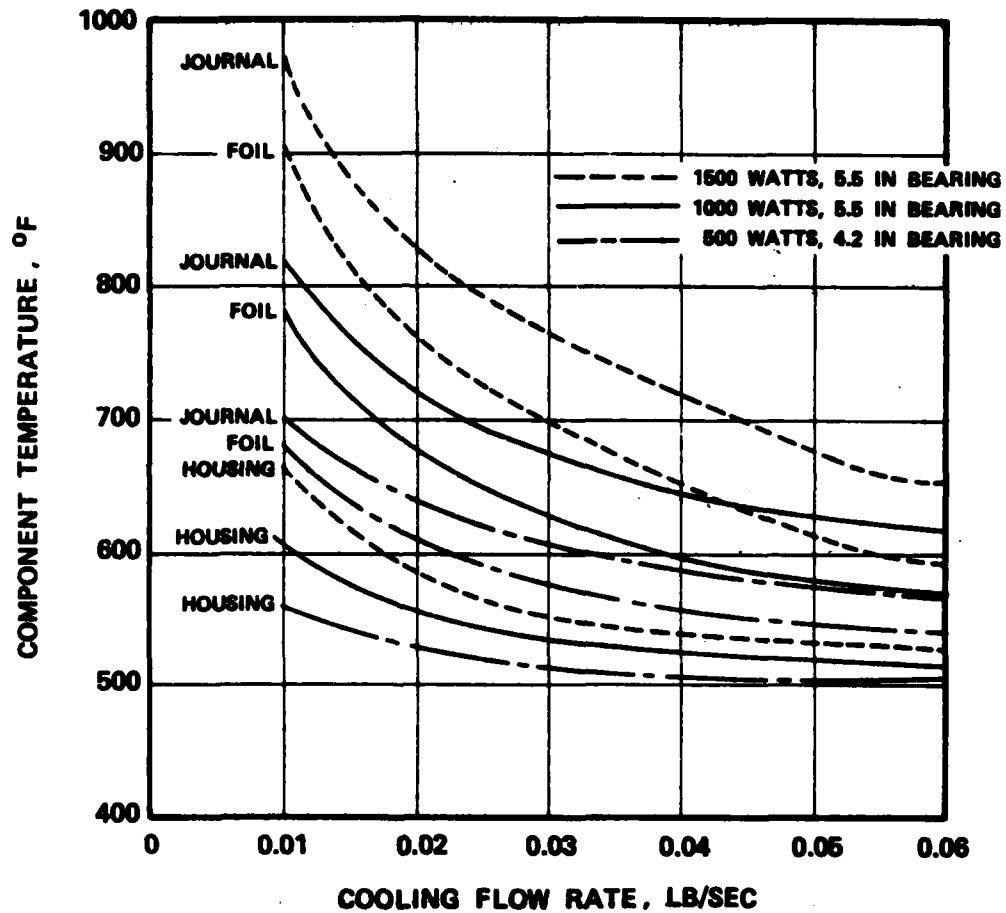


Figure 14. Effect of Cooling Flow Rate and Heat Generation on Bearing Component Temperatures.

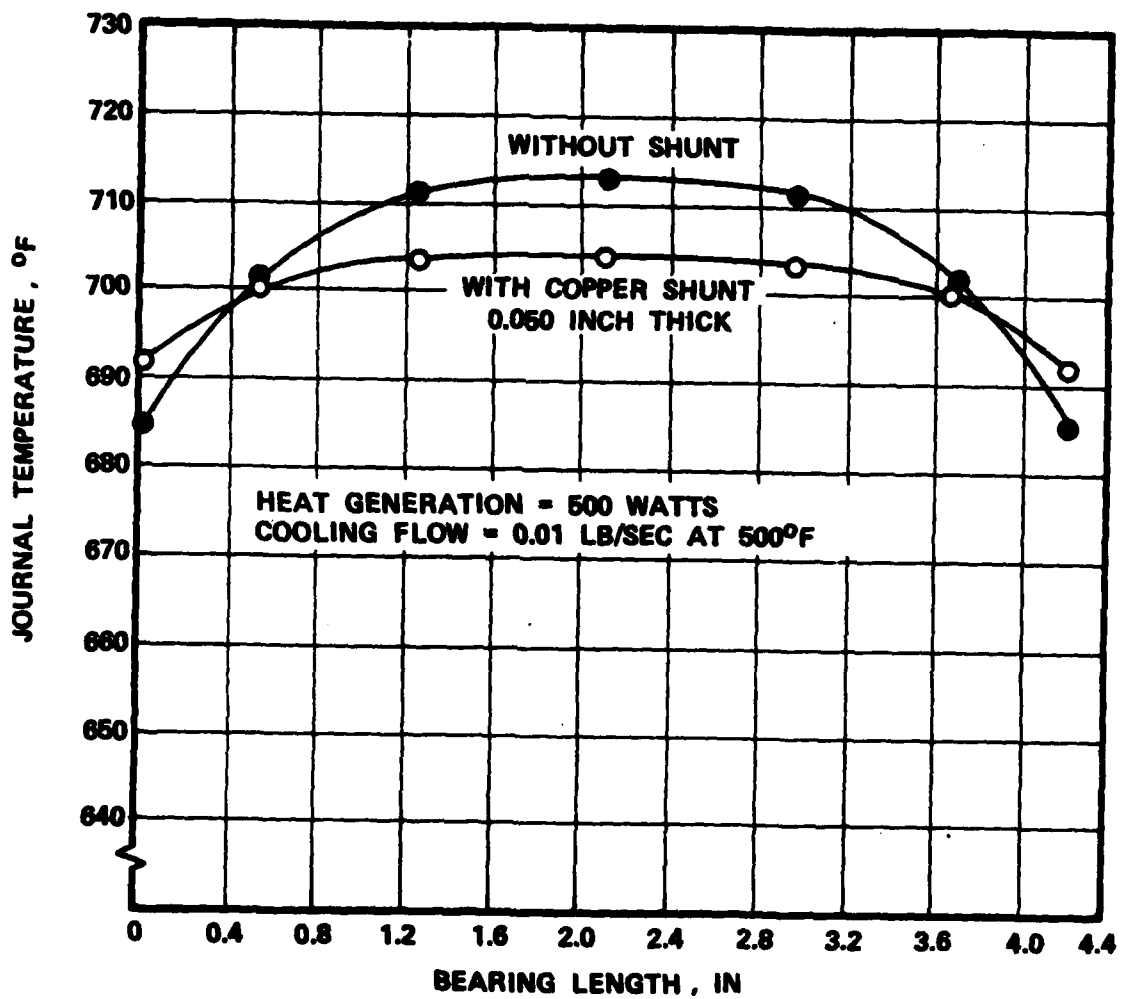


Figure 15. Effect of Copper Thermal Shunt Thickness on Foil Bearing Journal Axial Temperature Distribution.

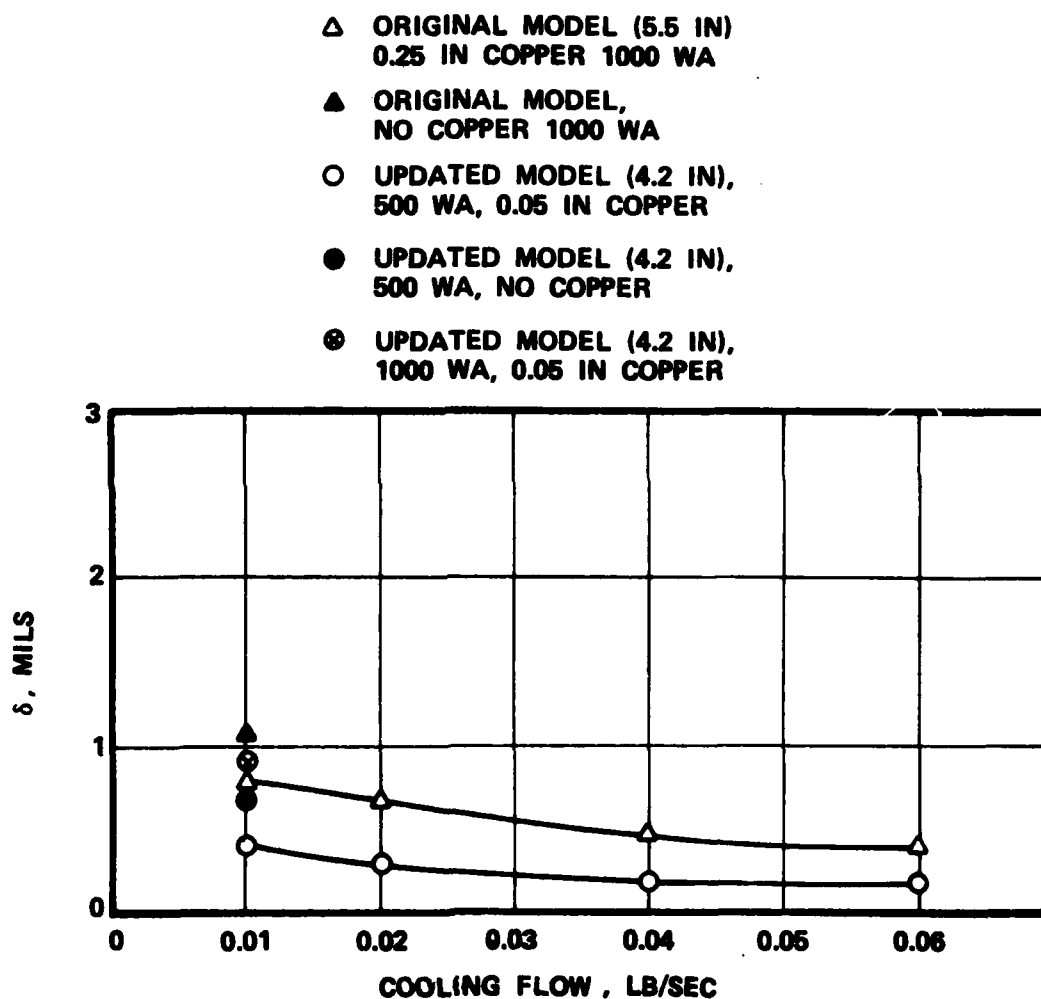


Figure 16. Axial Bearing Thermal Distortion for Various Configurations. Variation (δ) in Running Radial Clearance Between Bearing Center and Ends.

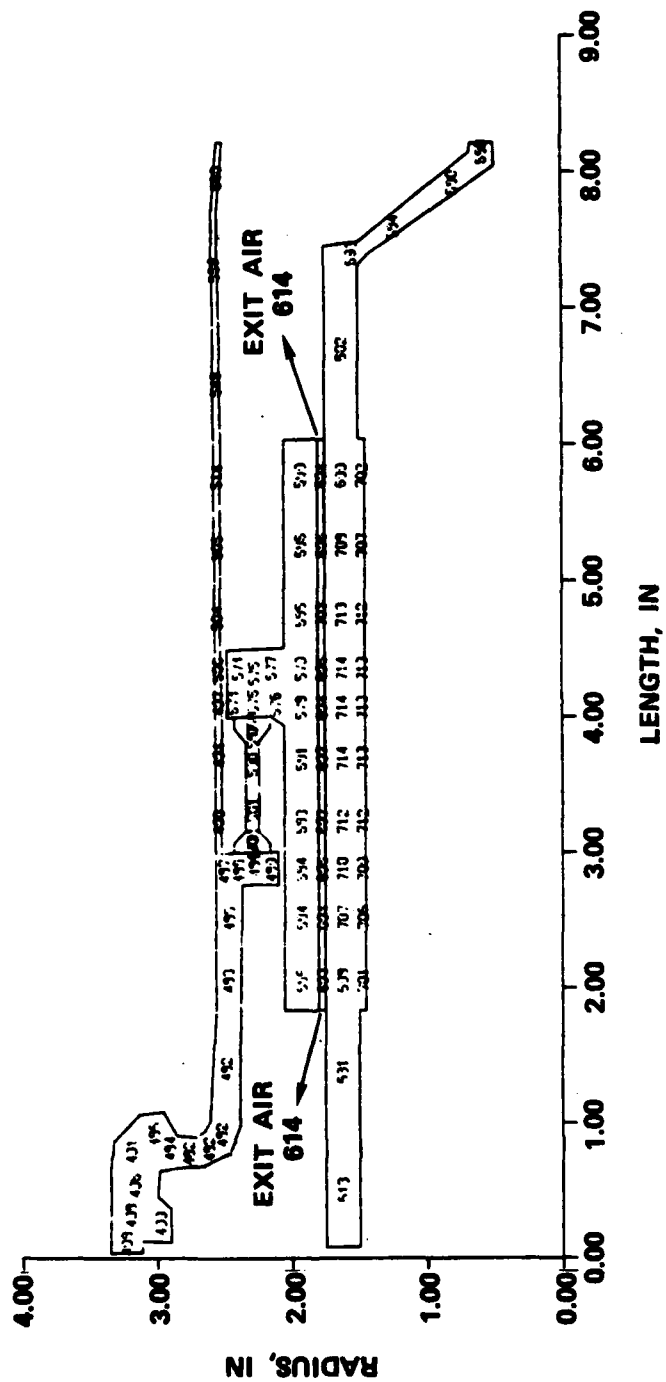


Figure 17. TJE331-1029 Hot End Foil Bearing Thermal Response at 500 Watts Power Dissipation and 0.01 Lbs/Sec Cooling Flow at 500°F Inlet Temperature.

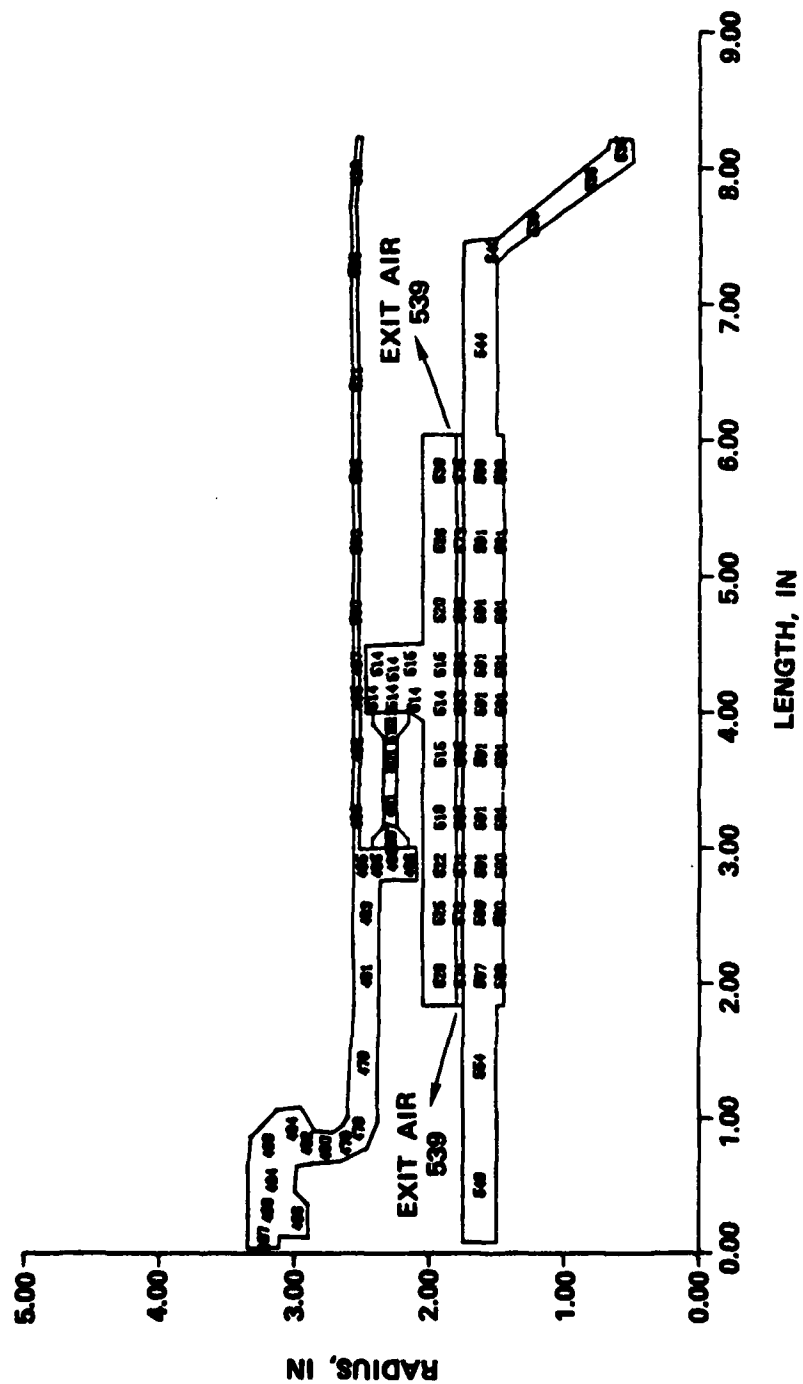


Figure 18. TJE331-1029 Hot End Foil Bearing Thermal Response at 500 Watts Power Dissipation and 0.04 Lbs/Sec Cooling Flow at 500°F Inlet Temperature.

data for 500 watts bearing power dissipation, and a bearing cooling flow of 0.01 and 0.04 lb/sec, respectively. These thermal responses are converted into journal and housing thermal growths. Journal centrifugal growth (adjusted for temperature) is then added to define a net change in sway space, as a function of axial length for the bearing.

Figures 19, 20, and 21 present plots of diametral sway space change as a function of axial length for various conditions. Figure 19 illustrates a diametral sway space change for 500-watts bearing power dissipation, a thermal shunt, and different cooling flows. Figure 20 is for 1000-watts bearing power dissipation, a thermal shunt, and different cooling flows. Figure 21 compares the results of copper shunt utilization with a no-shunt condition for 500-watts bearing power dissipation, and a cooling flow of 0.01 lb/sec.

A comparison of Figures 19 and 20 clearly shows the effects of steady state bearing power dissipation on sway space change. At midspan, the change in sway space is 7.6 mils for 500 watts bearing power dissipation, and 11.2 mils for 1000 watts bearing power dissipation, with a cooling flow of 0.01 lb/sec. Figure 21 illustrates the thermal shunt effect on sway space change. At midspan, the change in sway space is 7.6 mils with the thermal shunt and 7.82 mils without the thermal shunt, with a cooling flow of 0.01 lb/sec and 500-watts bearing power dissipation.

The bearing thermal response was evaluated for a case simulating the application of high maneuver loads. Starting with steady state operation at 1-g loading (500-watts bearing power dissipation, and 0.01 lb/sec bearing cooling flow) the bearing power dissipation was increased as a step function to 2000 watts, while holding the cooling flow constant. After 15 seconds, the journal temperature rose approximately 35 degrees, while the

CONDITIONS

- 1) COOLING FLOW AT 500°F INLET TEMPERATURE:

○	0.01 LB/SEC
●	0.02 LB/SEC
□	0.04 LB/SEC
■	0.06 LB/SEC
△	0.10 LB/SEC
- 2) BEARING POWER DISSIPATION 500 WATTS
- 3) WITH THERMAL SHUNT

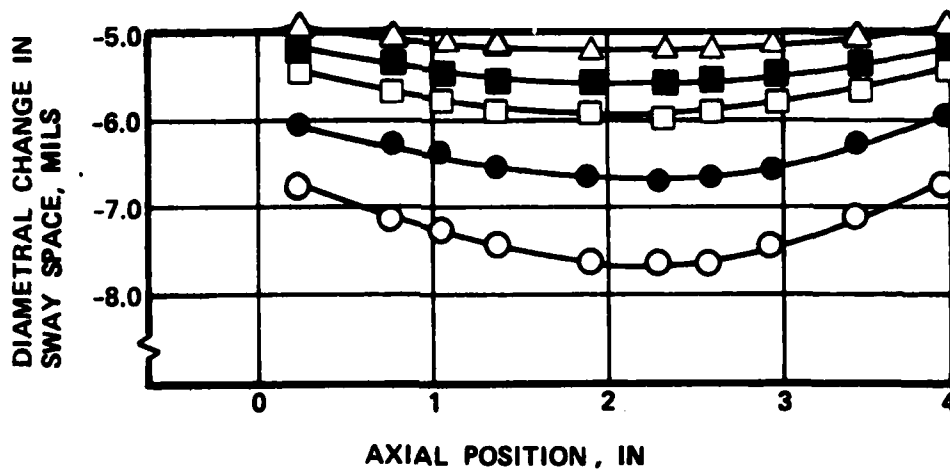


Figure 19. TJE331-1029 Hot End Foil Bearing Diametral Change in Sway Space Due To Combined Thermal and Centrifugal Effects.

CONDITIONS

- 1) COOLING FLOW AT 500°F INLET TEMPERATURE: { ○ 0.01 LB/SEC
□ 0.04 LB/SEC
△ 0.10 LB/SEC
- 2) BEARING POWER DISSIPATION OF 1000 WATTS
- 3) WITH THERMAL SHUNT

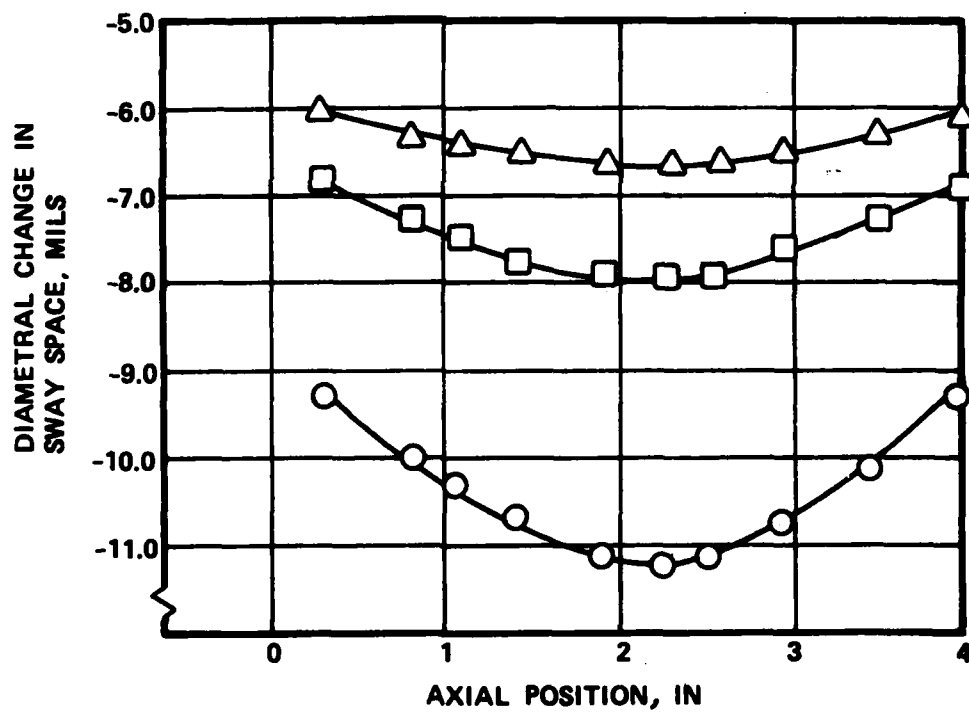


Figure 20. TJE331-1029 Hot End Foil Bearing Diametral Change in Sway Space Due To Combined Thermal and Centrifugal Effects.

CONDITIONS

- 1) COOLING FLOW AT 500°F INLET TEMPERATURE
- 2) COOLING FLOW RATE OF 0.01 LB/SEC
- 3) BEARING POWER DISSIPATION OF 500 WATTS
- 4) ○ WITH COPPER SHUNT (0.05 IN THICK)
● WITHOUT COPPER SHUNT

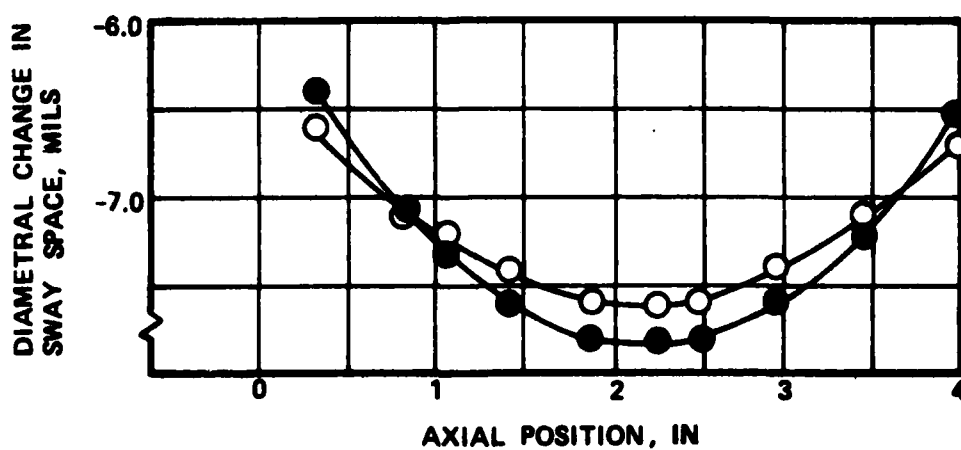


Figure 21. TJE331-1029 Hot End Foil Bearing Diametral Change in Sway Space Due To Combined Thermal and Centrifugal Effects.

housing remained essentially at the same temperature. This temperature difference would result in a diametral sway space loss of approximately 1 mil.

d. Similitude of Data for TJE331-1029 and GTCPl65 Basic Simulator Test Rig Bearings

Testing on the basic bearing rig for this program was conducted utilizing bearing journals from the basic simulator rig for the GTCPl65 APU from Contract F33615-78-C-2044. The operating similitude of the GTCPl65 journals and the TJE331-1029 journals are discussed as follows.

TJE331-1029 journal displacements under combined centrifugal and tieshaft loads are presented in Figure 12. Centrifugal stress in the GTCPl65 basic simulator journal is shown in Figure 22. Displacements of the solid web GTCPl65 journal under centrifugal loads is presented in Table 5. Comparison of this data shows that both the level of displacement and the axial variation of these displacements are similar for these two journals. The thermal responses (hence, the thermal growths) of the two bearings also are similar, as shown in Figure 23. Foil carrier and housing temperatures are almost the same in each case. TJE331-1029 journal temperature levels are slightly lower than those of the GTCPl65 basic simulator journal, but a small change in build sway space can compensate for these differences. Overall, the operating similitude of these two bearings was clearly established.

e. Alternate Bearing Cooling Designs

Test runs on the basic simulator test rig from Contract F33615-78-C-2044 clearly indicated that both the bearing power absorption and journal temperatures rose during even short-duration loads above the bearing normal 1-g operating condition. The potential for increased bearing cooling effectiveness via

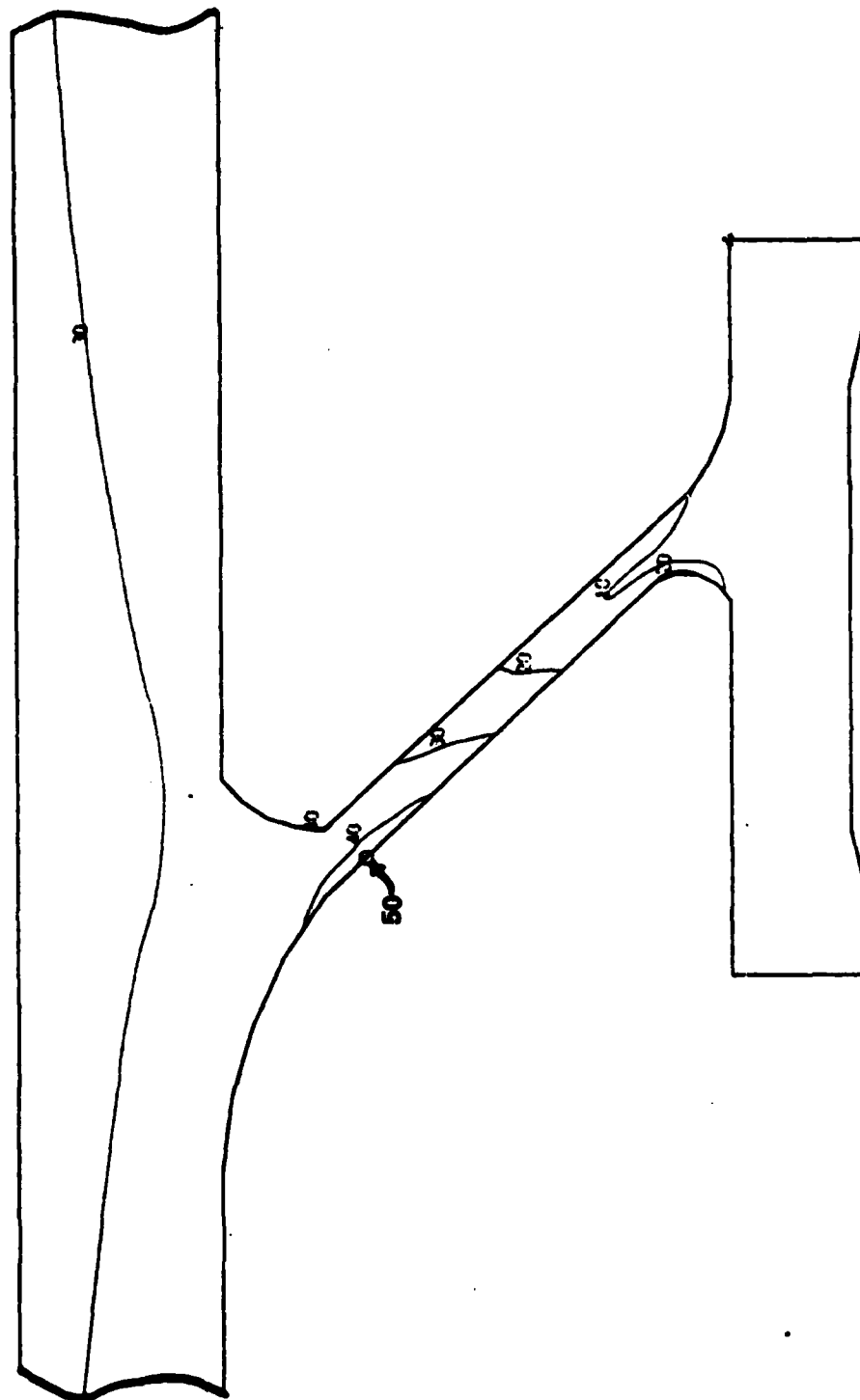


Figure 22. Solid-Web Journal Centrifugal Stress (ksi) 38,800 rpm.

**TABLE 5. SOLID WEB GTCPI65 JOURNAL STRESS
AND DISPLACEMENTS**

Parameter	Units	Solid Web
Peak Web Effective Stress	ksi	50
End Radial Displacement	in	0.00166
Center* Radial Displacement	in	0.00151

*Where web joins to outer cylinder

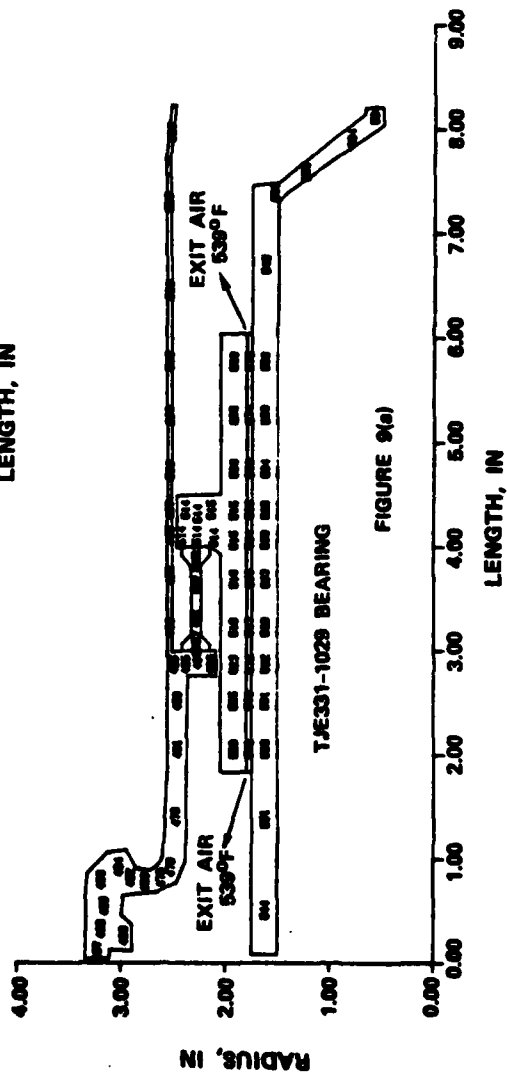
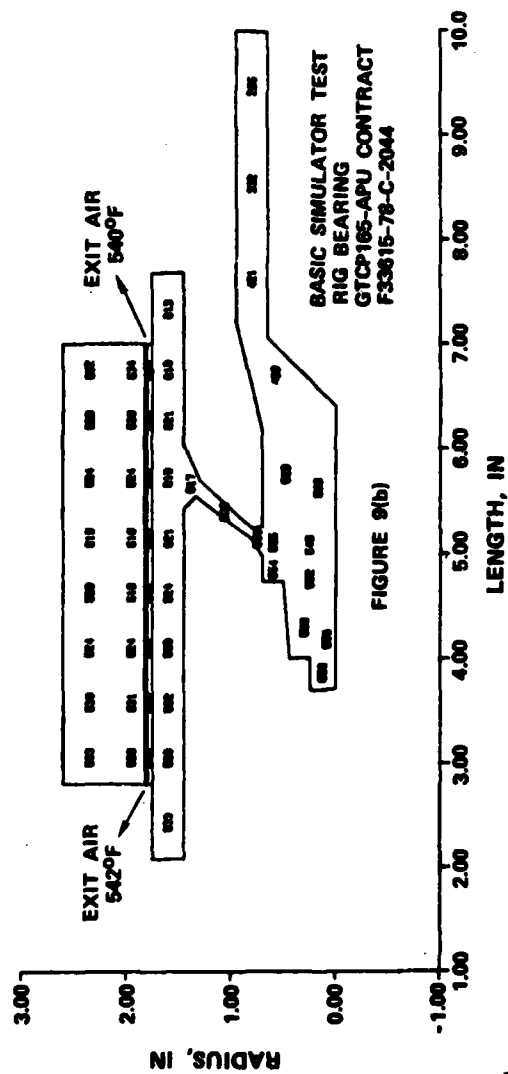


Figure 23. Foil Bearing Thermal Responses With 500 Watt Bearing Power Dissipation and 0.04 lbs/sec Cooling Flow at 500°F Inlet Temperature.

multiple axial cooling air entry positions was evaluated. Figure 24 is a sketch of the TJE331-1029 hot end foil bearing installation, locating the three different axial cooling flow entry positions on the bearing at $1/4 L$, $1/2 L$, and $3/4 L$, where "L" is the bearing length. Flows W_{C2} and W_{C3} enter the bearing at $1/2 L$; flows W_{C1} and W_{C2} are assumed to flow axially forward through the bearing; flows W_{C3} and W_{C4} are assumed to flow axially rearward through the bearing.

Bearing thermal response was calculated for several cooling flow distributions (cataloged in Table 6). The baseline single-entry cooling distribution is identified as Configuration 1. Figure 18 presents bearing thermal response to the baseline cooling Configuration 1. Bearing thermal response to the Configuration 2 cooling flow distribution is presented in Figure 25. A comparison of Figures 18 and 25 indicates that temperature distribution variations are quite small, with the largest differences at the bearing mid-position. These temperature distribution variations are converted to sway space changes in Figure 26. The overall loss in sway space is slightly less for Configuration 2 than for Configuration 1, but the distribution is "wavy", rather than smooth. Configurations 3 and 4 results were similar to Configuration 1, while Configuration 5 resulted in unacceptable axial temperature variations.

To compare the bearing load-carrying capacity for the cases for which data are presented in Figures 19, 20, 21 and 26, a method to quantify the differences was developed. This was done on a relative basis by comparing the estimated load-carrying capacity for each bearing to that of a bearing that undergoes no axial distortion. To calculate this relationship exactly would require a solution of the two-dimensional Reynold's equation coupled with a three-dimensional elastic model of the foils, which is not a practical procedure. However, the pressure developed in the bearing is inversely related to some power of the

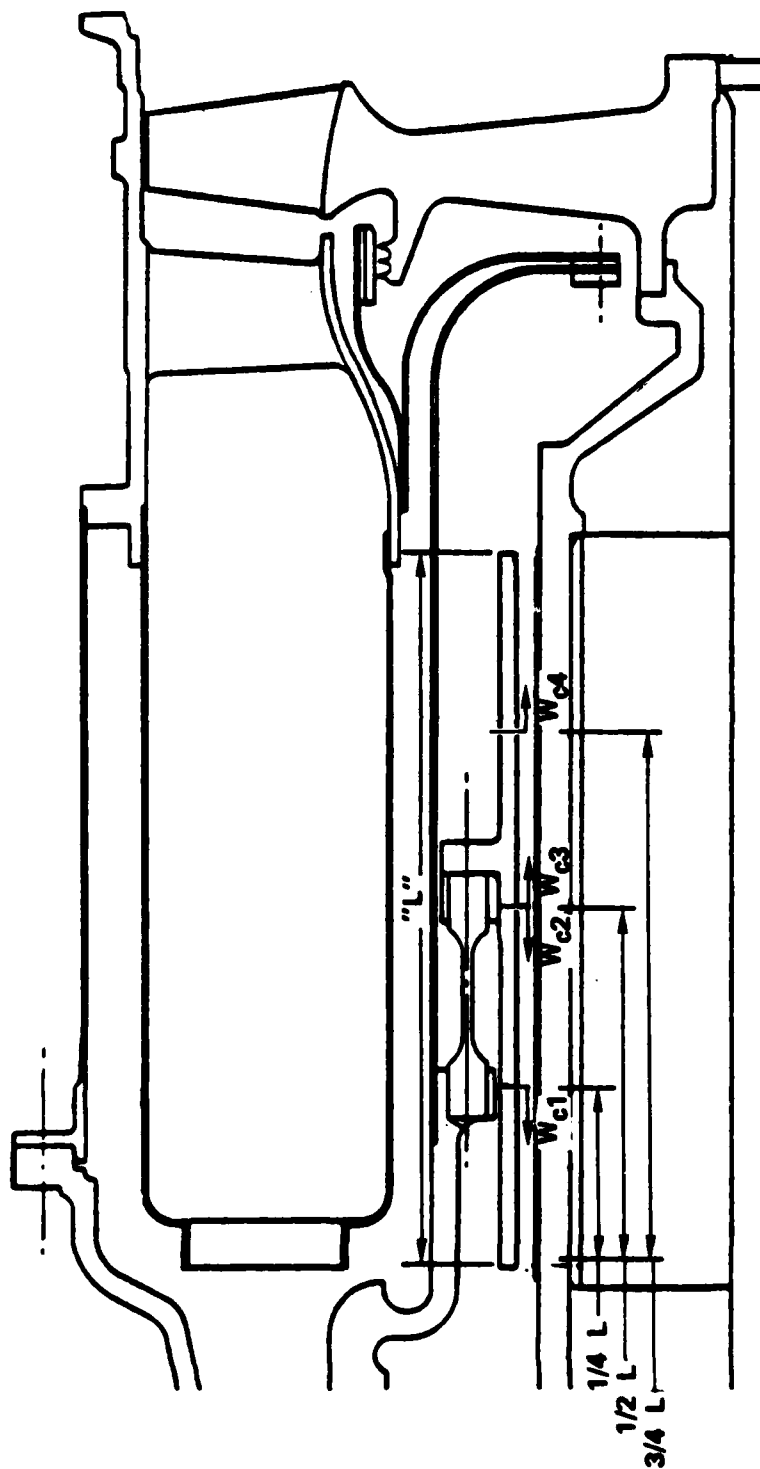


Figure 24. Schematic of Multiple Entry Cooling Flow.

TABLE 6. TJE331-1029 MULTIPLE ENTRY COOLING
FLOW DISTRIBUTION

Configuration	Fraction of Total Cooling Flow			
	W_{C1}	W_{C2}	W_{C3}	W_{C4}
1	0	0.5	0.5	0
2	0.375	0.125	0.125	0.375
3	0.25	0.25	0.25	0.25
4	0.125	0.375	0.375	0.125
5	0.5	0	0	0.5

$$W_{C_{TOTAL}} = W_{C1} + W_{C2} + W_{C3} + W_{C4}$$

$$W_{C_{TOTAL}} = 0.04 \text{ lb/sec at } 500^{\circ}\text{F}$$

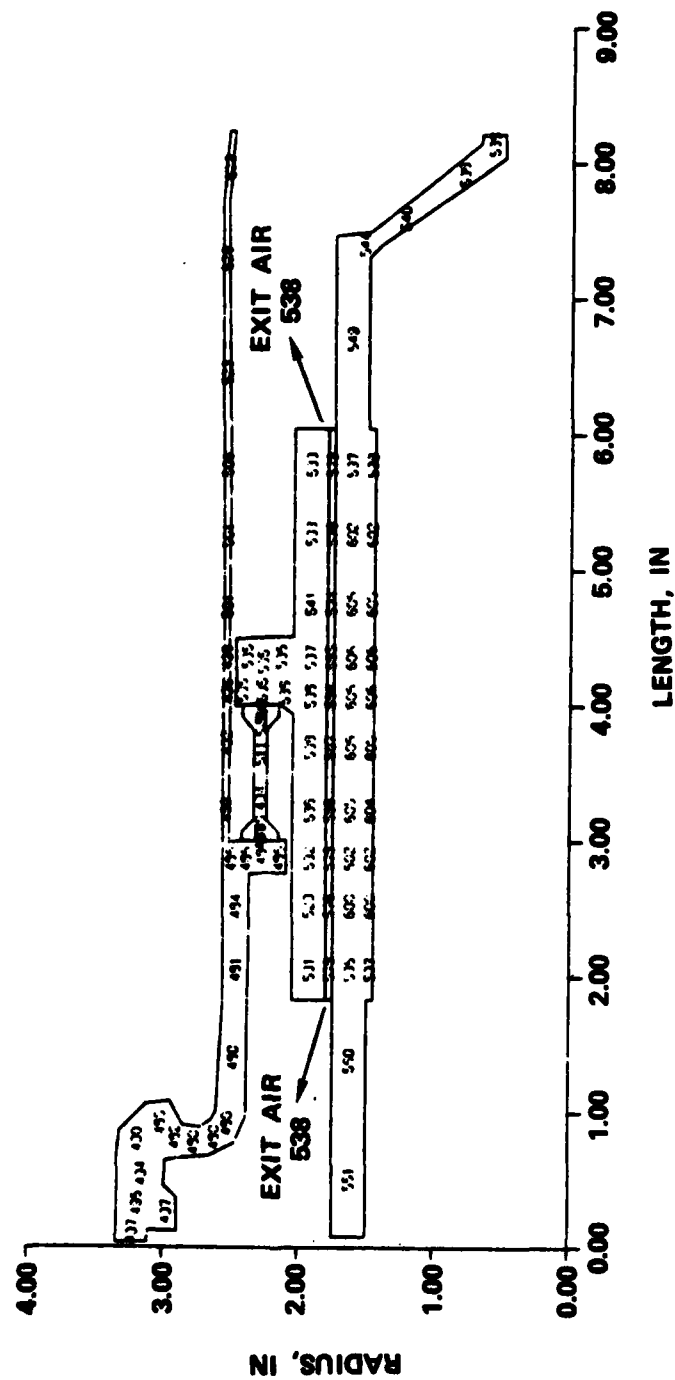


Figure 25. TJE331-1029 Hot End Foil Bearing Thermal Response with Configuration 2 Cooling Flow at 500°F Inlet Temperature.

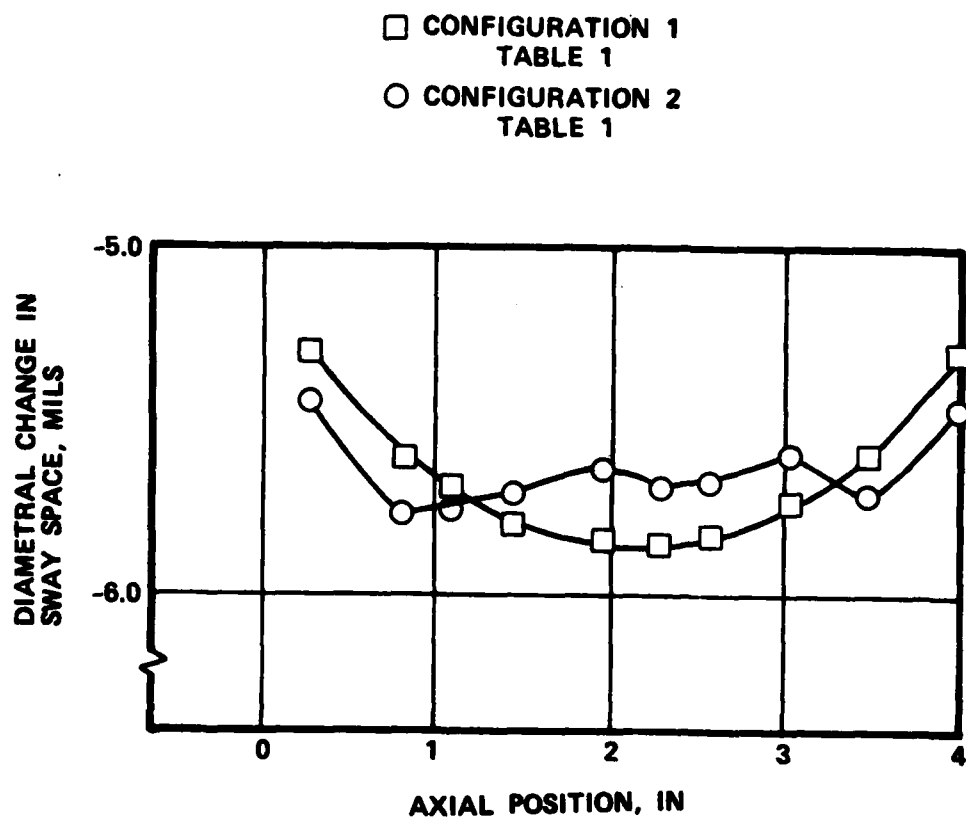


Figure 26. TJE331-1029 Hot End Foil Bearing Diametral Change in Sway Space for 2 Cooling Configurations.

film thickness, and the axial variation in film thickness can be obtained from Figures 19, 20, 21, and 26. Therefore, the integrated pressure can be estimated by calculating $\int 1/h^n dx$ where x is the axial coordinate. Using $n = 3$ and $h_{\min} = 0.001$, load capacities for the bearings considered in Figures 19, 20, 21 and 26 can be calculated and compared with a bearing having a uniform axial film of 0.001 inch, to establish a relative capacity.

This relative bearing load-carrying capacity is presented in Table 7. The estimated load capacities were normalized relative to the highest calculated bearing load. While recognizing that absolute load levels are not reliable, the following trends were identified from these calculations:

- o Certain multiple-entry cooling flow schemes have the potential for increasing bearing load capacity (calculation 10 versus calculation 3). However, other multiple-entry schemes show no benefit (calculation 11 and 12 versus calculation 3) over single-entry cooling
- o Addition of a copper thermal shunt to the journal increases bearing load capacity. (Calculation 1 versus calculation 9)
- o Doubling the bearing power dissipation causes a significant reduction in bearing load capacity (calculations 6, 7, 8 versus calculations 1, 3, 5)

Although the preceding analyses provide additional insight into bearing cooling schemes, the original, single, mid-entry cooling design (Configuration 1, Table 1) performed effectively and was retained as the primary cooling design.

TABLE 7. TJE331-1029 HOT END FOIL BEARING RELATIVE LOAD CARRYING CAPACITY
(COMPARED TO AXIALLY UNIFORM 0.001-INCH FILM)

Calculation Number	Bearing Power Dissipation (watts)	Thermal Shunt	Cooling Flow Configuration (Table 1)	Total Cooling Flow (lb/sec)	Load* Ratio
1	500	Yes	1	0.01	0.64
2	500	Yes	1	0.02	0.74
3	500	Yes	1	0.04	0.83
4	500	Yes	1	0.06	0.86
5	500	Yes	1	0.10	0.96
6	1000	Yes	1	0.01	0.45
7	1000	Yes	1	0.04	0.64
8	1000	Yes	1	0.10	0.79
9	500	No	1	0.01	0.60
10	500	Yes	2	0.04	1.00**
11	500	Yes	3	0.04	0.84
12	500	Yes	4	0.04	0.83
13	500	Yes	5	0.04	0.56

*Load Ratios Normalized by Setting Largest Calculated Value to 1.0
**Maximum Load Ratio

f. Hydrodynamic Analysis

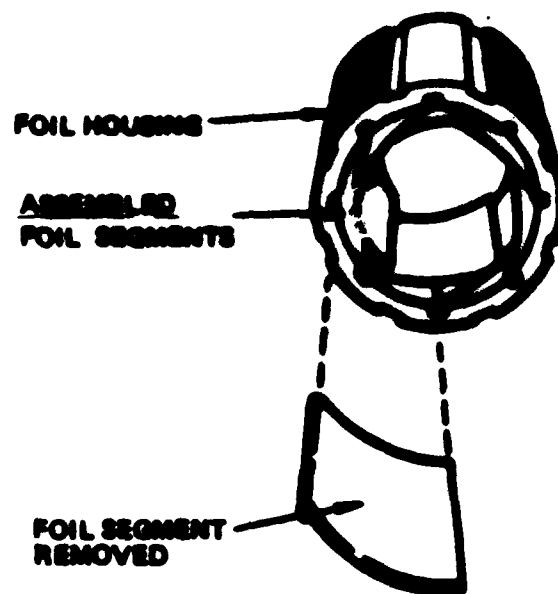
(1) Hydrodynamic Analysis Computer Program

The latest Garrett foil bearing analysis computer program was utilized to accomplish a thorough analysis and to perform parametric studies for design guidance. This program utilizes a model wherein the bearing journal is concentric within the bearing housing.

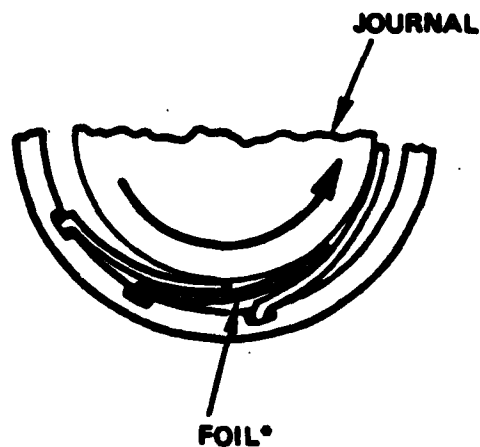
For a typical foil bearing used in the analysis (Figure 27), the compliant portion of the bearing consists of a number of overlapping foils and backing springs retained by grooves in the inside diameter of the foil carrier. The assembly configuration requires that the foils be elastically deflected to insert the journal. When stationary, the foils contact and center the journal in the bearing bore. Shaft rotation induces gas flow into the converging channels formed between the journal and the foils, generating hydrodynamic lift. At a sufficiently high shaft speed, the foils lift off the journal, eliminating any contact with the shaft. The journal is now supported entirely by the hydrodynamic film generated between the foils and journal.

The stress state of the elastically deformed foils determines the initial preload of the foils against the journal, influencing rotor starting-torque requirements. After foil lift-off, the foil configuration is determined by the loads imposed by the self-generated hydrodynamic pressure. This pressure distribution is determined by the gas film thickness distribution. The steady-state foil operating configuration must simultaneously satisfy both the foil elastic and gas film hydrodynamic constraints.

The computation iterates between these two constraints to converge to the final solution.



A. FOIL HOUSING AND FOIL CARRIER



B. CLOSE-UP OF INSTALLED JOURNAL

***BACKING SPRING ASSEMBLIES BETWEEN FOIL
AND FOR HOUSING. FOR CLARITY, NOT
INCLUDED IN THIS FIGURE**

Figure 27. Self-Acting Compliant Foil Bearing Geometry.

An initial gas film thickness distribution is determined by an estimate of foil configuration. The pressure loads computed from the resultant gas film thickness distribution then determine a new foil deflected state. Using a sufficiently small under-relaxation parameter usually ensures a slow but continuous convergence to the solution.

(2) Candidate Foil Bearing Configurations

Three candidate foil bearing configurations were analyzed. The configurations are summarized briefly below:

Number of Foils	Foil Thickness (Inch)
12	0.006
10	0.007
8	0.008

The 12-foil bearing configuration is the same as that utilized on Contract F33615-78-C-2044 for the GTCP165 APU foil bearing program. The 10- and 8-foil bearings were identified as additional configurations having the potential to meet or exceed the increased load carrying requirements of the current program.

(3) Hydrodynamic Analysis of Candidate Bearings

The load deflection curve for a single foil from the 12-foil bearing is presented in Figure 28, with the assembly state noted. The individual foil spring rate is 538 lb/in, and the spring rate for the total 12-foil bearing is 3408 lb/in. The geometry of the 12-foil system as well as the non-linear spring rate of an individual foil segment (Figure 28) can be considered in combination to obtain an overall bearing load deflection curve. The analytically derived curve is shown in Figure 29

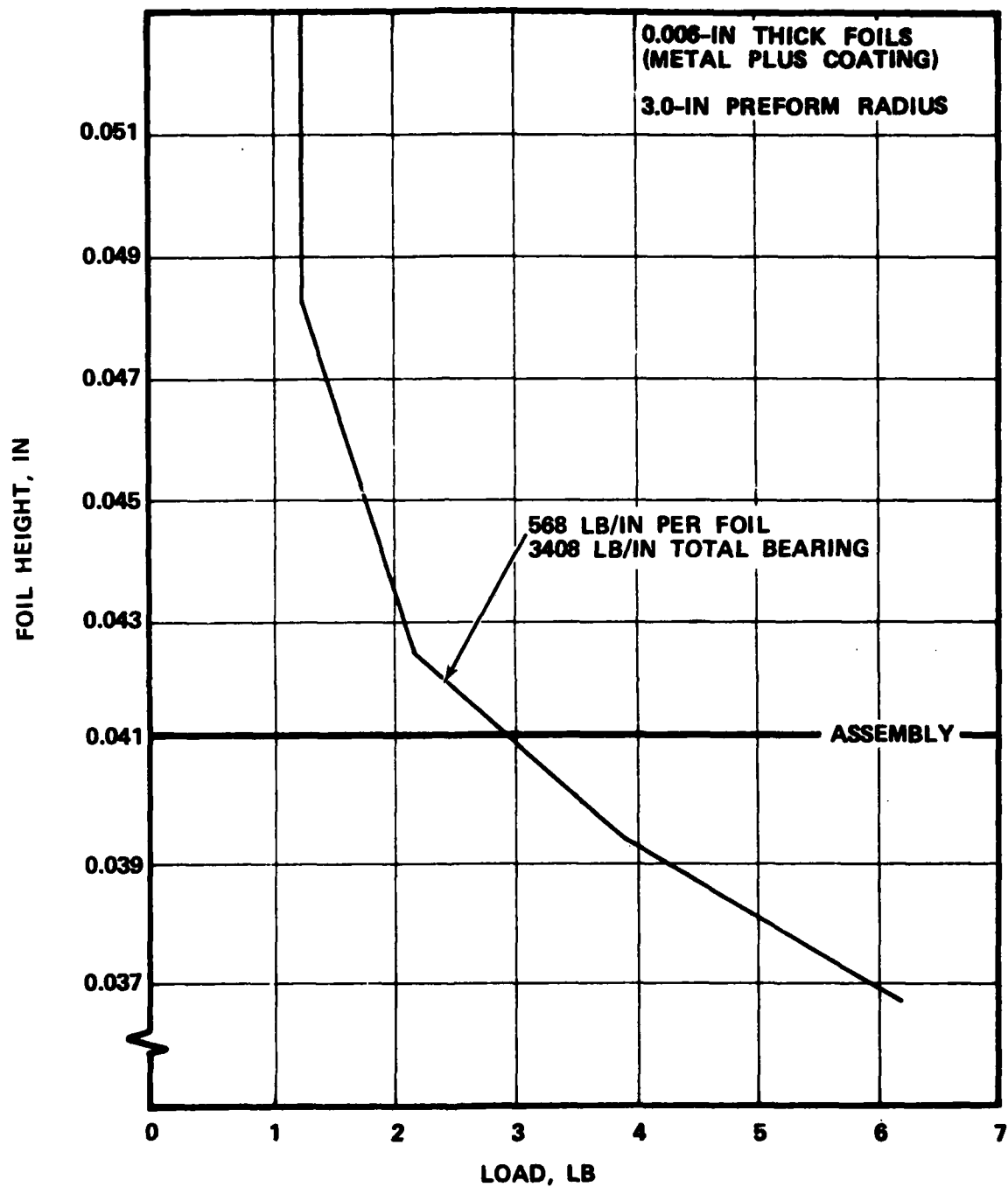


Figure 28. Load Deflection Curve For the 12-Foil Bearing.

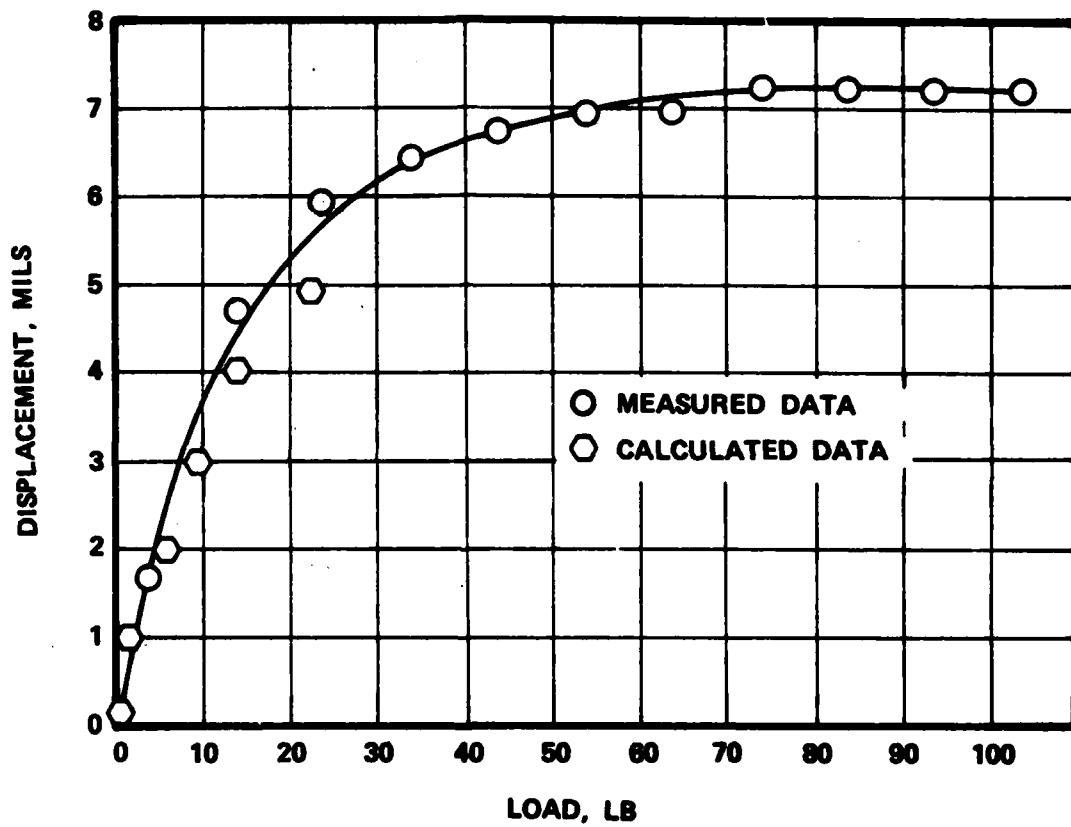


Figure 29. Comparison of Measured to Calculated Load Deflection Curve, Twelve-Segment Foil Bearing.

along with data obtained experimentally on Contract F33615-78-C-2044. Analytical data is plotted out to about a 1-g load. The agreement between measured and calculated results is good.

Figures 30 through 32 show the assembled foil deflected states for loads of 1.0, 3.0 (assembly) and 5.5 pounds, respectively. The vertical axis is radial height from the bearing housing and has been distorted relative to the horizontal axis. At assembly (3-pound load), the foil has made double contact underneath with the downstream foil as well as single contact with the backing spring. Under the 5.5 pound load shown in Figure 32, the foil is flattening out at both the journal interface and foil-foil interface, and the stiffness would increase markedly from that point.

The load-deflection curve for a 1-foil segment (0.007-inch thick, 3-inch preform radius) from the 10-foil bearing is shown in Figure 33 and the corresponding assembly state for this bearing is presented in Figure 34. The individual foil spring rate of 505 lb/in for this bearing is similar to that for the 12-foil bearing. The 2525-pound spring rate for the total 10-foil bearing at assembly is less than that for the 12-foil bearing because of fewer foils. The load-deflection curve for a 1-foil segment (0.007-inch thickness, 3-inch preform radius) from the 8-foil bearing is shown in Figure 35, and the corresponding assembly state for this bearing is presented in Figure 36. The individual foil spring rate is 184 lbs/in for the 8-foil bearing, and the total bearing spring rate at assembly is only 736 lbs/in. The reduced spring rate of the individual foils and the increased assembly height (3.4 mils higher) due to the reduced foil number, both contribute to the reduction in total bearing spring rate. Figure 35 also presents spring rate data for 8-foil bearings utilizing foils of increased thickness and a reduced preform radius.

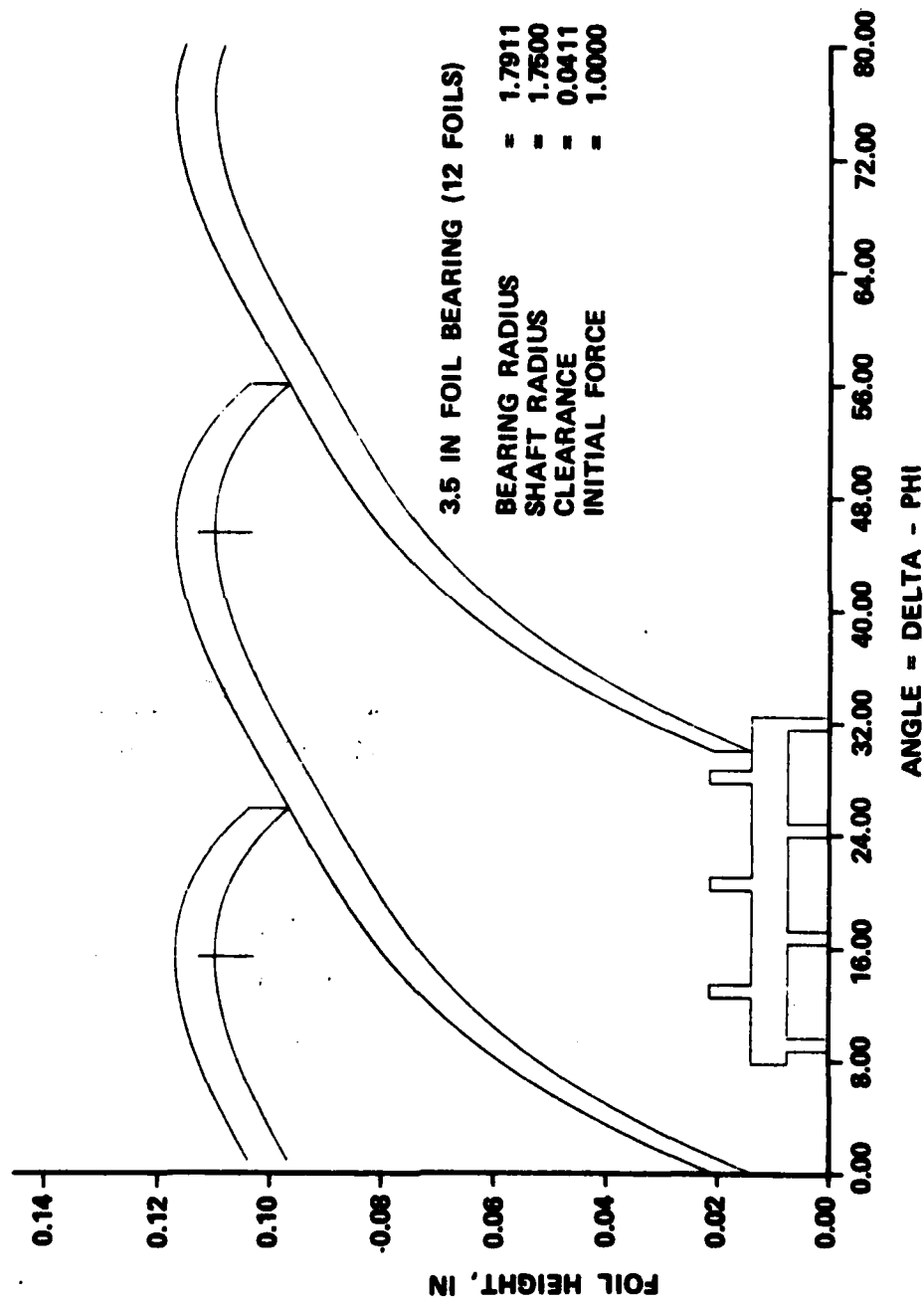
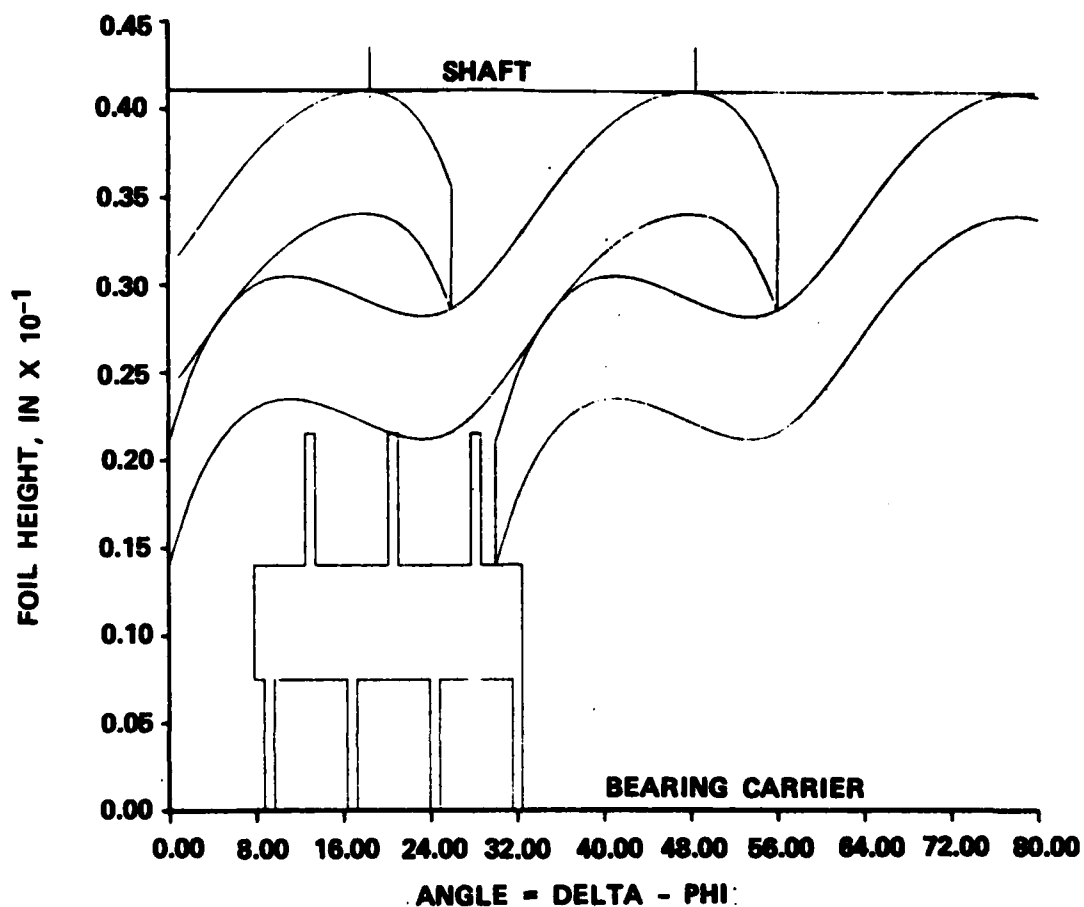


Figure 30. Deflected Foil State Under 1.0 Load For 12-Foil Bearing.



3.5 IN FOIL BEARING (12 FOILS)

FOIL RADIUS	= 3.0000
BEARING RADIUS	= 1.7911
SHAFT RADIUS	= 1.7500
CLEARANCE	= 0.0411
INITIAL FORCE	= 3.0000

Figure 31. Deflected Foil State at Assembly (3-Pound Load).

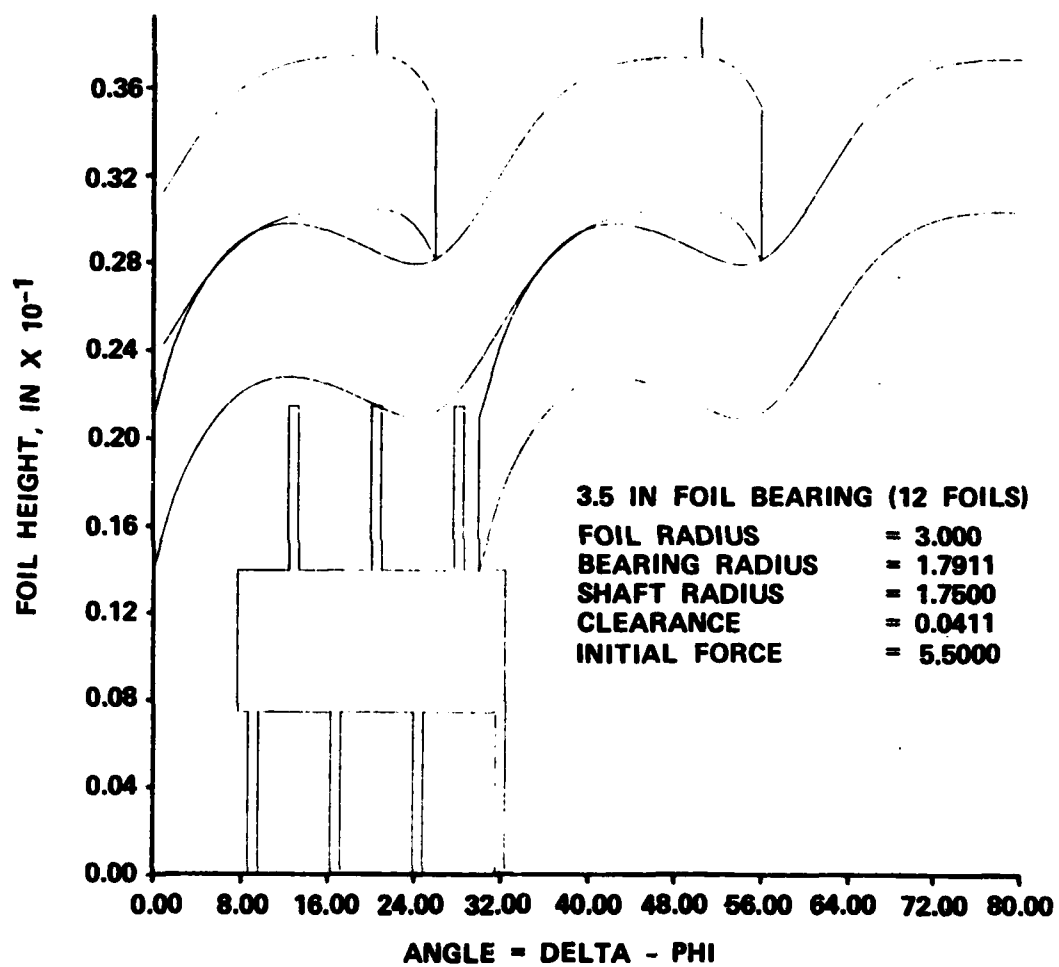


Figure 32. Deflected Foil State Under 5.5-Pound Load.

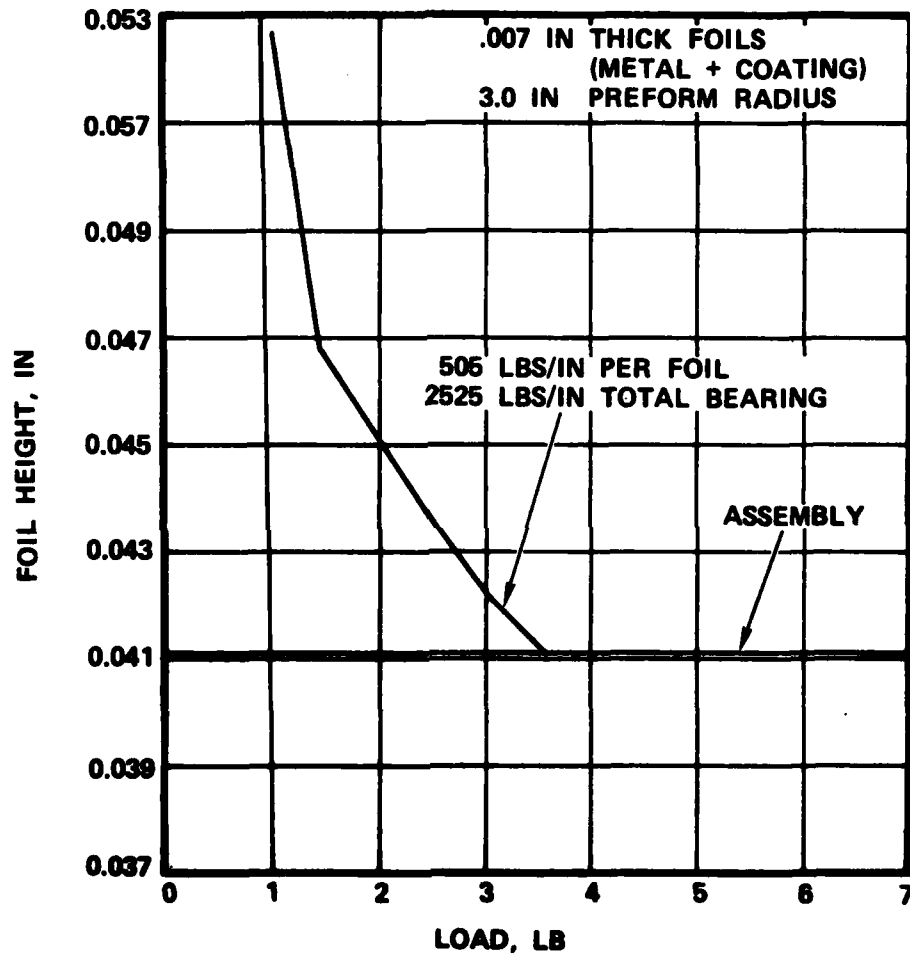


Figure 33. TJE331-1029/Foil Load-Deflection Curve for the 10-Foil Bearing.

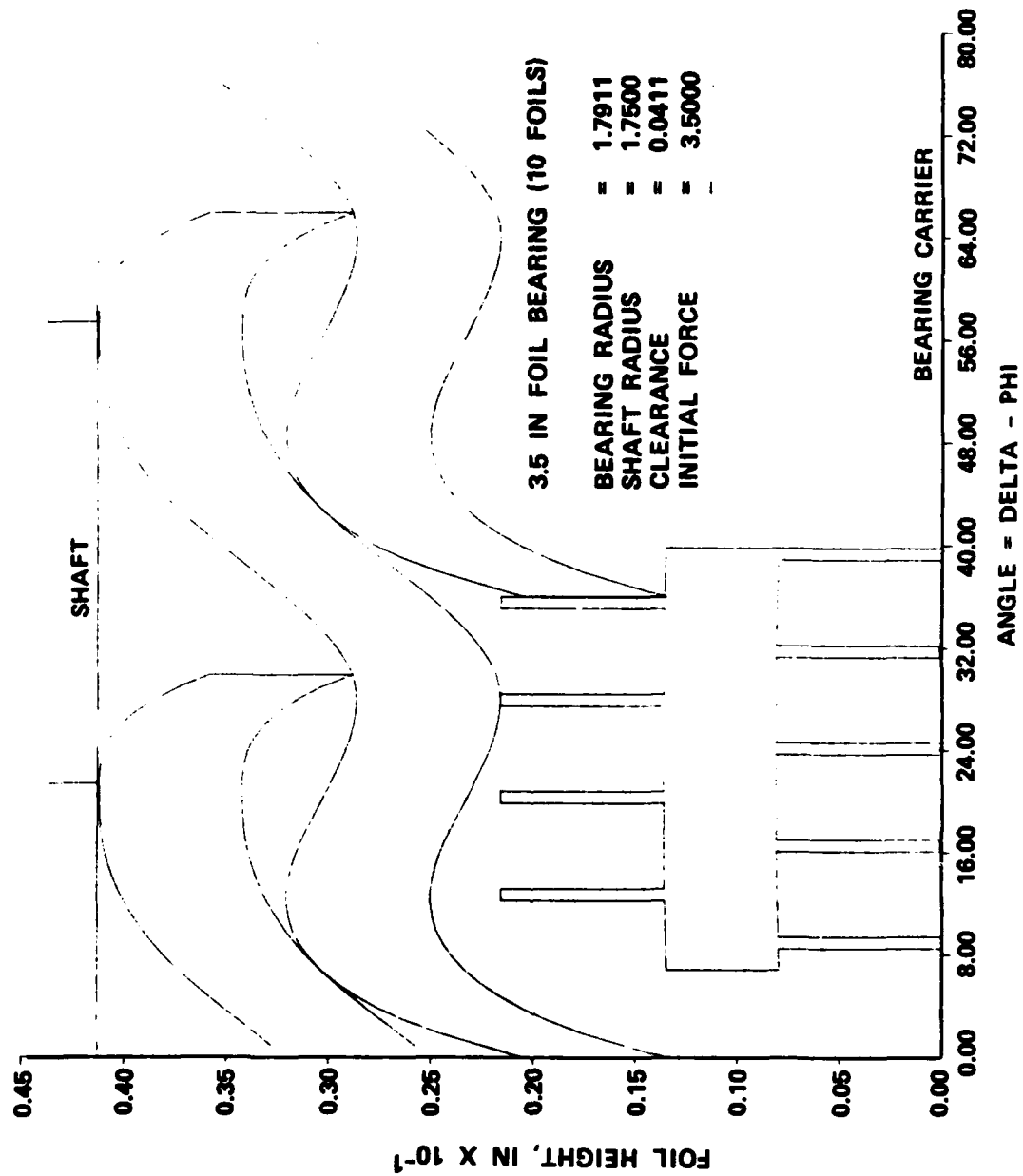


Figure 34. TJE331-1029 10-Foil Bearing Assembly State.

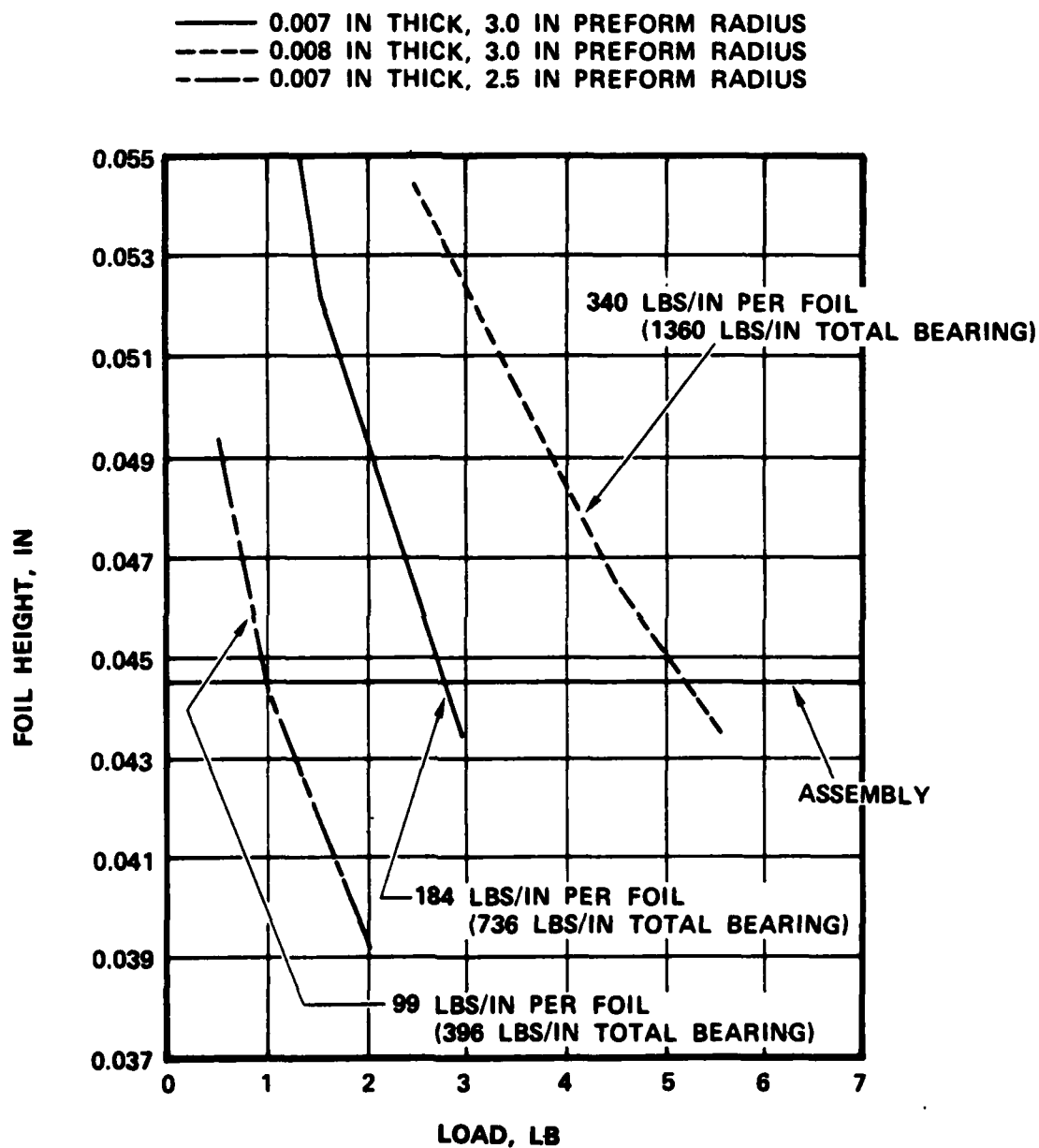


Figure 35. TJE331-10 Foil Load-Deflection Curve
 for the 8-foil Bearing.

A more detailed examination of the foil bearing assembly state (Figures 31, 34 and 36, for the 12, 10 and 8-foil bearings, respectively) begins to provide additional insight into the potential load carrying capability of each of these bearings. These figures show that as the number of foils in a configuration decreases, the contact region between the foil and shaft at the foil trailing edge "flattens out" at the same applied load level. The flattening out of the foil will produce a broader region of pressure buildup in the bearing, which translates in greater load carrying potential. A combined elasto-hydrodynamic solution for a concentric journal orientation was run for the 12-, 10-, and 8-foil bearings. Calculated pressure plots are presented in Figures 37 through 39 with corresponding foil shapes in Figures 40 through 42. The calculated pressures have been normalized, where 1 equals ambient pressure. Comparison of Figures 37, 38, and 39 shows that as the number of foils is reduced, the calculated peak pressure decreases, and the breadth of the pressure profile and minimum film thickness increase. The only anomaly in these calculated trends can be seen in Table 8. Note that the integrated load on one foil is only 3.71 pounds for the 8-foil bearing, versus 4.08 and 4.70 pounds for the 12- and 10-foil bearings. However, in the above analysis, the build clearance for the 8-foil bearing is greater than for the other two bearings. If the build clearance for the 8-foil bearing were reduced to that of the other bearings, it is expected that the pressure peak and especially the total integrated load for the 8-foil bearing will rise.

TABLE 8. TJE331-1029 FOIL BEARING HYDRODYNAMIC ANALYSIS RESULTS

Number of Foils	Minimum Film Thickness	Normalized Pressure Peak	Integrated Total Load	Build Clearance
12	0.00084	1.329	4.08	0.0411
10	0.00108	1.252	4.70	0.0411
8	0.00146	1.161	3.71	0.0445

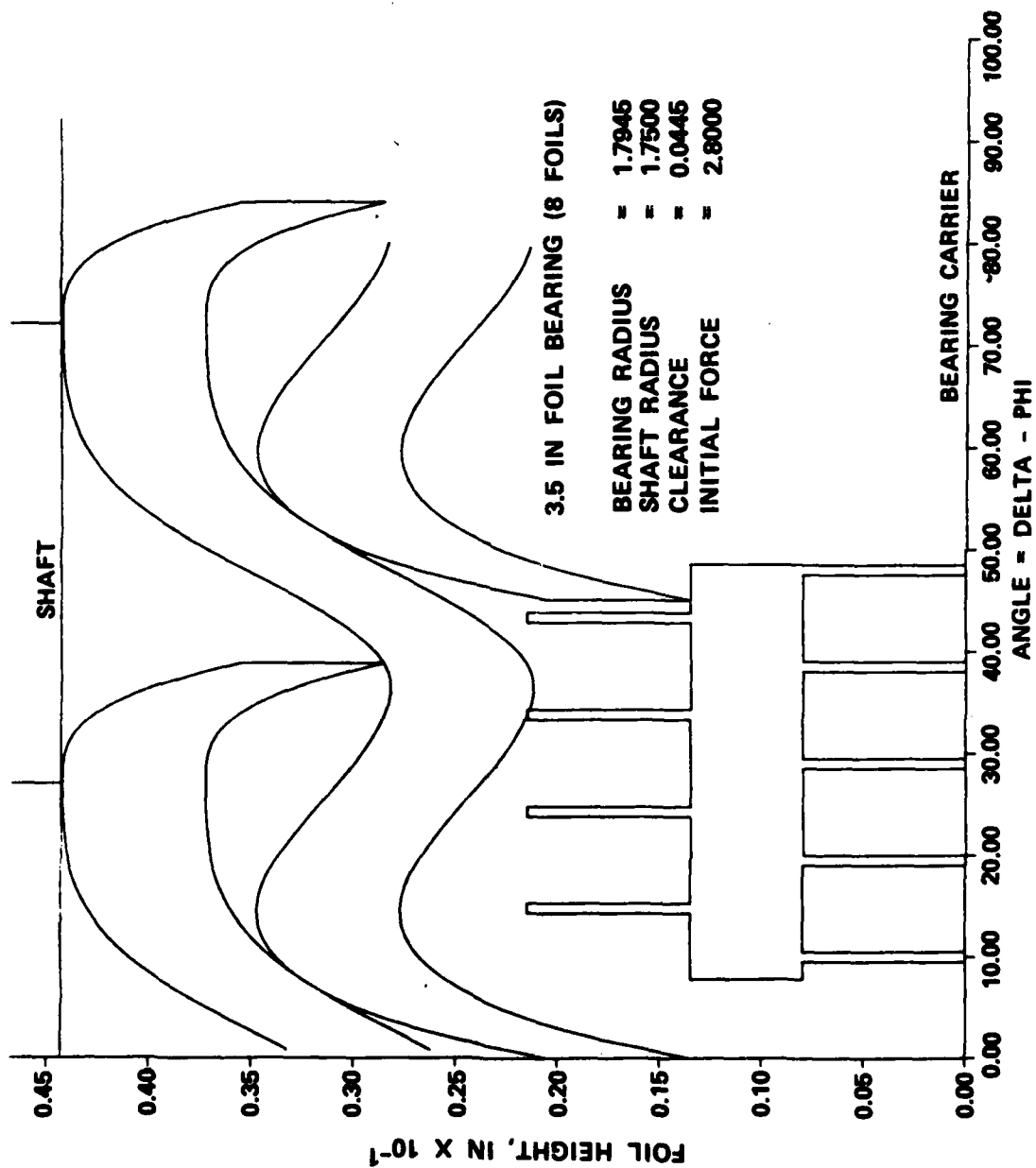


Figure 36. TJE331-1029 8-Foil Bearing Assembly State.

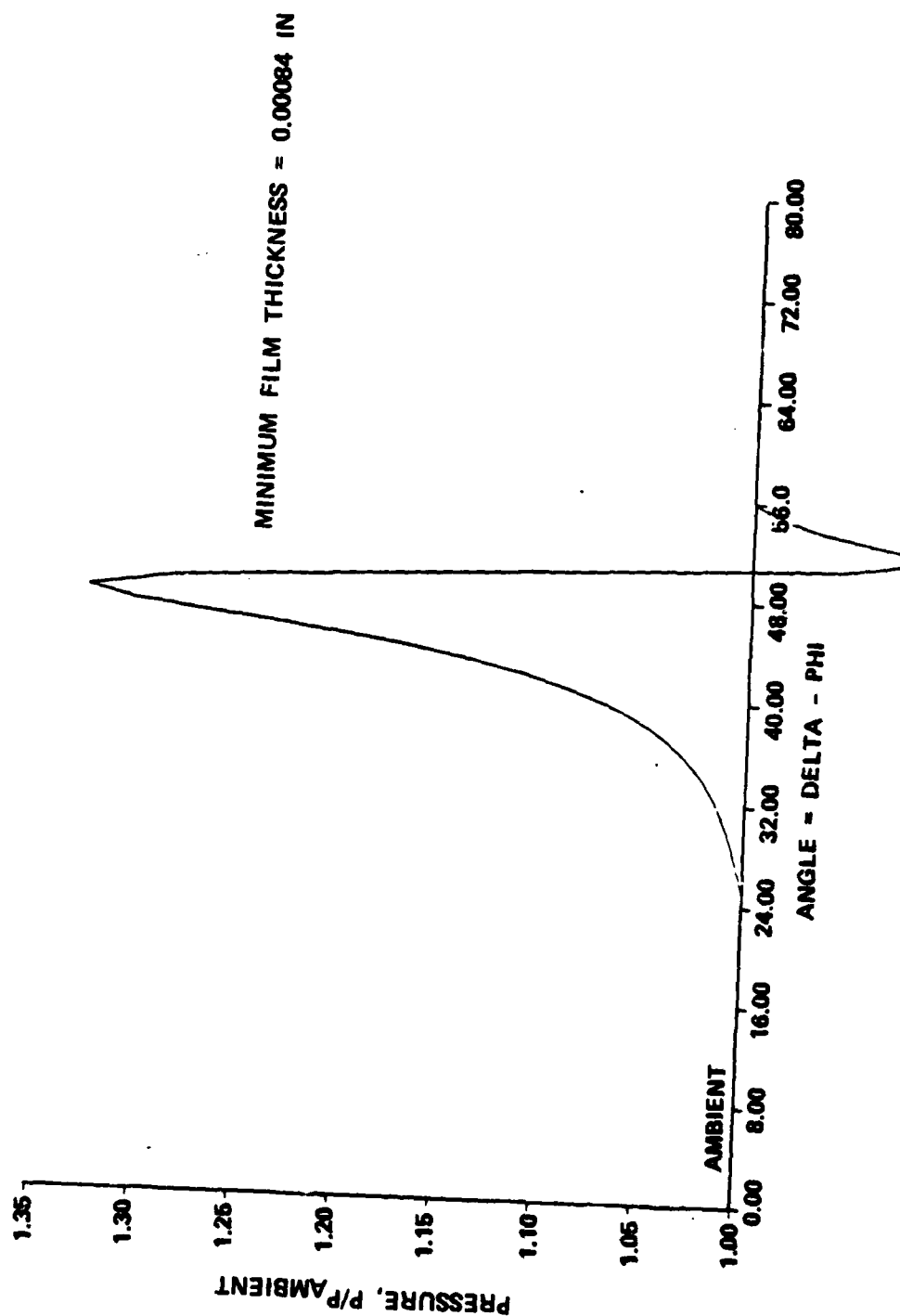


Figure 37. TJE331-1029 Normalized Pressure on Foil Segment for the Concentric 12-Foil Bearing.

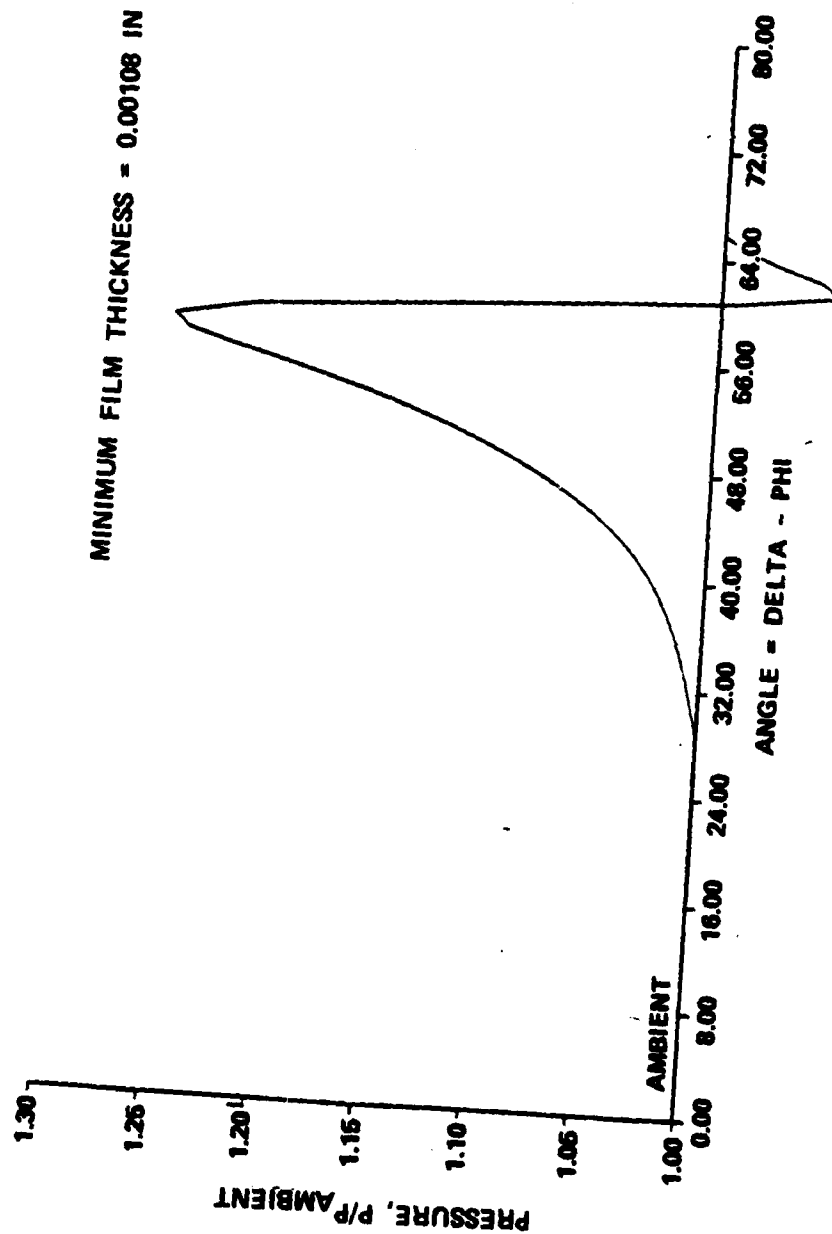


Figure 38. TJE331-1029 Normalized Pressure on Foil Segment for the Concentric 10-Foil Bearing.

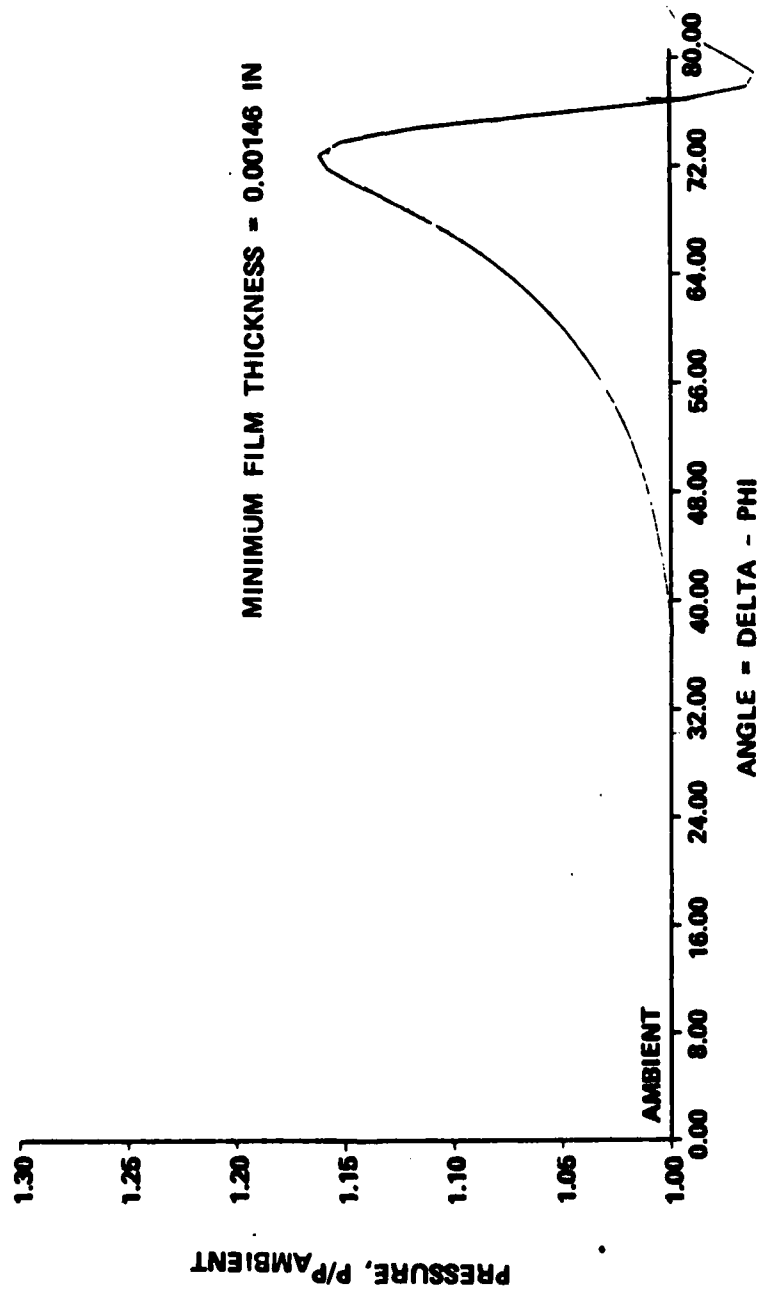


Figure 39. TJE331-1029 Normalized Pressure on Foil Segment for the Concentric 8-Foil Bearing.

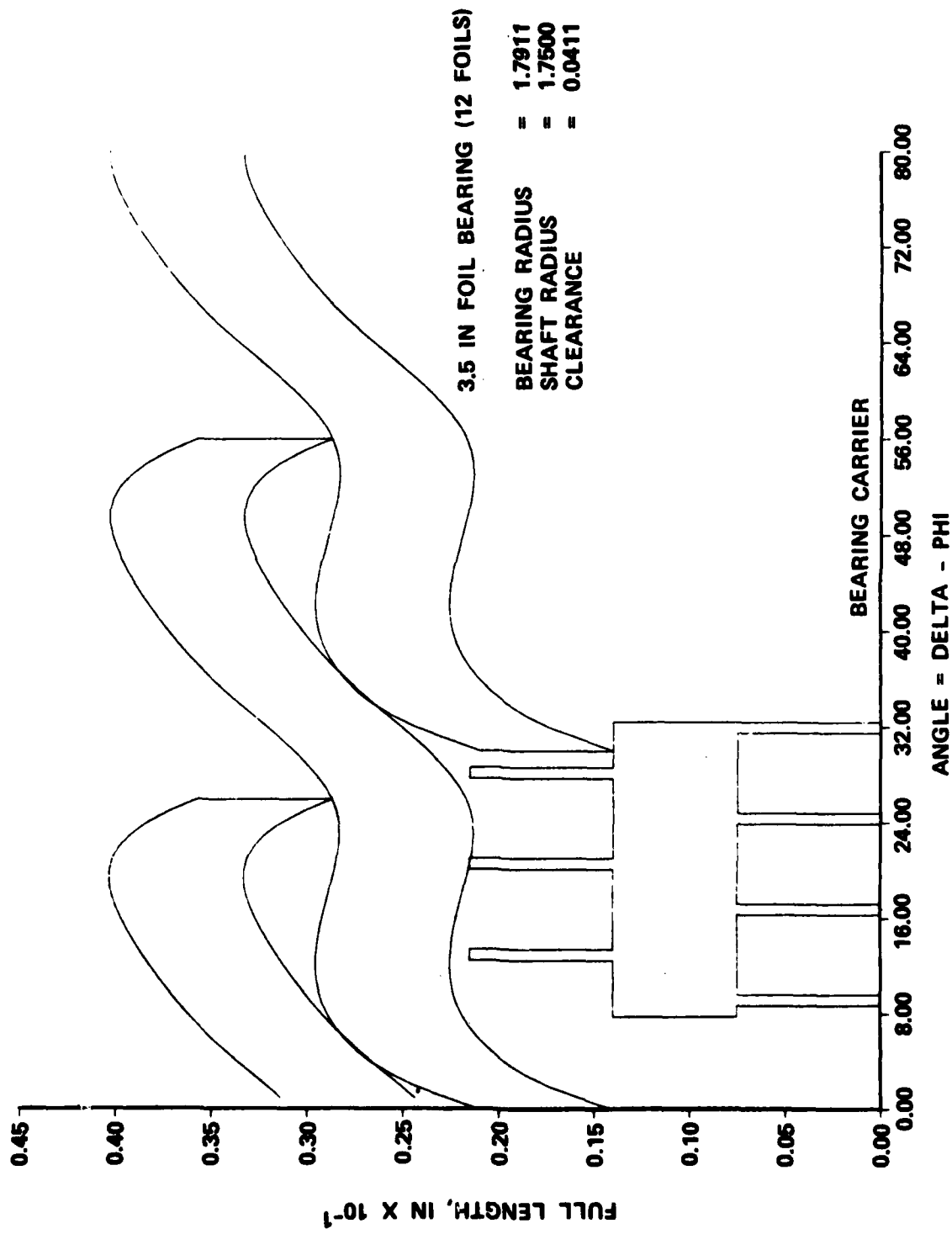


Figure 40. TJE331-1029 Foil Shape Under Pressure Load for the Concentric 12-Foil Bearing.

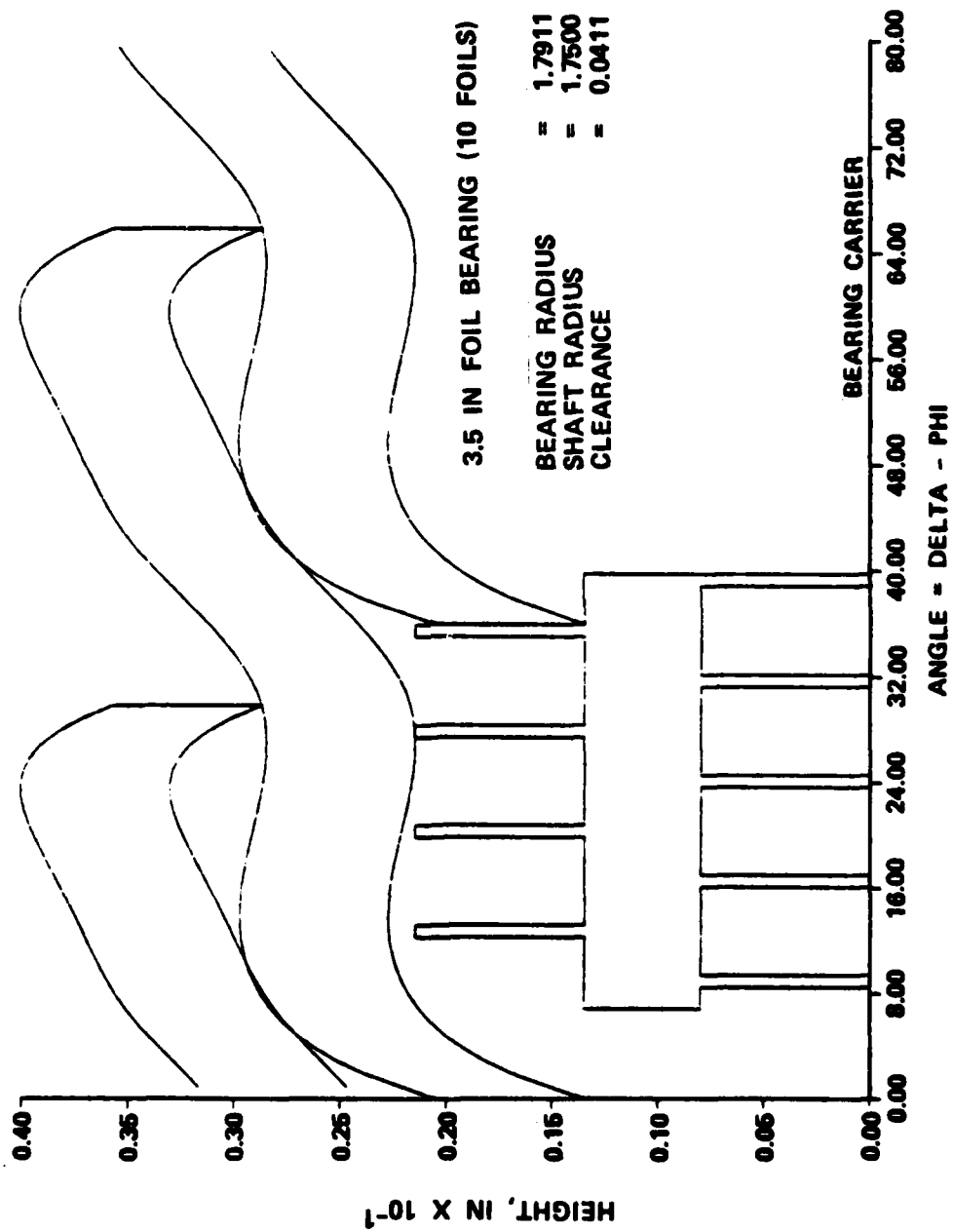


Figure 41. TJE331-1029 Foil Shape Under Pressure for the Concentric 10-Foil Bearing.

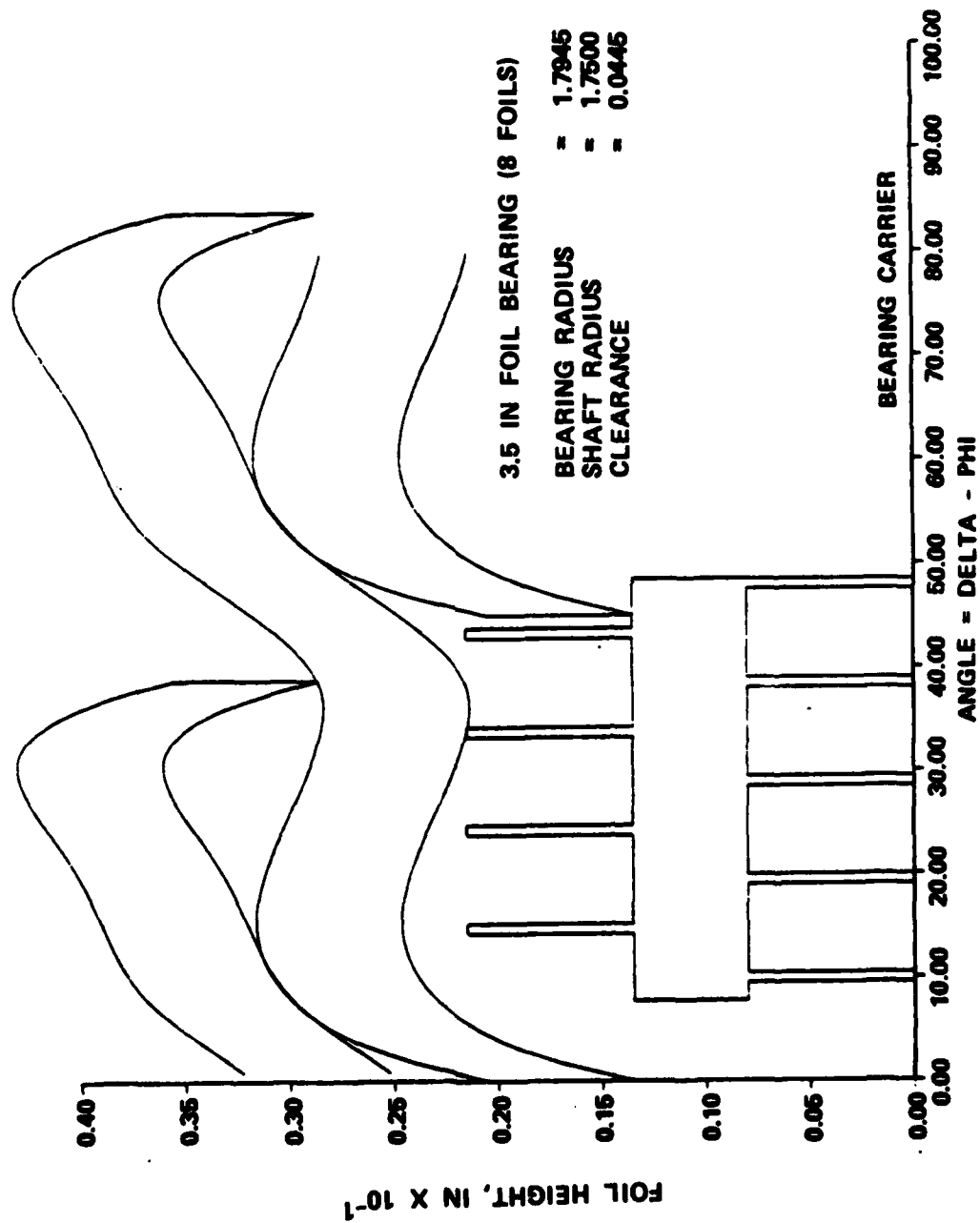


Figure 42. TJE331-1029 Foil Shape Under Pressure for the Concentric 8-Foil Bearing.

3. TEST RIG

a. Test Rig Configuration

The bearing test rig used was that designed for the U.S. Air Force APU Foil Bearing Program, Contract No. F33615-78-C-2044. This rig, shown in Figure 43, comprises an air turbine drive coupled to the test rotor by means of a splined shaft. The test rotor is supported by rolling element bearings with the test foil bearing suspended at one end. The test foil bearing was enclosed with thermal insulation (Figure 44) to permit testing at bearing temperatures up to 1200°F.

The bearing housing simulated the geometry applicable to the TJE331-1029 as closely as possible from a thermal standpoint. The similitude of the APU and Thrust Engine foil bearings is discussed in Paragraph 2d.

b. Test Rig Instrumentation

Instrumentation was provided to monitor bearing friction, rotor speed, bearing load, journal and bearing carrier temperatures, and journal and bearing housing dynamic motions. Instrumentation used is listed in Table 9. Figures 45 through 47 show instrumentation locations. Data was visually monitored and manually recorded throughout this program.

c. Displacement Probe Monitoring During Load Application

Displacement probes were used to monitor journal-to-ground and journal-to-carrier operating displacements in the basic bearing test rig. Experience gained from monitoring the oscilloscope traces of these probes during test load application, (especially the carrier-to-journal probes), was extremely useful in assessing the bearing running condition. Rig running showed there are three distinct wave patterns (Figure 48):

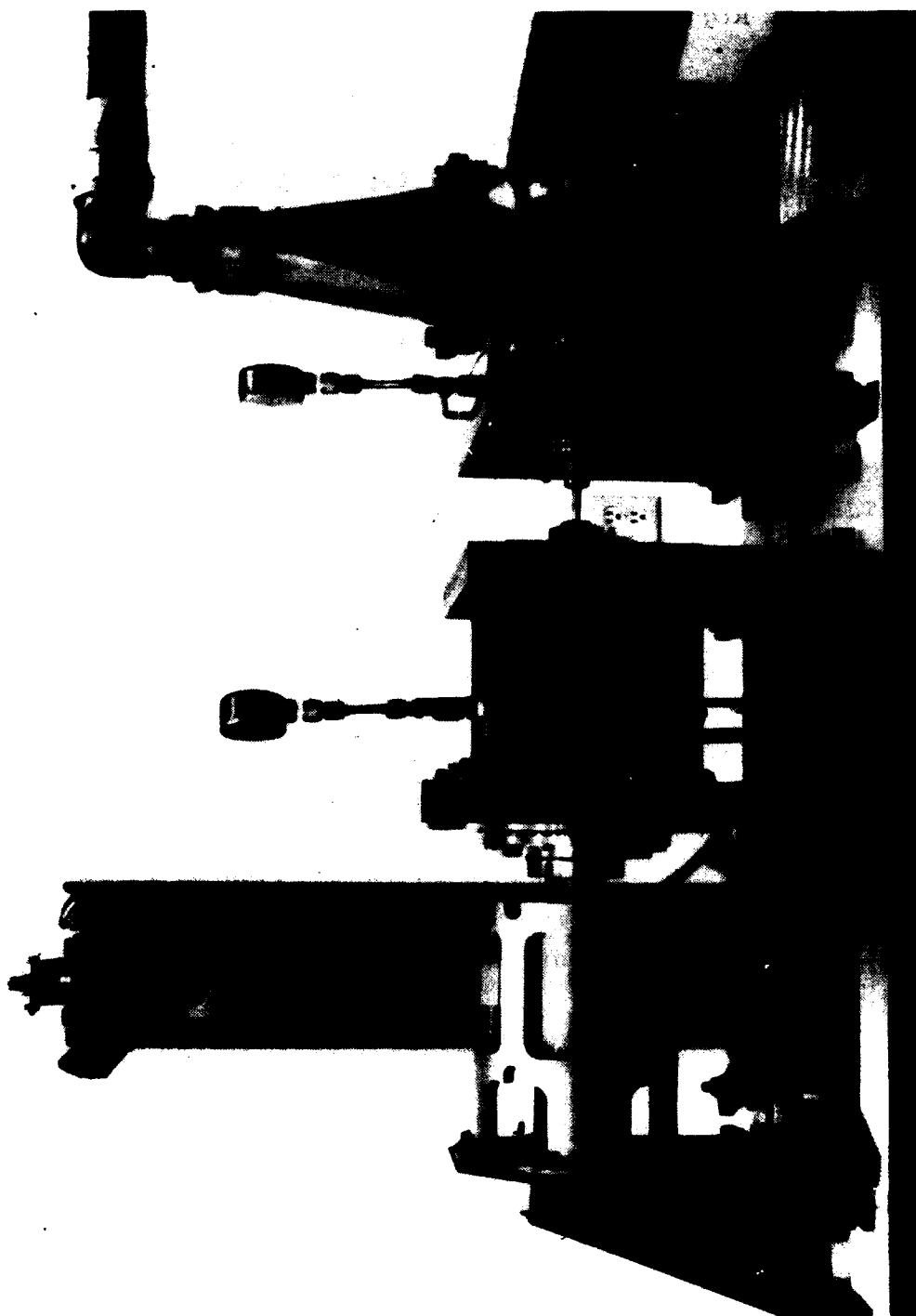


Figure 43. Basic Simulator Test Rig.



Figure 44. Basic Test Rig With Ambient Box Installed Over Test Bearing.

TABLE 9. FOIL BEARING BASIC SIMULATOR INSTRUMENTATION

Locations	Parameters	Symbol	Units	Range	Accuracy	Sensor Type
1	Speed	N	rpm	0-42,000	±1%	Bentley Probe
2	Vibration	G	mils	0-5	±5%	Accelerometer
3	Cooling Air: Flow Rate (design - 0.021 lb/sec)	W _C	lb/min	0-0.4	±1.5%	Orifice Plate
4	Pressure In	P _C	psig	0-75	±0.25%	Gauge
5	Temperature In	T _{Cl}	°F	0-1000	±8	C-A TC
6	Temperature Out- Top Bottom	T _{Cl}		0-1200		
8	Journal Temperature - Midspan	T _{J1}				Optical Pyrometer (Vanzetti)
9	- End	T _{J2}				Optical Pyrometer
10	Foil Carrier Rotational Displacement	D ₁ , D ₂	inch	0-0.030	±2%	Wayne-Kerr probe
11	Upper Cable Tension	F ₁	lb	0-500		Interface Load
12	Lower Cable Tension	F ₂	lb	0-500		Cell Model SM-500
13	Journal-to-Ground Proximity: Inboard (2)	C ₁	inch	0-0.030		Wayne-Kerr probe
14	Outboard (2)	C ₁		0-0.030		
15	Journal-to-Foil Carrier Proximity: Inboard (2)	S ₁		0-0.010		
16	Outboard (2)	S ₂		0-0.010		
17	Drive Turbine Air Supply: Pressure	P _T	psig	0-50	±0.25%	Gauge
18	Test Rig Oil Pressure	P _R	psig	0-50	±0.25%	

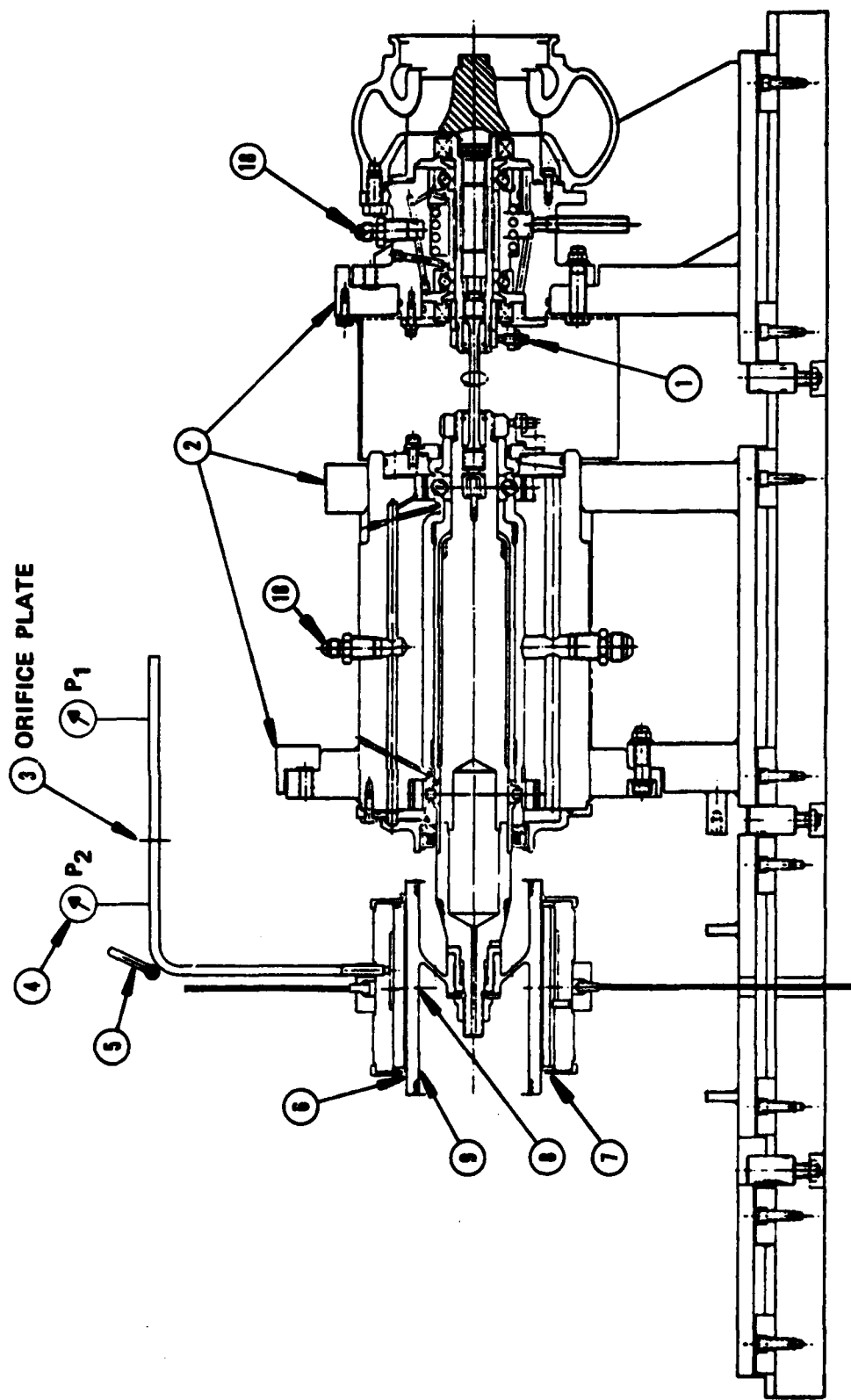


Figure 45. Instrumentation Locations.

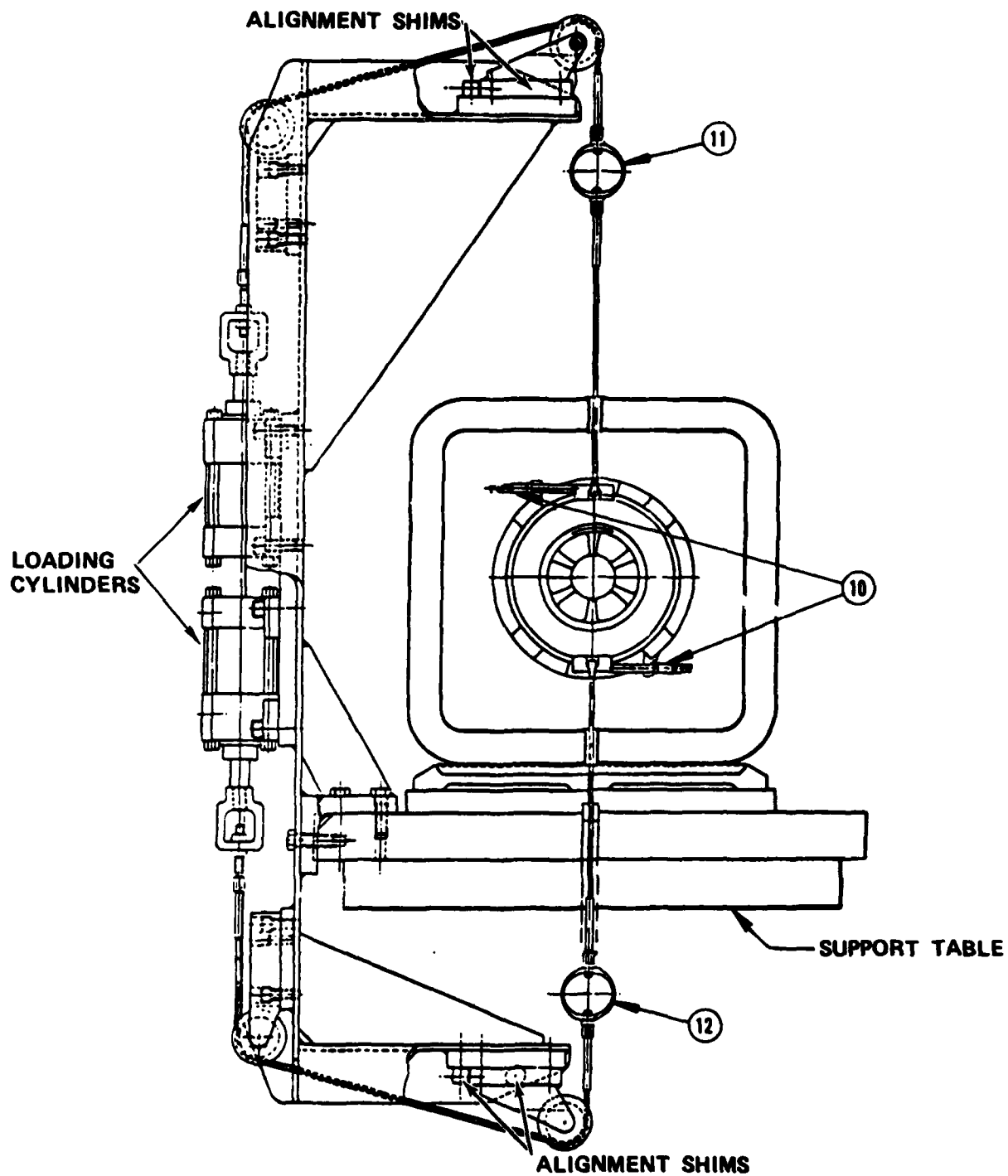


Figure 46. Instrumentation Locations.

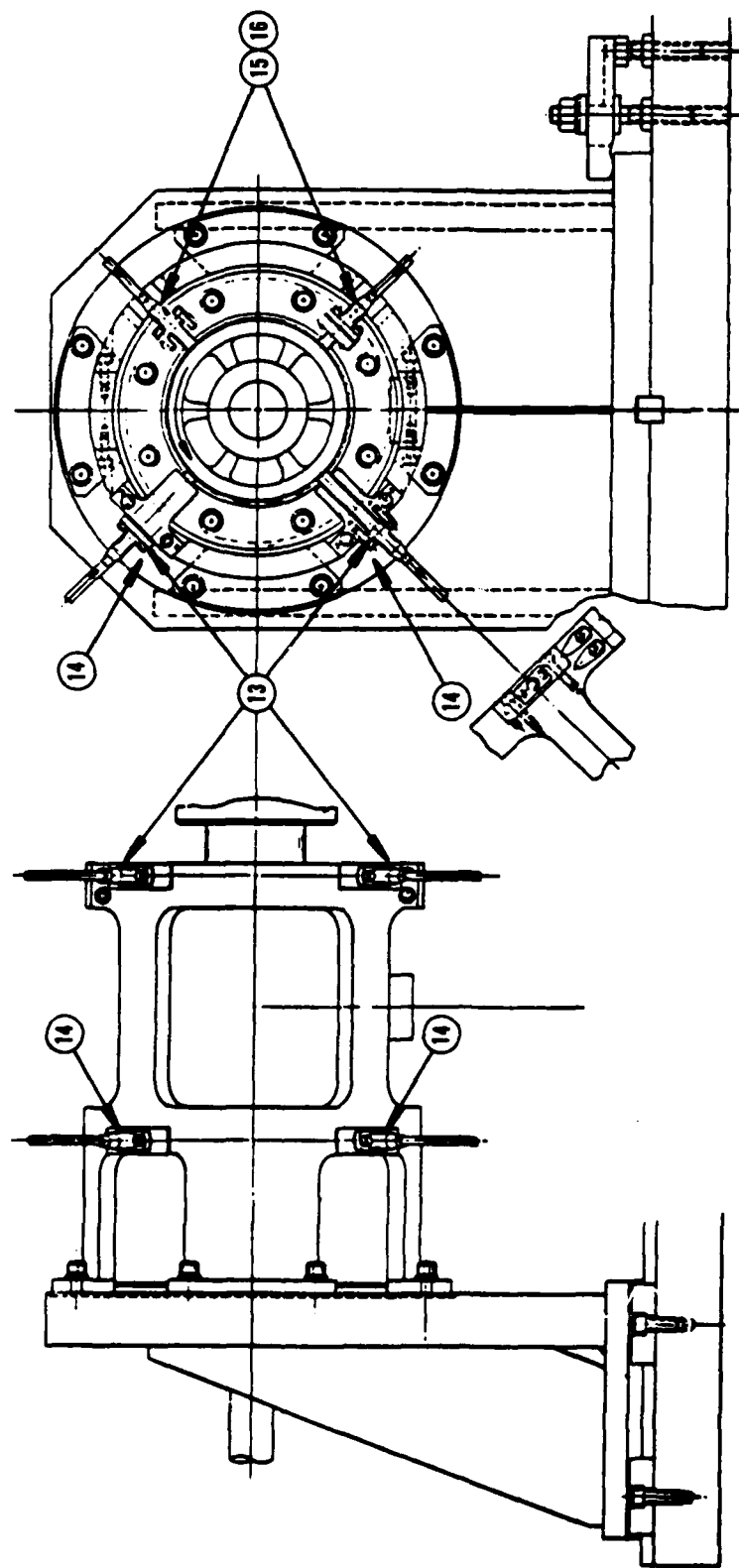
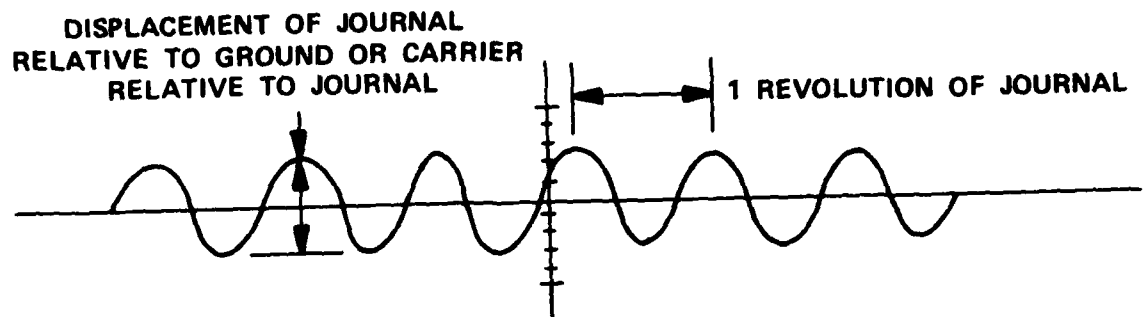
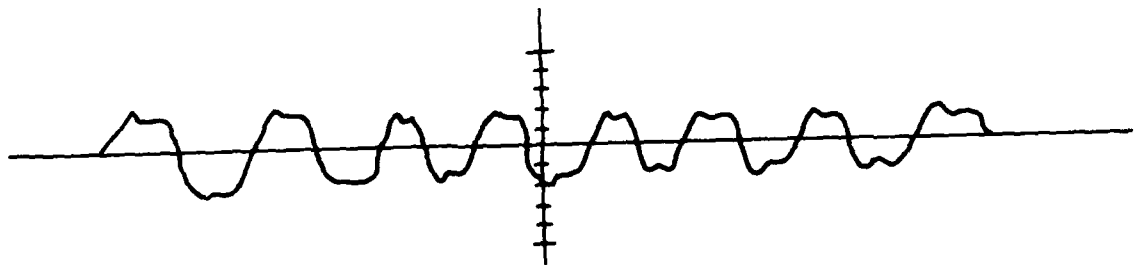


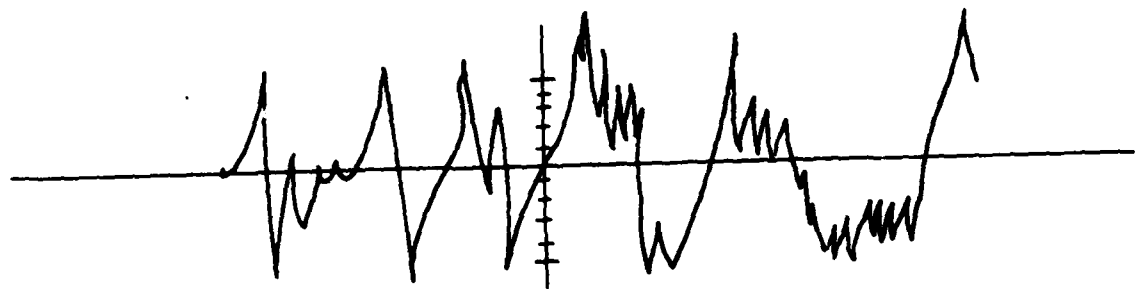
Figure 47. Instrumentation Locations.



a. NORMAL DISPLAY, 1-g LOAD, 33200 RPM



b. NORMAL DISPLAY, HEAVY LOAD STABILIZED, 33,200 RPM, LIGHT RUB
MAY BE OCCURRING OR INCIPIENT



c. ABNORMAL DISPLAY INDICATING HARD JOURNAL-ON-FO!! RUB

Figure 48. Typical Signals from Wayne-Kerr Capacitance
Type Displacement Probes.

AD-A114 692

GARRETT TURBINE ENGINE CO PHOENIX AZ
6AS FOIL BEARING DEVELOPMENT PROGRAM.(U)
SEP 81 F J SURIANO

F/8 13/9

UNCLASSIFIED

31-4089

AFWAL-TR-81-2095

F33615-79-C-2037

NL

2 2

2 2

2 2

2 2

2 2

2 2

2 2

2 2

2 2

2 2

2 2

2 2

2 2

2 2

2 2

2 2

2 2

2 2

2 2

2 2

2 2

2 2

2 2

2 2

2 2

2 2

2 2

2 2

2 2

2 2

2 2

2 2

2 2

2 2

2 2

2 2

2 2

2 2

2 2

2 2

2 2

2 2

2 2

2 2

2 2

2 2

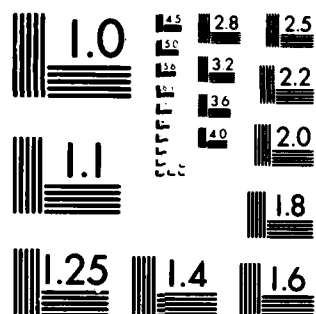
END

DATE

FILMED

6 82

DTIC



MICROCOPY RESOLUTION TEST CHART
NATIONAL BUREAU OF STANDARDS 1963 A

- o Normal display (Figure 48a). Smooth waveform. Constant amplitude and frequency
- o Hard journal-on-foil rub display (Figure 48c). Irregular waveform. Variation in amplitude and frequency
- o Light-to-incipient journal-on-foil rub (Figure 48b). Semiregular waveform. Characteristic flattened top exhibited by waveform. Reasonably regular amplitude and frequency

In actual testing, the oscilloscope traces described above are the principal mechanism for judging when the bearing has reached its load limit. This monitoring system also was a valuable tool in detecting when bearing overload occurred, allowing the load to be removed before serious overheating or seizure occurred.

4. BASIC BEARING TESTING

During this part of the program, a number of foil bearing configurations were tested. Table 10 presents a description of these bearing configurations.

a. Bearing Configuration 1

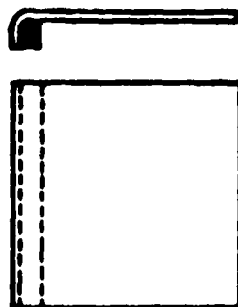
The basic bearing test rig was assembled with a 10-foil bearing configuration using Teflon-S coated foils and a chrome-plated journal. Since the 10-foil backing spring material was not yet available, a modified backing spring was fabricated from the 12-foil backing spring material available from Contract F33615-78-C-2044. Two modifications were considered (Figure 49):

(1) Cut foil trailing edge and lose at least one rib, with a potentially serious load carrying ability reduction (Figure 49a).

TABLE 10. CONFIGURATION DESCRIPTION

Config Number	No of Foils	Foils			Journal Coating	Sway (1) Space (inch)
		Length/Diameter (L/D) Ratio	Thickness (inch)	Coating		
1	10	1.2	0.00785	Teflon-S	Chrome	0.020
2	8	1.2	0.0091	Teflon-S	Chrome	0.021
3	10	1.2	0.0080	DES+Au Overcoat	SCA	0.022
3a	10	1.2	0.0080	DES	SCA	0.022
3b	10	1.2	0.0080	DES	SCA	0.022
4	8	1.2	0.0084	DES+Au Overcoat	SCA	0.023
4a	8	1.2	0.0084	DES+Au Overcoat Journal Side only	SCA	0.023
4b	8	1.2	0.0084	DES+Au Overcoat; Journal Side Trailing Edge only	SCA	0.023
4c	8	1.2	0.0084	DES	SCA	0.023
5	10	1.2	0.007	Co-20Ni	SCA	0.024
6	10	1.2	0.007	TiC	SCA	0.024

FOIL LEADING EDGE CONFIGURATION



$$(1) \text{ Sway Space} = D_H - D_J - 2(t_b + t_s) - 4 t_f$$

Foil carrier inside diameter = D_H

Journal diameter = D_J

Backing spring overall thickness = t_b

Backing spring shim thickness (if used) = t_s

Foil thickness = t_f

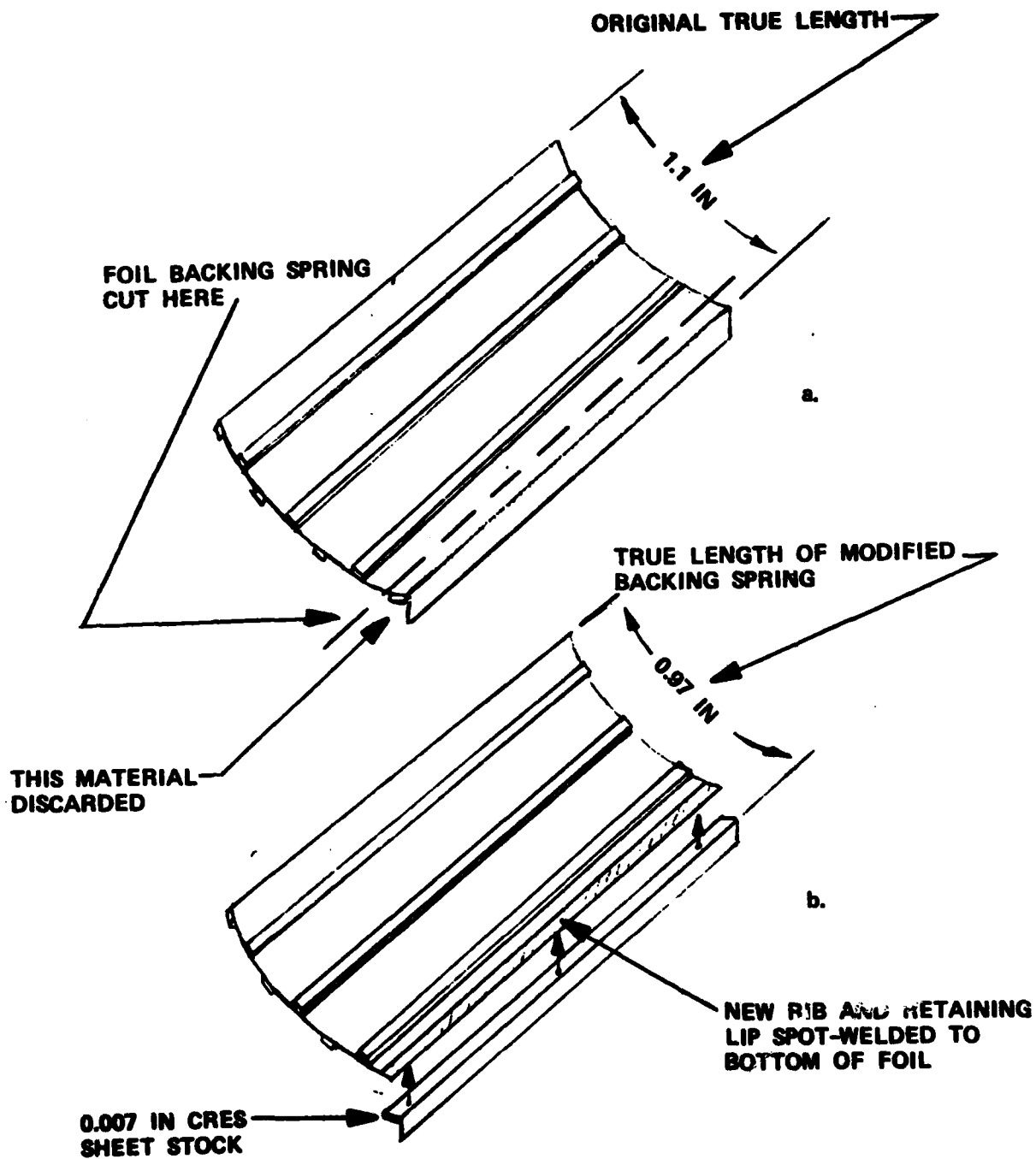


Figure 49. Foil Backing Spring Modification for 10-Foil Bearing.

(2) Cut foil leading edge and maintain original design with a spot-welded retaining lip and rib, and retain load-carrying ability (Figure 49b).

Modification (2) was selected.

A break-in procedure was run with a 1-g load. The initial breakaway torque (measured with torque wrench on drive shaft) was 17.5 in-lb, which increased to a maximum of 35 in-lb before disassembly after break-in. On disassembly, the bearing showed even wear on the foils with evidence of some debris on the foils. Breakaway torque after reassembly was 18 in-lb, which increased to a 20 in-lb maximum after 10 start-stops. Disassembly revealed even, well distributed burnishing of the foils with minimal debris.

The bearing was operated at its design speed of 33,200 rpm with 2-, 3-, 4-, and 5-g loads for 15 seconds at each load. Bearing behavior was excellent at all loads. The bearing then was disassembled and inspection showed the same evenly distributed burnishing with minimal debris. At this point, the foil carrier was removed for alignment and pinning of the anchor points for the loading system. Testing resumed after loading system alignment was completed.

The following test results were obtained:

o Transient Load:

500 pounds for 30-seconds duration

o Steady-State Load:

255-pound load for 8.5 minutes/journal temperature limit of 470°F*

*Load removed when journal temperature reached the 470°F temperature limit of the Teflon foil coating. No bearing anomaly during loaded time.

200-pound load for 17 minutes/journal temperature limit of 470°F*

160-pound load for 20 minutes/journal equilibrium temperature less than 470°F

- o 5 hours 40 minutes total run time, 39 starts

The sustained loads of 255 and 200 pounds were removed after the times listed above because journal temperature rose to levels that could have caused thermal decomposition of the foil coating (Teflon-S can tolerate a maximum temperature of 475°F). No anomalous behavior was exhibited by the bearing during the load application. The load removal was precautionary only.

During the transient load testing, no attempts were made to ascertain the ultimate load capacity of the Configuration 1 bearing since:

- o The test rig load application system was approaching its limit
- o The bearing load/duration requirements (Table 2) had already been exceeded

The bearing was run with a nominal 0.015 lb/sec cooling air flow. Lower cooling flow levels were tried while operating with a 200-pound steady-state load. Flows of 0.010 lb/sec and 0.005 lb/sec resulted in excessive foil carrier and journal heating and were discontinued after 8 and 5 minutes, respectively.

*Load removed when journal temperature reached the 470°F temperature limit of the Teflon foil coating; no bearing anomaly during loaded time.

Post-test disassembly and examination showed the bearing to be in excellent condition. Figure 50 is a view of the load-carrying region of the bearing with the foils still installed in the foil carrier. Figure 51 shows the foils laid out after removal from the carrier. The wear patterns shown on the foils are the result of start-ups and shutdowns, since there was no indication of journal-on-foil rub during load testing. The post-test journal condition was essentially the same as when installed.

b. Bearing Configuration 2

The basic bearing rig was assembled with an 8-foil bearing configuration using Teflon-S coated foils and a chrome-plated journal. A break-in procedure was run with a 1-g load. After break-in, the following test results were obtained:

o Transient Load:

524 pounds for 15-seconds duration

502 pounds for 30-seconds duration

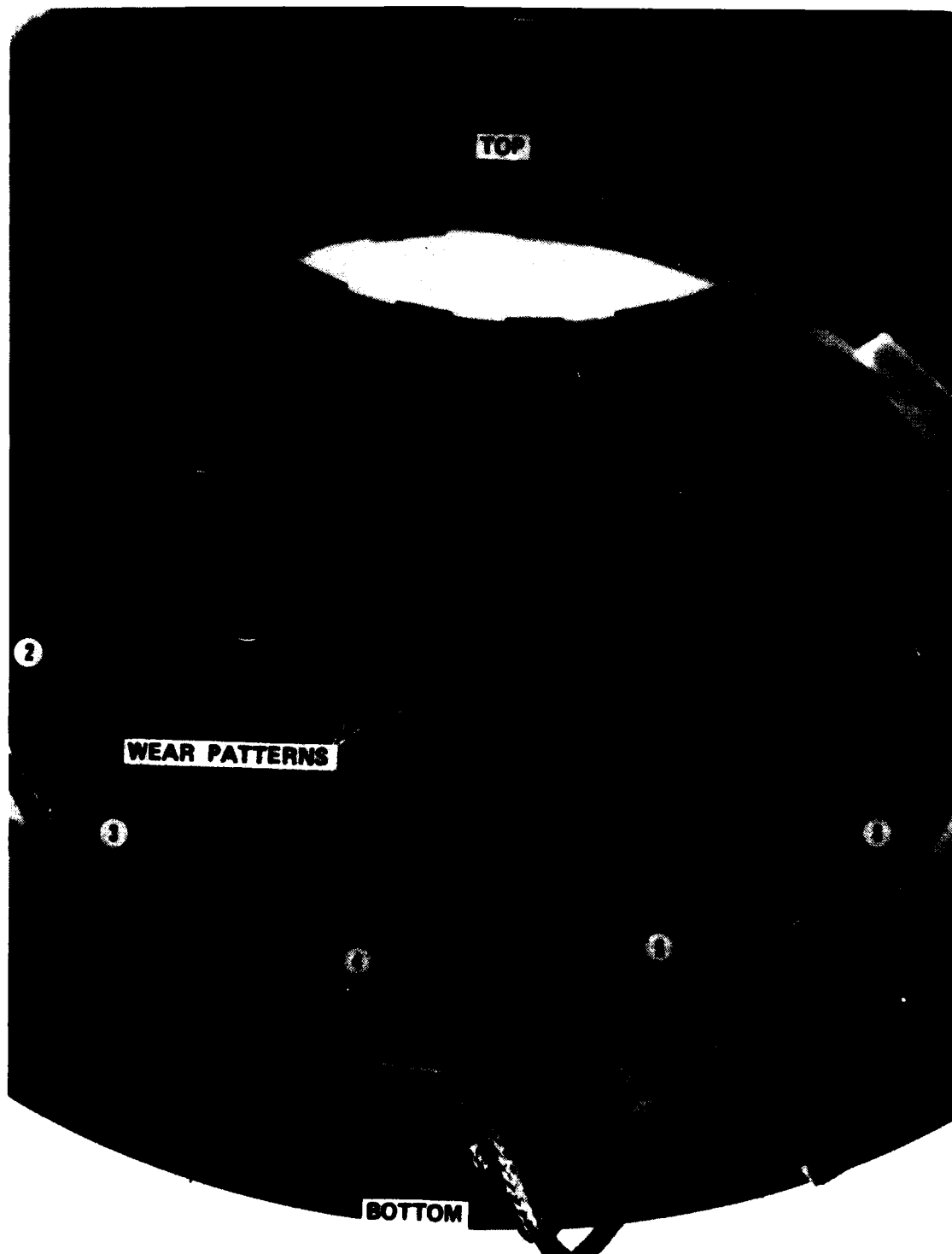
o Steady-State Load:

300 pounds for 6 minutes/journal temperature limit of 470°F*

250 pounds for 25 minutes/journal equilibrium temperature 470°F

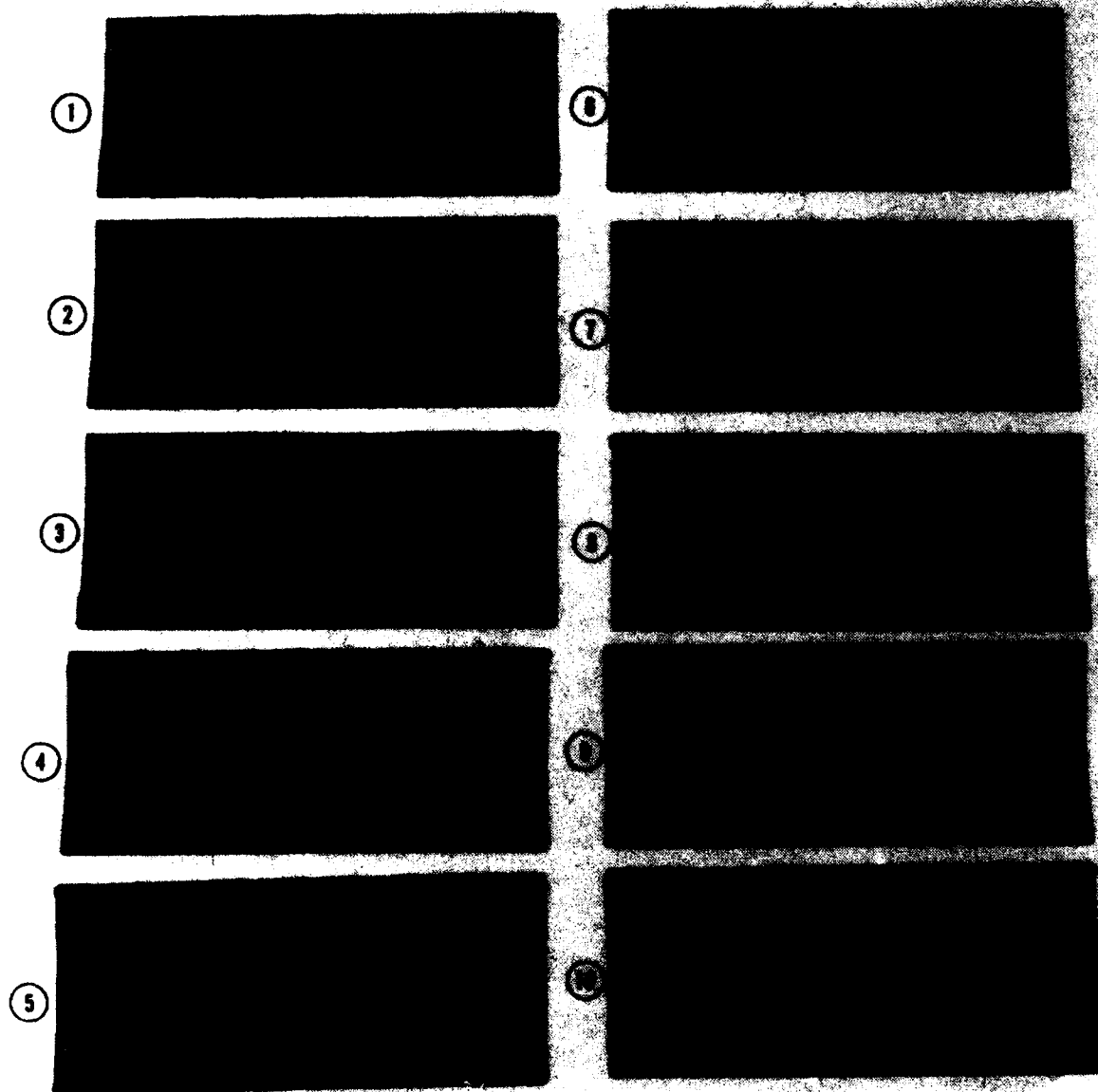
o 4 hours, 12 minutes total run time, 22 starts

*Load removed when journal temperature reached the 470°F temperature limit of the Teflon foil coating; no bearing anomaly during loaded time.



(CONFIGURATION 1)

Figure 50. 10-Foil Bearing Wear Pattern View of "LOAD CARRYING" Region.



(CONFIGURATION 1)

Figure 51. 10-Foil Bearing Post-Test Foil Condition.

The sustained 300-pound load on the bearing was removed as a precautionary measure when the journal temperature reached 470°F. Transient load testing also was limited for the same reasons as for the Configuration 1 bearing.

Post-test disassembly and examination showed the bearing to be in excellent condition. Wear patterns were essentially the same as the 10-foil, Configuration 1 bearing wear patterns shown in Figures 50 and 51. At no time during testing were any indications of journal-on-foil rub during loading noted.

c. Bearing Configurations 3, 3a, 3b

These bearings all were high-temperature, 10-foil configurations, characterized generally by utilizing Kaman SCA as the journal coating and Kaman DES as the "base" (or only) foil coating. Bearing configurations characteristics are described in Table 11.

(1) Bearing Configuration 3

Testing with the Configuration 3 bearing (essentially a high-temperature version of the Configuration 1 bearing) was conducted with journal operating temperatures ranging from 875 to 1040°F. The following test results were obtained:

o Transient Load

290 pounds for 20-seconds duration at a maximum temperature of 1015°F

o Steady-State Load

185 pounds for 105-seconds duration at a maximum temperature of 950°F

TABLE 11. BEARING CONFIGURATION
3, 3a, 3b CHARACTERISTICS

Configuration	Journal Coating	Foil Coating	Backing Spring	Comment
3	Kaman SCA	Kaman DES + Gold Overcoat	Narrow Rib Spacing (Same as Configuration 1)	Sputtered gold overcoat (15,000Å thick) All over foils
3a	Kaman SCA	Kaman DES	Narrow Rib Spacing (Same as Configuration 1)	
3b	Kaman SCA	Kaman DES	Wide Rib Spacing	

Testing with bearing Configuration 3 showed that both transient and steady load capacities were lower than for the 10-foil Teflon (Configuration 1) bearing upon which it is based. Disassembly of the bearing showed that the gold overcoat was lost from the foils, with subsequent gold "build-up" being deposited on the journal. A gold overcoat loss, and attendant reduction in bearing load capacity also had been encountered during fulfillment Contract F33615-78-C-2044.

(2) Bearing Configuration 3a

The Configuration 3a bearing was the same as the Configuration 3 bearing, except for removal of all foil gold overcoating.

This bearing configuration did not give good results, and displayed operating instability when carrying a 160-pound test load at 960°F journal temperature.

Disassembly examination of the bearing showed inordinately heavy wear marks aligned with the backing spring rib spacing (Figure 52). (Note that the "narrow spacing" backing springs utilized in Configuration 3a were originally designed for a 12-foil bearing, but were pressed into service when the proper "wide spacing" 10-foil backing springs were not yet available.)

(3) Bearing Configuration 3b

The most significant feature of the Configuration 3b bearing was the utilization of backing springs with the "wide spaced" ribs originally intended for use with the 10-foil bearing configuration. The following test results were obtained with this bearing configuration:

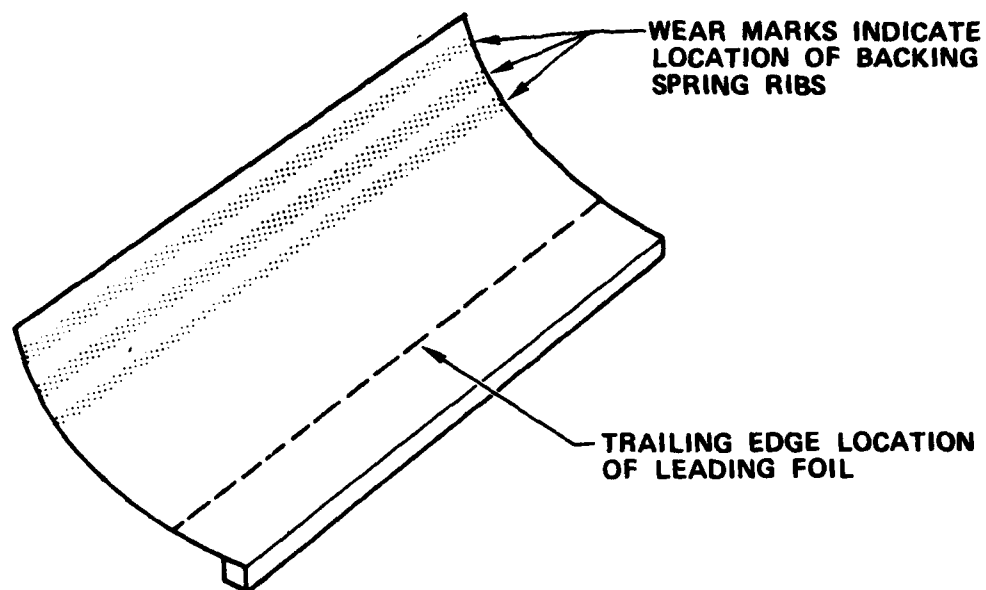


Figure 52. Configuration 3a Post-Test Foil Wear Pattern.

o Transient Load

310 pounds for 15-seconds duration at room temperature test conditions

340 pounds for 15-seconds duration at a maximum temperature of 995°F

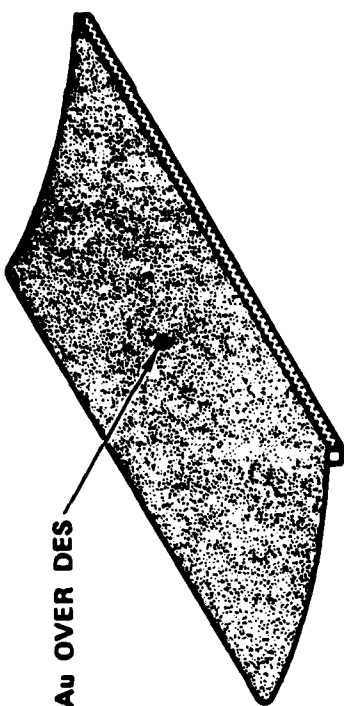
This bearing configuration performed very well throughout testing. Bearing operation was stable and free of anomalous behavior. Disassembly showed the bearing to be in excellent condition with a uniform, well-distributed wear pattern on the foils. The journal condition also was excellent, with a highly polished surface finish.

d. Bearing Configurations 4, 4a, 4b, 4c

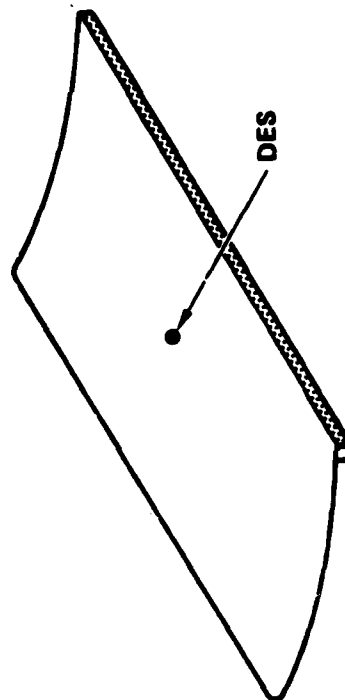
These bearings all were high temperature, 8-foil configuration, characterized generally by utilizing Kaman SCA as the journal coating and Kaman DES as the base foil coating. Several variations of gold overcoat to the Kaman DES coated foils also were tested. These variations are further described in Figure 53.

(1) Bearing Configuration 4

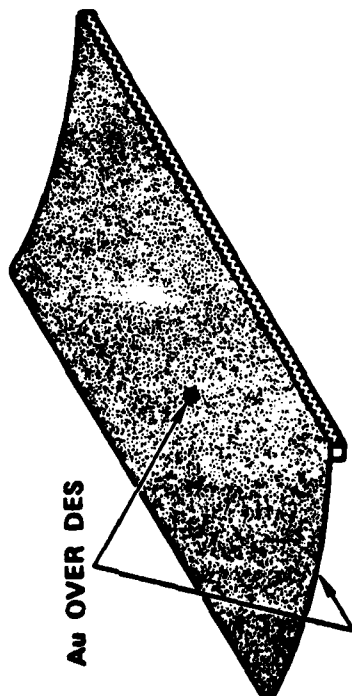
The Configuration 4 bearing, essentially a high-temperature version of the Configuration 2 bearing, utilizes a sputtered gold overcoat of 15,000Å thickness all over the foils, similar to the Configuration 3 foils. In initial ambient temperature testing, the Configuration 4 bearing would not sustain a 200-pound load for 15 seconds. In an effort to determine whether the low load capacity was bearing- or rig-related, the Configuration 2 Teflon-S foils were installed and run against the Configuration 4 Kaman SCA-coated journal. With the Teflon foils,



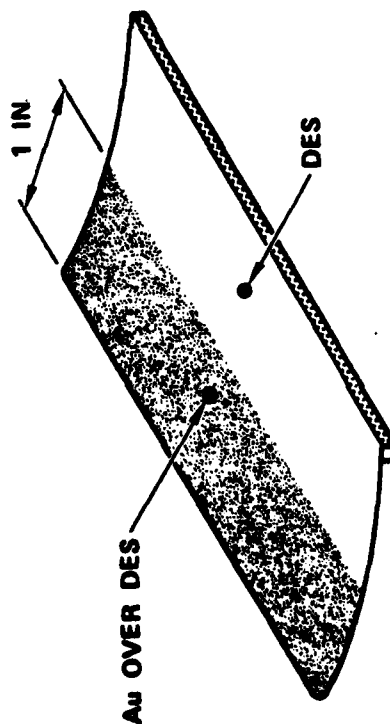
4a. GOLD OVERCOAT ON BEARING-
VS-JOURNAL SURFACE ONLY



4c. NO GOLD OVERCOAT
KAMAN DES ONLY



4. GOLD OVERCOAT 15,000 Å
OVER ENTIRE FOIL SURFACE



4b. GOLD OVERCOAT ON TRAILING EDGE
OF JOURNAL VS BEARING SURFACE

Figure 53. Configuration 4 Variations.

the bearing sustained a 439-pound load for 30 seconds, indicating that the low load capability was a bearing problem.

The gold coating was suspected as a possible cause of this problem due to the quantity of gold that was lost from the foils during running. Another factor was the high coefficient of friction of a gold-vs-gold friction couple, which exists when both sides of the foil are gold-coated. This high friction possibly could reduce the bearing compliance in the foil overlap regions.

(2) Bearing Configuration 4a

This bearing configuration had gold overlay on the foil-vs-journal side only (Figure 53). Both the gold and DES were removed from the back (foil carrier) side of the foils, exposing the X-750 foil substrate material. Coating removal was done by the vapor honing process.

Configuration 4a sustained a maximum load of 360 pounds for 15 seconds and a continuous load of 280 pounds for 2 minutes and 5 seconds. These loads, which were imposed at ambient temperature condition to expedite comparative testing of the gold overcoat, represent a substantial increase in load carrying capability over Configuration 4.

In spite of this improved bearing performance, post-test examination of the bearing suggested that there was merit in reducing the gold overcoat even further.

(3) Bearing Configuration 4b

For the Configuration 4b "reduced extent" gold overcoat foils, only the foil-vs-journal side of the foil was gold-coated, and then only in the trailing edge region (Figure 53) to a thickness of 15,000Å. In ambient temperature

testing, this configuration sustained a maximum load of 400 pounds for 10 seconds, representing a marginal improvement over Configuration 4a. Localized gold buildups resulting from gold-to-gold adhesion still were noted after bearing disassembly, in spite of the significant reduction of gold utilized in the foil configuration. It was speculated that these gold buildups, which induced localized foil warpage, caused air film disturbances that limited bearing load capacity. (Some gold buildups actually were higher than projected air film thicknesses on the load-bearing portion of the foil.) The next step was complete removal of the gold overcoat.

(4) Bearing Configuration 4c

Testing with the Configuration 4c bearing (no gold overcoat on foils) was conducted at temperatures from ambient up to 850°F. The following test results were obtained:

o Transient Load

405 pounds for 15-seconds duration at room temperature test conditions

425 pounds for 15-seconds duration at a maximum temperature of 840°F

490 pounds for 15-seconds duration at a maximum temperature of 900°F

o Steady-State Load

200-pound load for 20-minutes duration at a maximum temperature of 870°F

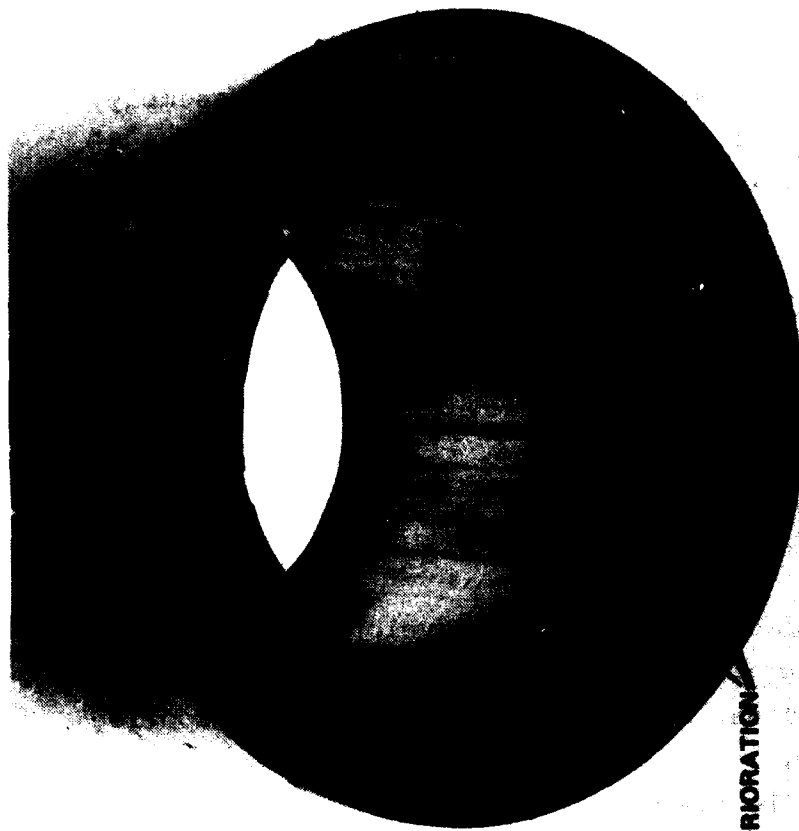
After successfully carrying the 490 pound test load for 15 seconds at 900°F (which satisfies the program requirements listed in Table 2), loading was continued for an additional 5 seconds, during which time foil-to-journal rub occurred. The rig was stopped and a restart made at a journal temperature of 850°F. Several unsuccessful attempts were made to reload the bearing with a 380-pound load. However, continued steady-state operation at 850°F with a 1-g load was satisfactory, with no performance anomalies indicated by the test instrumentation.

Figure 54 shows the bearing after disassembly. Edge region foil damage is apparent in the photo. Figure 55 shows the journal area where a small quantity of foil material adhered to the journal. The bearing damage is not considered severe. The journal probably was recoverable by a grinding and one-step recoating process to seal coating porosity. Had slightly less foil material adhered to the journal, it could have been made serviceable by a simple manual dressing and honing operation. The foil carrier is undamaged.

5. ALTERNATE FOIL COATINGS

A foil bearing coating materials development task was included in another on-going Garrett Program*. Two candidate foil coatings developed under this U.S. Navy program were applied to foils in this program, and tested against the previously used Kaman SCA coated journal in the basic bearing test rig at ambient and elevated temperatures.

*Navy Advanced SPS/APU Foil Bearing Development Program, Contract N00140--79-C-1296.



AREAS OF FOIL DETERIORATION
DUE TO HARD RUB

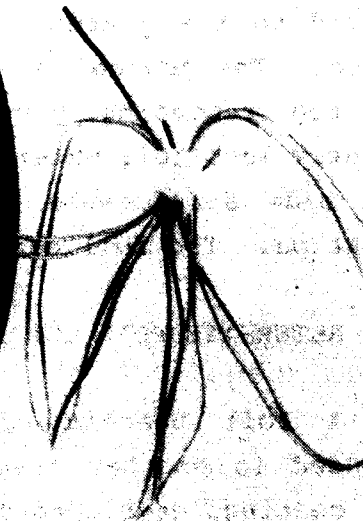
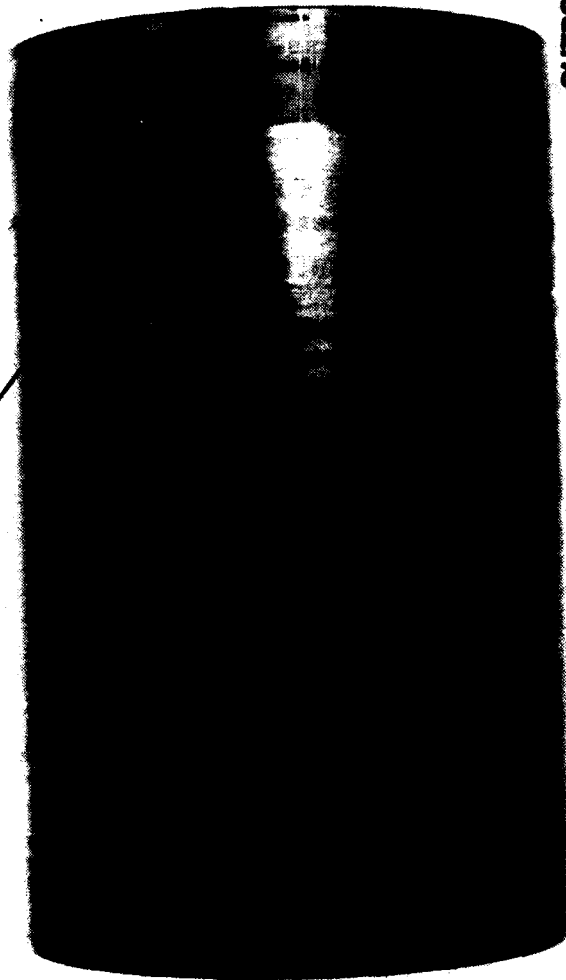


Figure 54. Configuration 4C Bearing. Post-Test Condition After High-Temperature, High-Load Testing.

WELDED ON
FOIL SUBSTRATE MATERIAL



OUTBOARD END

Figure 55. Configuration 4C Journal. Post-Test Condition After High-Temperature, High-Load Testing.

a. Bearing Configuration 5

The 10-foil, Configuration 5 bearing (Table 9) utilized electroplated Co-20Ni foils, that were heat-treated prior to use to develop a lubricious oxide layer on the coating surface.

Testing began with a series of start/stops at ambient temperature. Bearing breakaway torque increased steadily through the start/stop series. Disassembly of the bearing and visual inspection of the foil coating showed that the oxide layer on the foil surface was being rubbed off during the starts and stops.

High-temperature testing under load was initially performed with journal temperatures ranging from 765 to 820F and loads from 31 to 155 pounds. The rig then was stopped to reset the loading device. Journal temperature was maintained at approximately 765°F during this procedure. A restart could not be made, indicating a substantial increase in bearing breakaway torque. A check showed that the breakaway torque had increased to approximately 3 times the torque before hot load testing began.

Bearing disassembly again showed the foil oxide film was rubbing off in the area of foil-to-journal contact. Although the foil oxide film renews itself during operation at high temperature or at hot soak, when the bearing is stopped the oxide film is apparently rubbed off and does not renew itself sufficiently. This behaviour compromises the usefulness of Co-20Ni as a high-temperature foil coating when run against Kaman SCA journal coatings. Testing of Co-20Ni vs Kaman SCA was discontinued at this point.

Although Co-20Ni coated foils do not appear to be satisfactory where coupled with an SCA-coated journal, Co-20Ni

may still provide satisfactory results with less abrasive journal coatings, such as Triballoy 400.

b. Bearing Configuration 6

The 10-Foil Configuration 6 bearing (Table 9) utilized sputtered TiC-coated foils, and the same Kaman SCA-coated journal run with the Configuration 5 bearing.

A standard bearing break-in procedure at ambient temperature was run. Bearing breakaway torque did not increase significantly during this series of start/stops.

High-temperature testing began with 31- through 155-pound-loads applied for 15 seconds duration at a 765°F journal temperature. Bearing operation at this load and temperature level was very stable. The bearing temperature was therefore increased to 1200°F. Bearing operation at 1200°F journal temperature also was very stable with loads of 31- to 155-pounds. A 31-pound bearing restart was made at 1200°F with no apparent breakaway torque increase over previous levels.

Final high-temperature load testing resulted in a maximum load of 410 pounds for 15 seconds duration at 1256°F journal temperature. Another 31-pound hot start was made at 965°F without difficulty.

Bearing teardown revealed very little foil coating wear as shown in Figure 56. The most readily apparent change in the coating was a change in color from the original silvery TiC to a straw color. Very limited areas of coating discoloration were noted, but no flaking, peeling or chipping of the TiC occurred. TiC foil coating proved to be an extremely durable, heat resistant coating with minimal friction increases after repeated start/stops and operation at 1200°F. TiC does, however, exhibit

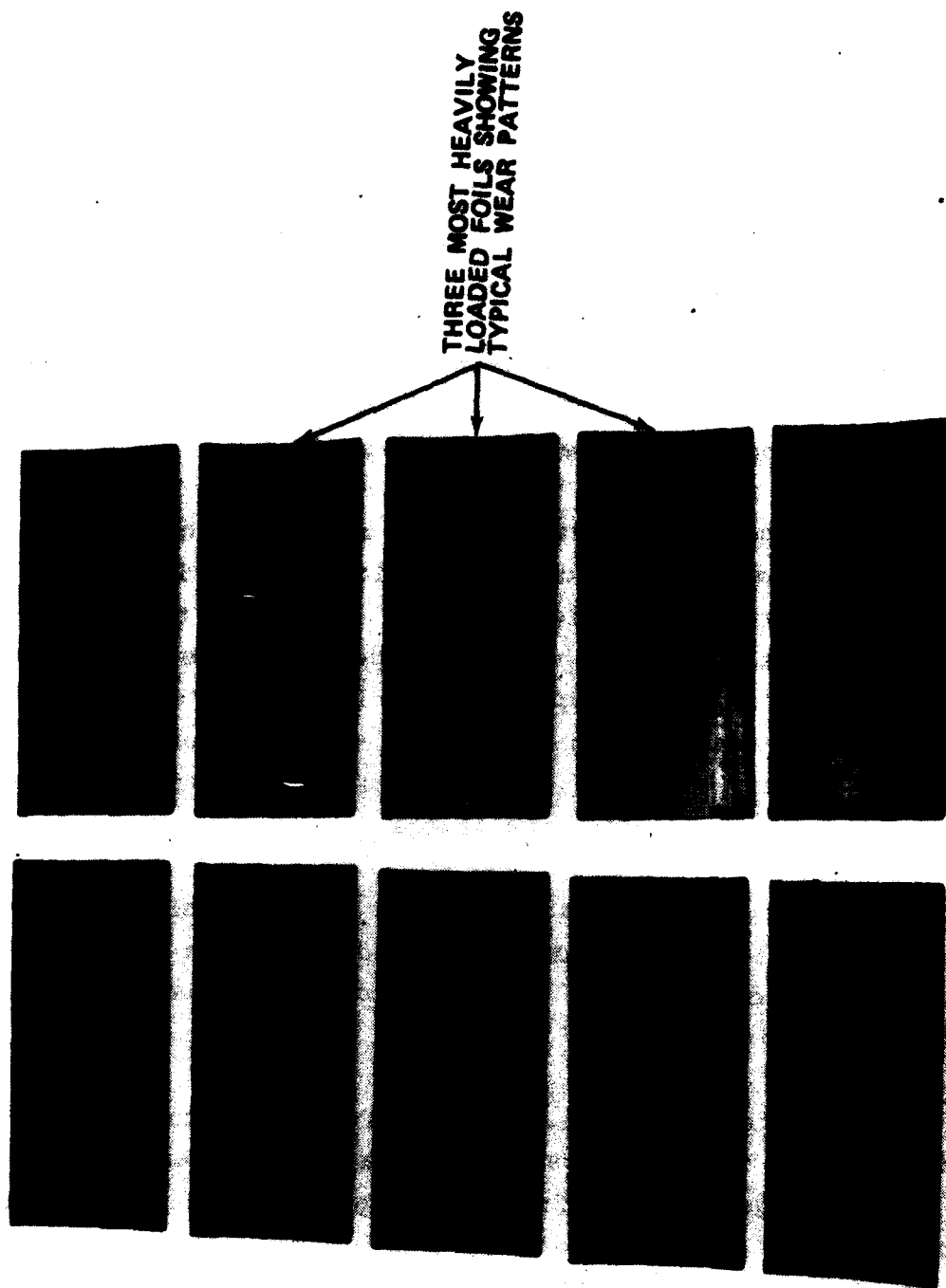


Figure 56. Configuration 6 TiC Coated Foils After Testing at 1200°F.

a reasonably high (but stable) breakaway torque when coupled with an SCA-coated journal.

6. INSTRUMENTED JOURNAL TESTING

As a final task in the basic bearing rig test program, a test foil bearing was specially instrumented to measure the film pressure and film thickness in an operating foil bearing. The bearing utilized for this task was the 8-foil, Configuration 2 bearing, employing Teflon-S coated foils and a chrome-plated journal. The pressure and clearance probes were installed in the journal and the sensor signals conveyed to signal conditioners by means of a slip-ring assembly.

a. Test Rig Setup

A Garrett-developed slip-ring assembly was adapted to the existing 3.5-inch foil bearing test rig. Figure 57 shows the basic rig layout. Figure 58 shows the slip-ring installation for the basic rig.

(1) Pressure Measurement Setup

Pressure probes were located in a modified journal as shown in Figure 59. Figure 60 details the pressure probe installation. The two pressure probes used were Entran Devices Inc. Model EPI-080-100. Calibration was accomplished with the probes in place in the journal.

(2) Film Thickness Measurement Setup

Film thickness (displacement) probes were located as shown in Figure 59. Probe faces were lapped to the journal radius in place. The two probes used were Wayne-Kerr type

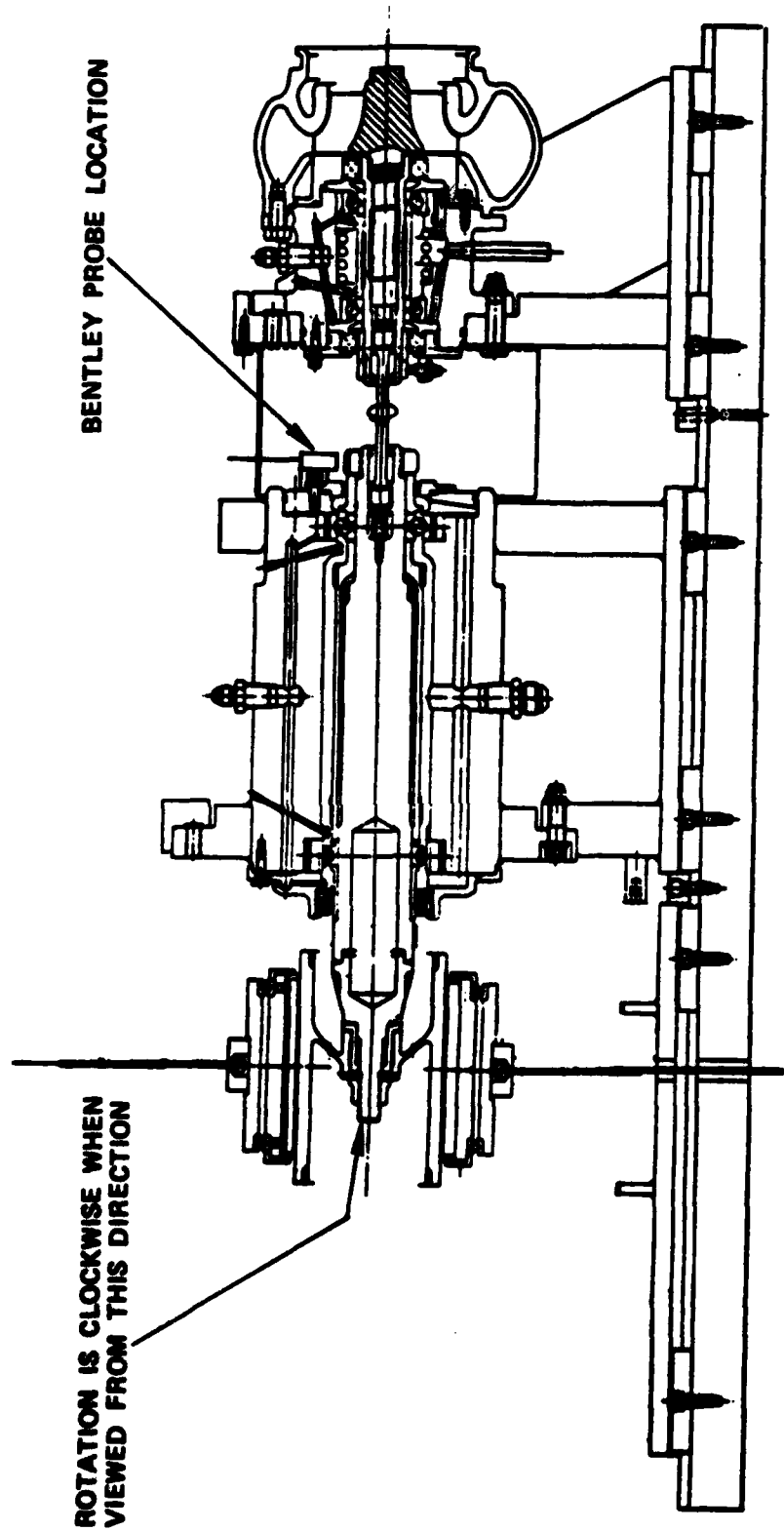


Figure 57. Test Rig Assembly Without Instrument Holder or Slip-Ring Assembly.

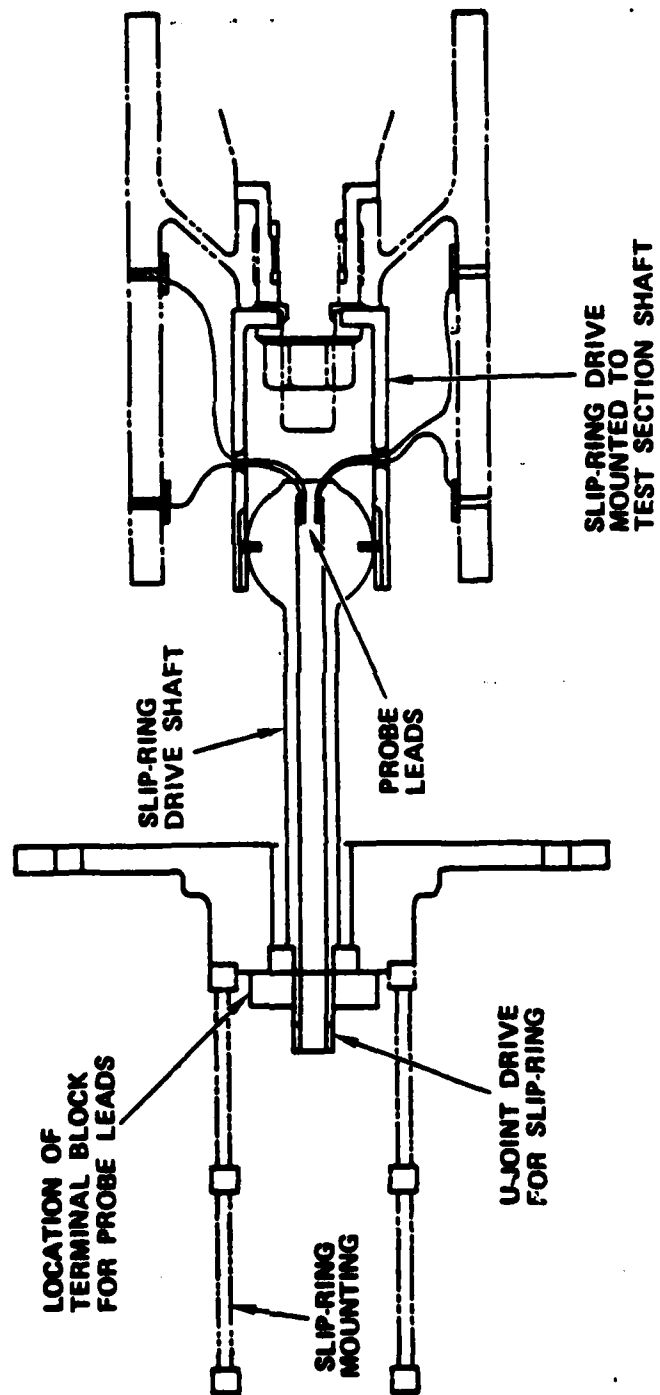


Figure 58. Probe Slip-Ring Installation on Basic Bearing Rig.

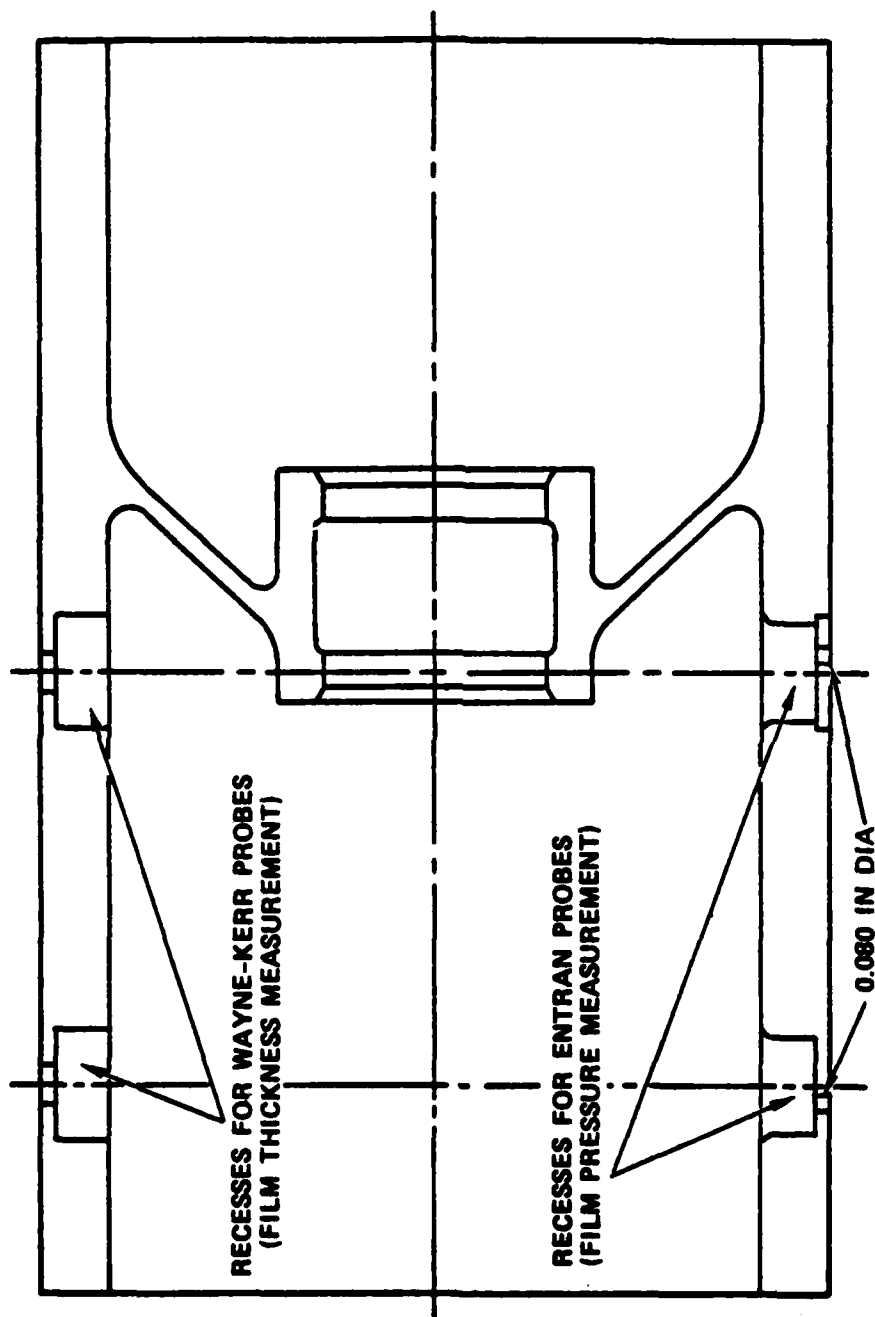


Figure 59. Pressure and Displacement Probe Locations.

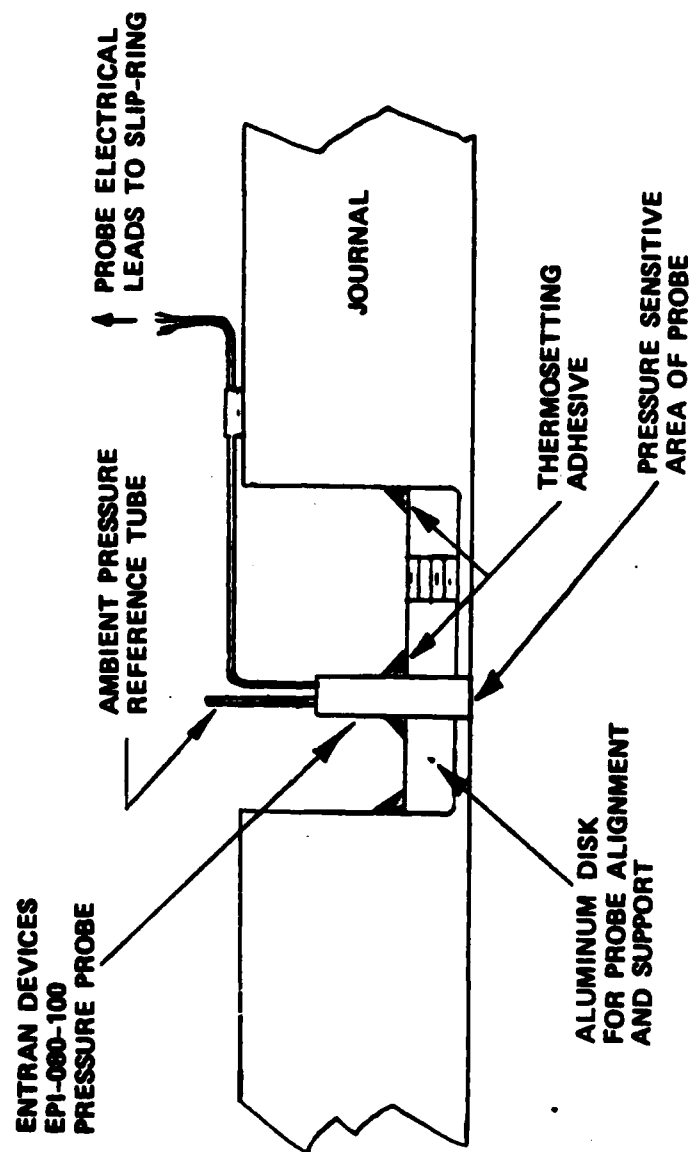


Figure 60. Detail of Pressure Probe Installation in Journal.

capacitance probes, fabricated by Garrett, and used with a Wayne-Kerr signal conditioner. Calibration was accomplished with the probes in the journal.

(3) Additional Instrumentation Setup Information

A Bentley probe was installed in the location shown in Figure 57. This probe was used with a single-flat nut to generate a 1/rev pulse as an oscilloscope display trigger.

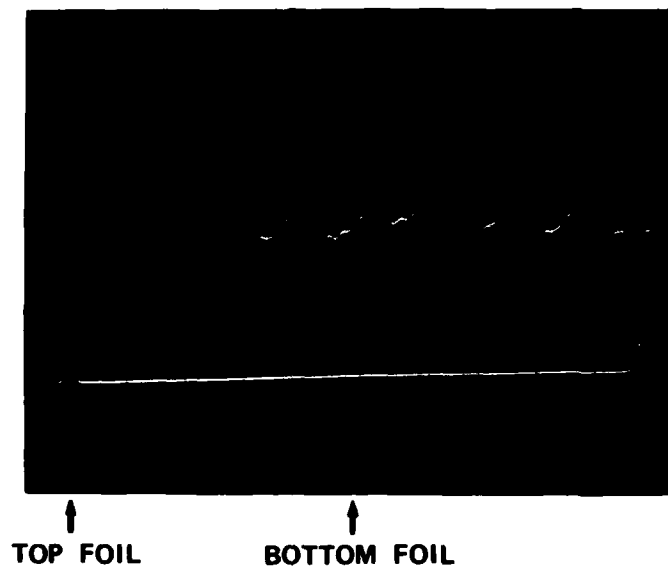
Dual trace oscilloscopes were used. Displays were photographed using a Polaroid camera.

b. Pressure Measurement Test Results

Only the outboard pressure probe was operational during testing. Oscilloscope display calibrations are noted in Figures 61 through 71. Noise problems were so severe that only a limited number of film pressure photos were taken.

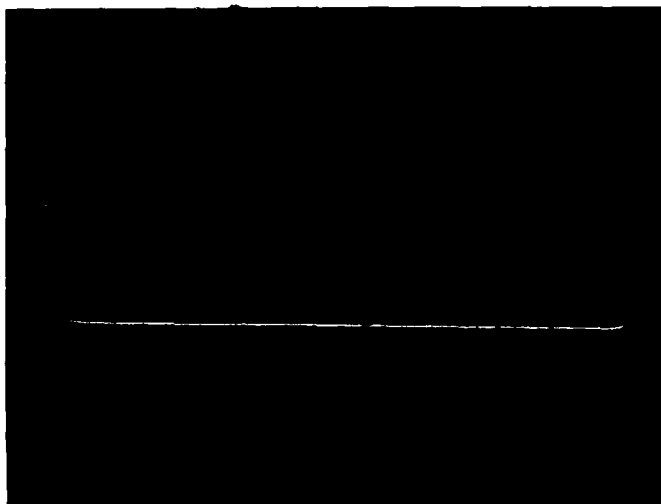
The pressure profiles displayed in Figures 61 through 71 represent clockwise rotation of the journal (looking at the open end of the journal) going from left to right. The trigger for the oscilloscope display was a Bentley probe located at top dead center on the test shaft nut. (See Figure 57). Refer to Figure 61 to determine radial location of foils in the bearing. Outboard pressure probe disintegration halted pressure testing.

The solid line in Figure 72 (which reproduces a portion of the pressure field data on Figure 68) shows a typical measured no-load pressure field profile, while the broken line presents the analytically determined curve for the same bearing and operating conditions. Note (in Figure 72) the relationship of the measured and calculated pressure profiles with each other and



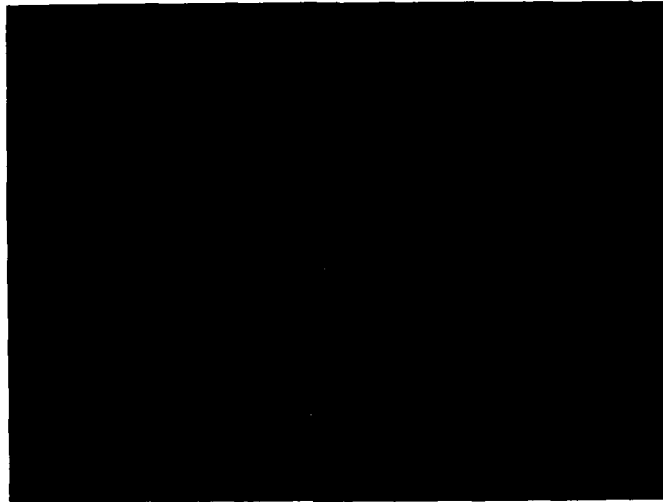
DATE: 3 FEB 81
SPEED: 12,000 RPM
LOAD: 0
PARAMETER: OUTBOARD PRESSURE
UPPER TRACE CALIBRATION: 1 MAJOR DIVISION/~2.0 PSI
LOWER TRACE CALIBRATION: 1 PULSE/REV.
COMMENTS: INITIAL PHOTO OF PRESSURES ACROSS ALL EIGHT FOILS

Figure 61. Instrumented Journal Data, 3.5-Inch Foil Bearing
(Photo No. 1).



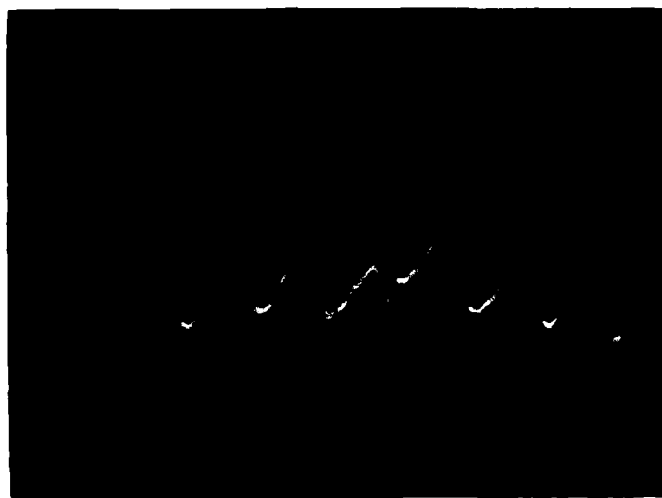
DATE: 3 FEB 81
SPEED: 12,000 RPM
LOAD: 0
PARAMETER: OUTBOARD PRESSURE
UPPER TRACE CALIBRATION: 1 MAJOR DIVISION/~2.0 PSI
LOWER TRACE CALIBRATION: 1 PULSE/REV.
COMMENTS:

Figure 62. Instrumented Journal Data, 3.5-Inch Foil Bearing
(Photo No. 2).



DATE: 3 FEB 81
SPEED: 12,300 RPM
LOAD: 0
PARAMETER: (UPPER) OUTBOARD PRESSURE, (LOWER) OUTBOARD FILM THICKNESS
UPPER TRACE CALIBRATION: 1 MAJOR DIVISION/~2.0 PSI
LOWER TRACE CALIBRATION: NONE
COMMENTS: FILM THICKNESS TRACE OVERCLAMPED AND NOISY, COMPLETELY
WITHOUT RESOLUTION

Figure 63. Instrumented Journal Data, 3.5-Inch Foil Bearing
(Photo No. 3).



DATE: 3 FEB 81
SPEED: 12,300 RPM
LOAD: 0
PARAMETER: PRESSURE ACROSS FOILS
UPPER TRACE CALIBRATION: 1 MAJOR DIVISION/~1.0 PSI
LOWER TRACE CALIBRATION: NONE
COMMENTS:

Figure 64. Instrumented Journal Data, 3.5-Inch Foil Bearing
(Photo No. 4).



← AMBIENT

DATE: 3 FEB 81
SPEED: 18,000 RPM
LOAD: 0
PARAMETER: PRESSURE
UPPER TRACE CALIBRATION: 1 MAJOR DIVISION = 2.5 PSI
LOWER TRACE CALIBRATION: NONE
COMMENTS: NOTE THE AMBIENT REFERENCE MARKED ON THE PHOTO AT THE
TIME IT WAS TAKEN. THIS CAN BE USED AS AN APPROXIMATE
AMBIENT PRESSURE REFERENCE FOR FIGURES 66 THROUGH 69.
SIGNAL IS ALSO NOISY.

Figure 65. Instrumented Journal Data, 3.5-Inch Foil Bearing (Photo No. 5).



DATE: 4 FEB 81

SPEED: 18,000 RPM

LOAD: 0

PARAMETER: (UPPER) PRESSURE, (LOWER) FILM THICKNESS

UPPER TRACE CALIBRATION: 1 MAJOR DIVISION = 2.5 PSIG

LOWER TRACE CALIBRATION: NOT ESTABLISHED

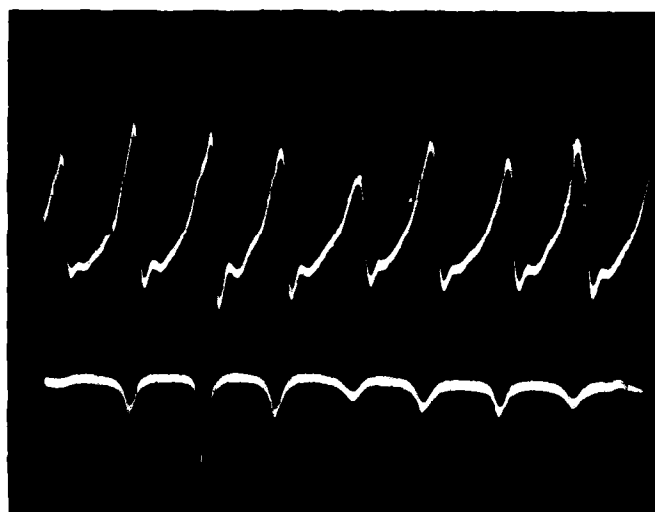
COMMENTS: PROPERLY FILTERED SIGNAL FOR PRESSURE TRACE. NOTE FILM THICKNESS NOTES TO THE RIGHT OF PHOTO 6.

Figure 66. Instrumented Journal Data, 3.5-Inch Foil Bearing (Photo No. 6).



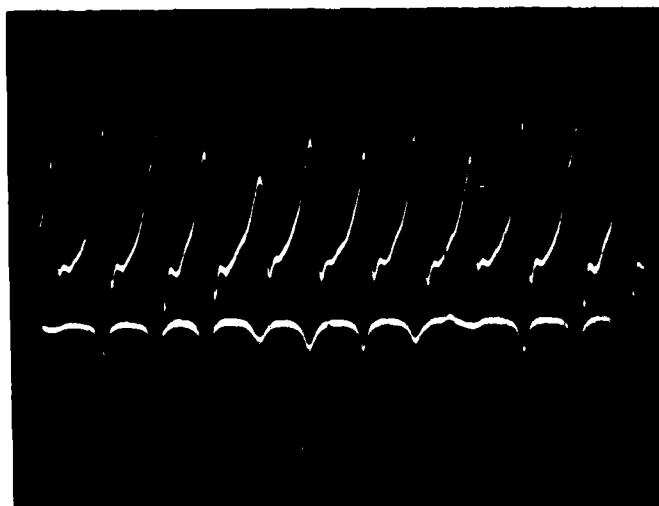
DATE: 4 FEB 81
SPEED: 18,000 RPM
LOAD: 0
PARAMETER: (UPPER) PRESSURE, (LOWER) FILM THICKNESS
UPPER TRACE CALIBRATION: 1 MAJOR DIVISION = 2.5 PSIG
LOWER TRACE CALIBRATION: NOT ESTABLISHED
COMMENTS:

Figure 67. Instrumented Journal Data, 3.5-Inch Foil Bearing
(Photo No. 7.)



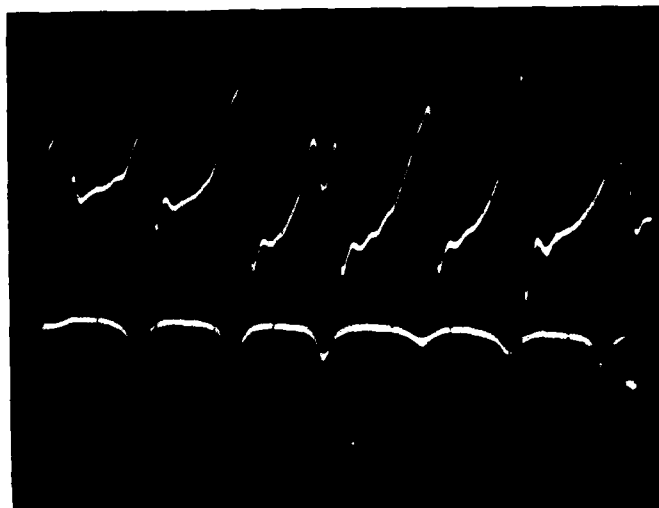
DATE: 4 FEB 81
SPEED: 18,000 RPM
LOAD: 0
PARAMETER: (UPPER) PRESSURE, (LOWER) FILM THICKNESS
UPPER TRACE CALIBRATION: 1 MAJOR DIVISION = 2.5 PSIG
LOWER TRACE CALIBRATION: NOT ESTABLISHED
COMMENTS:

Figure 68. Instrumented Journal Data, 3.5-Inch Foil Bearing
(Photo No. 8).



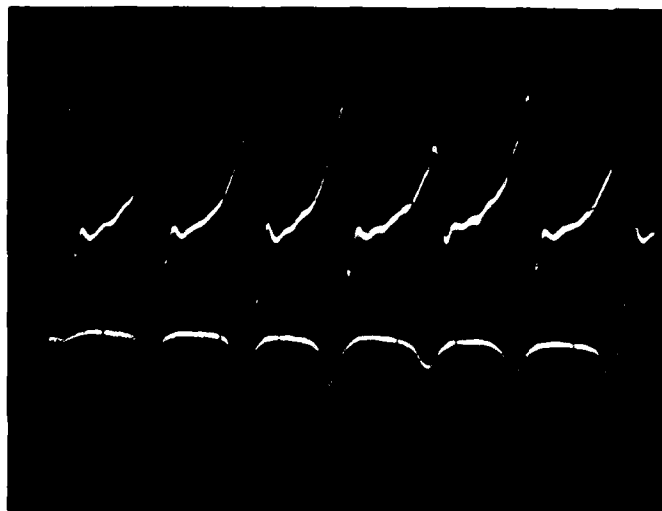
DATE: 4 FEB 81
SPEED: 18,000 RPM
LOAD: 0
PARAMETER: (UPPER) PRESSURE, (LOWER) FILM THICKNESS
UPPER TRACE CALIBRATION: 1 MAJOR DIVISION = 2.5 PSIG
LOWER TRACE CALIBRATION: NOT ESTABLISHED
COMMENTS:

Figure 69. Instrumented Journal Data, 3.5-Inch Foil Bearing
(Photo No. 9).



DATE: 4 FEB 81
SPEED: 13,500 RPM
LOAD: $\sim 1/2$ g
PARAMETER: (UPPER)
UPPER TRACE CALIBRATION: 1 MAJOR DIVISION = 2.5 PSIG
LOWER TRACE CALIBRATION: NOT ESTABLISHED
COMMENTS: NOTE THE DOUBLE PRESSURE PEAK ON THE BOTTOM FOIL
(THE ONE BEARING THE HIGHEST LOAD).

Figure 70. Instrumented Journal Data, 3.5-Inch Foil Bearing
(Photo No. 10).



DATE: 4 FEB 81

SPEED: 13,500

LOAD: 0

PARAMETER: (UPPER) PRESSURE, (LOWER) FILM THICKNESS

UPPER TRACE CALIBRATION: 1 MAJOR DIVISION = 2.5 PSIG

LOWER TRACE CALIBRATION: NOT ESTABLISHED

COMMENTS: AMBIENT PRESSURE REFERENCE MARKED AS
0 ON OSCILLOSCOPE SCREEN.

Figure 71. Instrumented Journal Data, 3.5-Inch Foil Bearing
(Photo No. 11).

with the foils and backing springs, whose relative positions are also shown. Of interest is the measured secondary pressure peak in the region immediately behind the trailing edge of an overlapping foil. The exact cause of this pressure peak is not yet known but it is in a region which experiences heavy recirculation, and is worth further analytical pursuit.

Figure 73 (which reproduces a portion of the pressure field data of Figure 70) shows the measured pressure profile on the heavily loaded foil when the bearing load was 1/2 to 1-g.

Even though a limited amount of data was obtained, this data was invaluable in improving the modeling of this type bearing.

c. Film Thickness Measurement

This measurement is regarded as inconclusive. The traces shown in the photos provide an indication of the point of minimum film thickness only (Figure 66). Oscilloscope calibration was set at 50mv/cm. This calibration gives 30cm (30 major divisions on display screen) for no-clearance to saturation voltage spread. Saturation voltage of the film thickness probe shown in the photos is 1.8v/6mil (this is for the outboard probe).

When the pressure probe noise problems were solved, allowing time to debug the Wayne-Kerr probe noise and calibration problem, the lead to the outboard probe failed. An effort to proceed using data from the inboard probe was made, but was unsuccessful because of extraneous signals that appeared to be slip ring noise.

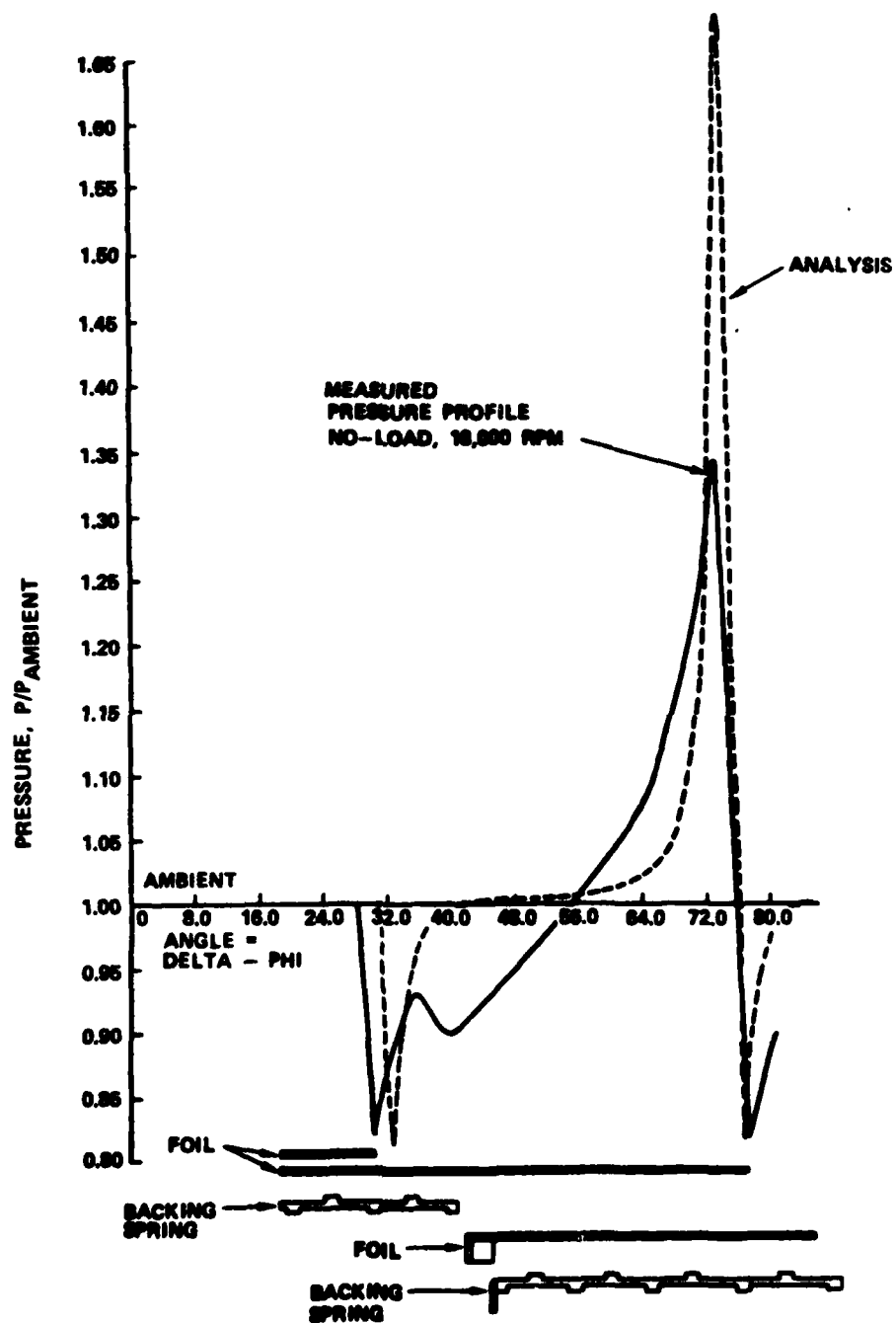


Figure 72. Pressure Field Relationship With Foils and Backing Springs.

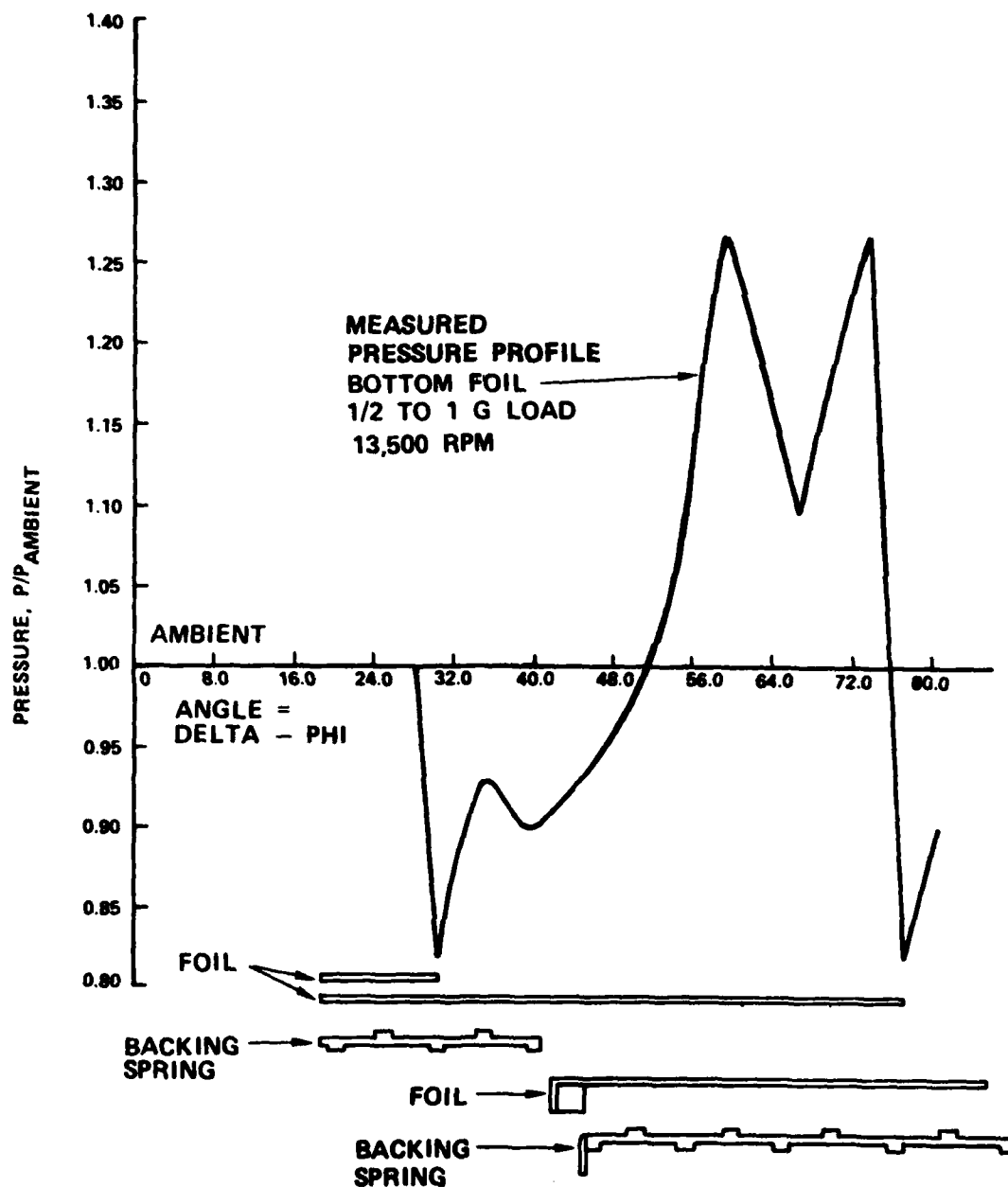


Figure 73. Measured Pressure Field Relationship With Foils and Backing Springs.

d. Additional Comments

Bearing air film pressure and thickness measurements were halted by probe failure and malfunction. Figure 74 shows the result of pressure probe disintegration. The bearing area adjacent to the outboard pressure probe (Figure 75) has all of the Teflon-S coating worn away. Some of the foil material is eroded, but the bearing was still operating without undue distress. Figure 76 shows the Wayne-Kerr probes. There was no physical or electrical damage to the film thickness probes resulting from pressure probe disintegration. Electrical problems prevented the acquisition of meaningful film thickness data. These problems resulted from severe noise, calibration difficulties, and probe lead failure from centrifugal force.



Figure 74. Bearing Showing Damage Resulting From Pressure Probe Disintegration.

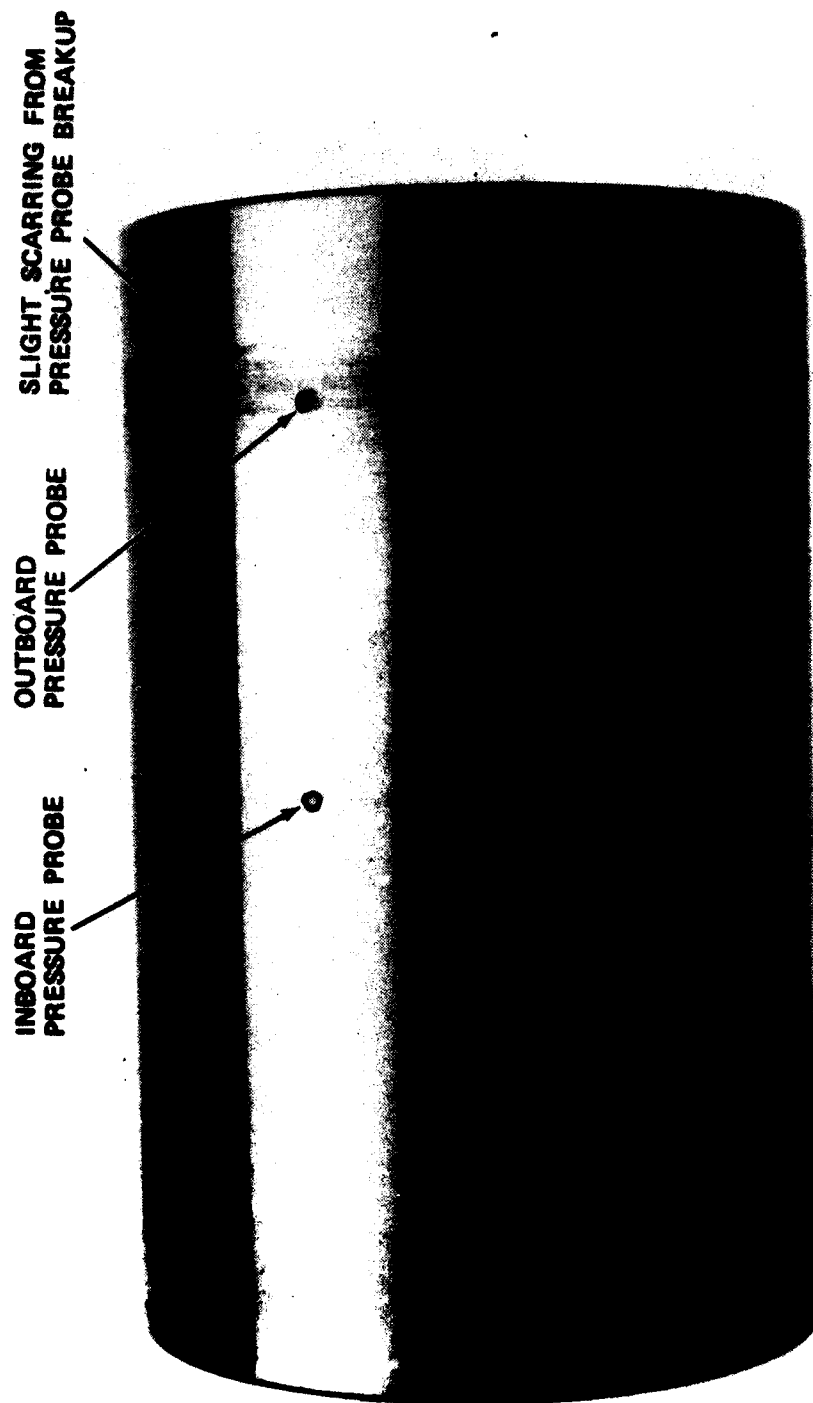


Figure 75. Instrumented Journal; Inboard Pressure Probe in Place. Outboard Pressure Probe Missing. Scarring is a Result of Probe Centrifuging Out and Breaking Up.

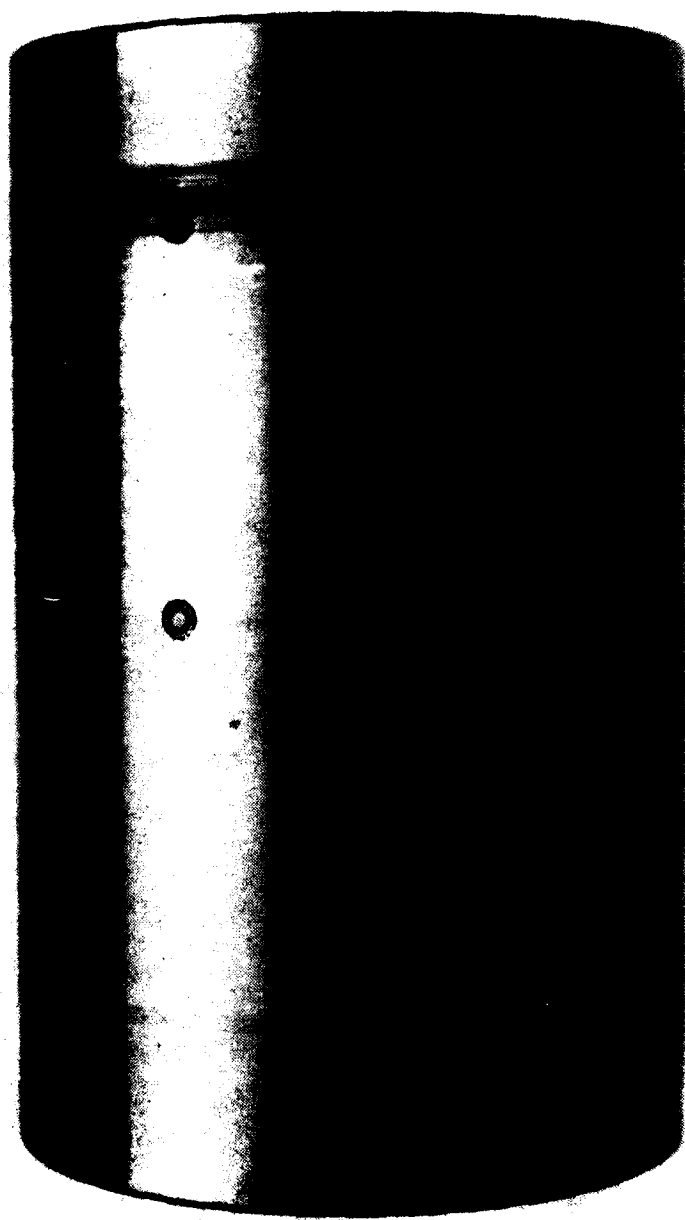


Figure 76. Instrumented Journal; Wayne-Kerr Probe Installation.

SECTION IV

CONCLUSIONS AND RECOMMENDATIONS

Table 12 summarizes the major steps in the development of the 3.5-inch bearing. The basic bearing design was successful in meeting program objectives in both the baseline ambient and high-temperature configurations.

1. ANALYSIS/DESIGN

a. Mechanical Design - Conclusions

The mechanical design of the bearing was acceptable. The bearing operated satisfactorily over the range of loads and temperatures imposed in the test program. Minimal axial variations in radial growth were achieved in design. Bearing dynamic behavior was acceptable, provided journal static runouts were maintained as low as possible. Bearing materials, foils, backing springs and bearing housing also were acceptable.

b. Mechanical Design - Recommendations

Bearing and journal design should be retained as is if a follow-on engine demonstration program is to be initiated.

c. Thermal Design - Conclusions

Bearing thermal response was in good agreement with analysis. The thermal model correlated well with measured data for different cooling flow rates and bearing power consumptions. The maximum bearing cooling flow attainable at about 50 psig (a reasonable approximation of compressor discharge pressure in an engine of this type) was 0.0125-0.015 lb/sec. This flow at

TABLE 12. CONFIGURATION AND PERFORMANCE DESCRIPTION

Config Number	No of Foils	Foil			Journals	Sway (1)	Test Results	
		Length/Dia (L/D Ratio)	Thickness (inch)	Coating			Max Load/Duration/Temp	Max Sustained Load/Duration/Temp
1	10	1.2	0.00785	Teflon-S	Chrome	0.020	500 lb/30 sec/amb	255 lb/85 min/470°F
2	8	1.2	0.0091	Teflon-S	Chrome	0.021	524 lb/15 sec/amb	300 lb/6 min/470°F
3	10	1.2	0.0080	DES+Au Overcoat	SCA	0.022	290 lb/20 sec/amb	185 lb/1 min 45 sec/amb
3a	10	1.2	0.0080	DES	SCA	0.022	340 lb/15 sec/994°F	--
4	8	1.2	0.0084	DES+Au Overcoat	SCA	0.023	--	--
4a	8	1.2	0.0084	DES+Au Overcoat; Journal Side only	SCA	0.023	360 lb/15 sec/amb	200 lb/2 min/amb
4b	8	1.2	0.0084	DES+Au Overcoat; Journal Side Trailing Edge only	SCA	0.023	400 lb/10 sec/amb	--
4c	8	1.2	0.0084	DES	SCA	0.023	490 lb/20 sec/900°F	200 lb/20 min/870°F
5	10	1.2	0.007	Co-20Ni	SCA	0.024	155 lb/15 sec/820°F	--
6	10	1.2	0.007	TiC	SCA	0.024	410 lb/15 sec/1256°F	--

FOIL LEADING EDGE CONFIGURATION



- (1) Sway Space = $D_H - D_J - 2(t_b + t_s) - 4t_f$
- D_H Foil carrier inside diameter
 - D_J Journal diameter
 - t_b Backing spring overall thickness
 - t_s Backing spring shim thickness
 - t_f Foil thickness

50 psig varied little with temperature or changes in sway space. The cooling air flow at 50 psig provided good cooling at ambient and high temperatures. Flows lower than 50 psig resulted in bearing heat buildup and consequent reduction in sway space, which compounds the problem.

d. Thermal Design - Recommendations

Thermal analysis was adequate for this program. Data taken should be used to improve thermal modeling of the bearing and its installation in a TJE331-1029 as part of a follow-on engine demonstration program.

e. Integrated Mechanical-Thermal Design - Conclusions

The original, single mid-entry cooling system performed effectively during testing. Cooling flows at 50 psig were adequate with bearing sway space chosen during baseline bearing tests to give bearing performance capable of meeting load and temperature goals.

f. Integrated Mechanical-Thermal Design - Recommendations

The single mid-entry cooling system should be retained for any further rig testing as well as incorporated in the TJE331-1029. The bearing and bearing cooling design is compatible with the installation envelope and should be retained for this reason.

g. Hydrodynamic Analysis - Conclusions

The elasto-hydrodynamic analysis used for 12-, 10-, and 8-foil bearings indicated that load capacity increased as number of foils decreased. Test data bore this out. Measured load deflection curves agreed with analysis data. The program used is

adequate for modeling the test bearing. The only portion of this analysis that is not substantiated by empirical data is prediction of air film thickness in the bearing under various operating conditions. Further instrumented journal testing should be able to improve this analysis.

h. Hydrodynamic Analysis - Recommendations

Current hydrodynamic analysis should be used in conjunction with test results to improve both the bearing analytical model and bearing design and performance. This analysis should be correlated and improved with any future instrumented journal testing.

2. BASIC BEARING TEST RIG

a. Basic Bearing Test Rig - Conclusions

The basic bearing test rig was successful in proving the satisfactory operation of the designed bearing to full required load and temperature levels. The use of an optical pyrometer to measure journal temperatures was highly successful.

b. Basic Bearing Test Rig - Recommendations

Use of this rig should be continued for further foil bearing testing of either 3.5-inch or other bearing sizes. However, the methods of test journal attachment to the test shaft should be improved to eliminate journal assembly and runout problems.

3. BASIC BEARING TESTING/AMBIENT FACILITY

a. Basic Bearing Testing/Ambient Facility - Conclusions

The baseline bearing on both 10- and 8-foil configurations met load goals, proving the adequacy of the basic design. Sufficient starts and operation of these bearings with Teflon-S coated foils and chrome-plated journals were accumulated to verify the validity of this bearing.

b. Basic Bearing Testing/Ambient Facility - Recommendations

The baseline bearing should be used to further refine present analytical models of this type foil bearing. Additionally, with expanded instrumentation, further exploration of maximum load capability should be considered.

4. BASIC BEARING TESTING/HIGH-TEMPERATURE FACILITY

a. Basic Bearing Testing/High-Temperature Facility - Conclusions

The high-temperature bearing met program load and temperature goals. As predicted, the 8-foil bearing showed higher load capacity than the 10-foil design. The Kaman DES foil coating and Kaman SCA journal coatings tolerated 400 start/stops without serious degradation and then were used successfully for maximum load and temperature testing.

b. Basic Bearing Testing/High-Temperature Facility - Recommendations

Because of successful testing with this bearing, high-temperature coating improvement would be the most worthwhile area

to investigate. Kaman SCA and DES are compatible, but thicker DES coatings should be investigated in an effort to obtain improved foil coating wear characteristics.

5. ALTERNATE FOIL COATING TESTING

a. Alternate Foil Coating Testing - Conclusions

For 1200°F use, sputtered TiC proved to be far superior to electroplated Co-20Ni as a foil coating when used in conjunction with an SCA coated journal. TiC wear and friction characteristics were exceptional in maintaining low bearing breakaway friction.

b. Alternate Foil Coating Testing - Recommendations

TiC should be considered as a candidate high-temperature foil coating if thicker, more wear resistant DES coatings cannot be successfully used.

6. INSTRUMENTED JOURNAL TESTING

a. Instrumented Journal Testing - Conclusions

Instrumented journal testing was partially successful. Pressure measurement was of great value in that the current analytical bearing model predicted a bearing pressure field similar to that measured. Also, it is significant that pressure measurement was accomplished by using commercially available pressure transducers. The technology for making successful pressure measurements from transducers in a rotating journal has been firmly established. Film thickness measurements were inconclusive; only areas of maximum and minimum film thickness could be determined.

b. Instrumented Journal Testing - Recommendations

Due to the successful nature of the instrumented journal testing, further work in this area should be pursued. The following improvements can be made:

- o Improved transducer lead design (both pressure and proximity)
- o Improved shielding, filtering and isolation of all associated data acquisition equipment
- o Improved physical mounting of the pressure probes in the journal to allow higher rotational speeds

7. OVERALL CONCLUSIONS AND RECOMMENDATIONS

The foil bearing designed and tested in this program exceeded program load requirements at sea level while operating at temperatures in excess of program requirements.

Test results demonstrated the validity of analytical tools used to develop and characterize this bearing design. Bearing air film pressure measurement significantly advanced techniques for improving bearing design, and load capacity.

It is recommended that:

- o The foil bearings developed should be used in a follow-on engine demonstration program
- o A separate instrumented journal program be undertaken to provide the analytical tools necessary to substantially improve bearing design and performance

DATE
FILME
—8